Distribution Agreement

In presenting this thesis or dissertation as a partial fulfillment of the requirements for an advanced degree from Emory University, I hereby grant to Emory University and its agents the non-exclusive license to archive, make accessible, and display my thesis or dissertation in whole or in part in all forms of media, now or hereafter known, including display on the world wide web. I understand that I may select some access restrictions as part of the online submission of this thesis or dissertation. I retain all ownership rights to the copyright of the thesis or dissertation. I also retain the right to use in future works (such as articles or books) all or part of this thesis or dissertation.

Signature:

_____ _____

Leila Myrick Date

Pathogenesis of novel *FMR1* mutations in fragile X syndrome

By

Leila Khoogar Myrick
Doctor of Philosophy

Graduate Division of Biological and Biomedical Science
Neuroscience

_____
Stephen T. Warren, Ph.D.
Advisor

_____
Gary J. Bassell, Ph.D.
Committee Member

_____
Christine M. Dunham, Ph.D.
Committee Member

_____
Peng Jin, Ph.D.
Committee Member

_____
James J. Lah, M.D., Ph.D.
Committee Member

Accepted:

_____
Lisa A. Tedesco, Ph.D.
Dean of the James T. Laney School of Graduate Studies

_____
Date

Pathogenesis of novel *FMR1* mutations in fragile X syndrome

By

Leila Khoogar Myrick
B.S., Emory University, 2007

Advisor: Stephen T. Warren, Ph.D.

An abstract of
A dissertation submitted to the Faculty of the
James T. Laney School of Graduate Studies of Emory University
in partial fulfillment of the requirements for the degree of
Doctor of Philosophy
in Graduate Division of Biological and Biomedical Sciences, Neuroscience
2014

Abstract

Pathogenesis of novel *FMR1* mutations in fragile X syndrome
By Leila Khoogar Myrick

Fragile X Syndrome (FXS) is the most common form of inherited intellectual disability (ID) and also the leading monogenic cause of autism spectrum disorder. In most cases, FXS is caused by a trinucleotide repeat expansion within the *FMR1* gene that causes transcriptional silencing and loss of the encoded protein, FMRP. *FMR1* missense mutations that disrupt FMRP function are also expected to cause FXS, however, in over two decades since *FMR1* was discovered, only a single pathological missense mutation has been reported (I304N). Recently we identified two novel variants, G266E and R138Q, in males with ID who tested negative for repeat expansion. To determine if these variants are pathological, we infected *Fmr1* KO cells with either G266E-FMRP or R138Q-FMRP lentivirus. We found that G266E behaves like a functional null and is unable to rescue any of the functions associated with FMRP's canonical role as a postsynaptic translation regulator. Specifically G266E failed to rescue AMPAR trafficking, associate with polyribosomes, or bind mRNA. We also modeled the G266E mutation onto crystallographic data of FMRP's KH1-KH2 domain and found this mutation is likely to cause significant structural disruption. Conversely, R138Q-FMRP rescued all the phenotypes associated with translation regulation. However, when neuronally expressed in transgenic *dfmr1*-deficient *Drosophila*, R138Q did not rescue synaptic overgrowth at the neuromuscular junction, suggesting this mutation specifically impairs FMRP's presynaptic function. Electrophysiological and biochemical studies confirmed the presynaptic defect and revealed that R138Q-FMRP is unable to modulate action potential duration through loss of interaction with presynaptic BK_{Ca} channels. In order to determine if R138Q causes any structural changes, we solved the crystal structure for the amino terminal domain where R138Q resides. We did not find any significant conformational changes between wild-type or R138Q crystal structures, however we unexpectedly discovered a novel RNA binding domain instead. In conclusion, G266E is a pathological null mutation while R138Q is a partial loss-of-function mutation that confers isolated loss of FMRP presynaptic function. These results separate the pre- and postsynaptic functions of FMRP and demonstrate investigational and clinical utility of screening for conventional *FMR1* mutations in individuals with ID.

Pathogenesis of novel *FMR1* mutations in fragile X syndrome

By

Leila Khoogar Myrick
B.S., Emory University, 2007

Advisor: Stephen T. Warren, Ph.D.

A dissertation submitted to the Faculty of the
James T. Laney School of Graduate Studies of Emory University
in partial fulfillment of the requirements for the degree of
Doctor of Philosophy
in Graduate Division of Biological and Biomedical Sciences, Neuroscience
2014

Acknowledgements

This dissertation would not have been possible without the support of a number of individuals to whom I am greatly indebted. First, I would like to express my appreciation for my advisor, Dr. Stephen Warren, for his continuous support, invaluable guidance, and undeniable foresight. Thank you for teaching me the rigors of science and providing an environment that fosters quality research above all things. You set the bar high and I have been very fortunate to be trained by such an exceptional scientist.

I must also thank my thesis committee members, Drs. Gary Bassell, Christine Dunham, Peng Jin, and James Lah for their selfless investment into my training. Your encouragement, patience, and intellectual contributions have been crucial to my success and professional development over the years. I especially thank Dr. Gary Bassell for always being my advocate, even when things looked "abysmal", and Dr. James Lah for his frank and honest advice at all times.

I am incredibly grateful for my collaborations with the Klyachko and Cheng labs. Dr. Vitaly Klyachko not only contributed tremendous amount of resources towards all the electrophysiology work presented here, but he also showed me that being the biggest critic of your own research is quite commendable. I learned the intricacies of biochemistry and crystallography in Dr. Xiaodong Cheng's lab, and I thank him and the other lab members for treating me as if I were genuinely a part of the lab. I especially appreciate the countless hours Hideharu Hashimoto spent technically training me, answering my never-ending questions, and putting me to shame with his undying work ethic; thank you for all your help Hassie.

Additionally, I would like to thank the entire Warren lab (both former and current members). You all made this process fun and provided me with constant sources of inspiration, technical advice, and open scientific discussion along the way. And I cannot go without saying thanks to the directors of the MD/PhD program, specifically Dr. Chuck Parkos and Mary Horton,

who helped me overcome my frustrations during difficult times and celebrated my successes at joyful times.

To my two wonderful sets of parents, thank you so much for loving me and being so supportive. Mom and Dad, from day one you taught me the value of education, gave me self-discipline, and encouraged me to constantly challenge myself. Without those virtues I would never have made it this far and I hope you know how much I love you both. Mama Jan and Big Dex, I am so lucky to have married into such a loving and supportive family. You have poured into me your love, support, encouragement, motivation, and practical advice and I would not be who I am today without you guys. Thank you from the bottom of my heart.

Last but not least, to my husband Dexter, you are my rock and I am so blessed that God put you in my life. When I was unsure and discouraged, your unfaltering confidence picked me back up and gave me motivation to continue. You have been in constant support of me achieving my goals and I literally could not have done this without you, literally. From our dinnertime conversations about failed PCR reactions to serious scientific debates about theory of science, you get it and I love that we share our passion for science together. Thank you for listening to my daily groans, thank you for bringing me food during those late nights in lab, thank you for always believing in me, and thank you for being you. You are my best friend and the best husband. I love you more than words can express.

Table of Contents

List of Figures and Tables

Chapter 1

Chapter 2

Chapter 3

Chapter 4

Chapter 5

Chapter 1. Introduction and Background

1.1 Fragile X syndrome

Fragile X syndrome (FXS) is the most common hereditary cause of intellectual disability (ID), affecting approximately 1:5000 males (Coffee et al., 2009) and 1:8000 females (Crawford et al., 2001). FXS accounts for approximately 2% of all intellectual disability and is also the leading monogenic cause of autism spectrum disorders (ASD) (Jacquemont et al., 2007, Wang et al., 2010b). In addition to ID, the syndrome is characterized by a wide array of behavioral and neurological symptoms (see **Section 1.1.1** Clinical description), and it is most often caused by a trinucleotide repeat expansion mutation that transcriptionally silences the *FMR1* gene (see **Section 1.1.2** Genetics of FXS). Loss of the encoded protein, Fragile X Mental Retardation Protein (FMRP), is the underlying basis of FXS pathophysiology and has been the focus of intense study for over 20 years (see **Section 1.2** Fragile X Mental Retardation Protein). However, repeat expansion mutations are not the only mode for acquiring FXS. Conventional mutations within *FMR1*, such as gross deletions, small indels, and missense/nonsense mutations have also been reported (see **Section 1.3** Conventional mutations). The focus of this present dissertation is to characterize two novel *FMR1* missense mutations, G266E and R138Q, and determine their pathological relevance in FMRP function and FXS.

1.1.1 Clinical description

The cardinal symptom in FXS is intellectual disability (ID). Male patients typically have IQ scores in the mild to severe ID range (FSIQ 25-70), while female patients are usually higher functioning and have IQ scores in the average to mild ID range (FSIQ 55-110) (Hessl et al., 2009). In fact, most females with FXS are not considered intellectually disabled and only about 30% have FSIQ < 70 (Hessl et al.,

2009). Since FXS is an X-linked disorder, the generally less severe female phenotypes are believed to be due to the production of FMRP by cells with the normal *FMR1* allele on the active X chromosome, also known as the X activation ratio (Abrams et al., 1994). Along with ID, patients experience global developmental delay and their intellectual functioning typically develops 2.2 times slower than unaffected children (Hall et al., 2008).

Other features commonly associated with FXS include autism, attention deficit hyperactivity disorder (ADHD), anxiety, seizures, macroorchidism, distinct facial characteristics, and connective tissue abnormalities (Chudley and Hagerman, 1987, Jacquemont et al., 2007). The facial abnormalities are often subtle but include long narrow face, large prominent ears, and a large forehead. Connective tissue problems include mitral valve prolapse, flat feet, joint hyperextensibility, and high arched palate, however these connective tissue manifestations, along with the dysmorphic facies, have an unknown relationship with intellectual disability and have received little research attention.

Conversely, the neuropsychiatric disorders contribute significantly to the morbidity of FXS and their molecular bases within the context of FXS are beginning to be understood (Tranfaglia, 2011). ADHD is present in an overwhelming 80% of FXS patients, and anxiety has been reported to affect anywhere from 70-100% of individuals (Jacquemont et al., 2007). In one rigorous study of 97 patients affected with FXS, 82.5% met the criteria for any anxiety disorder and 58.3% met the criteria for multiple anxiety disorders, with social phobia and specific phobia as the most common diagnoses (Cordeiro et al., 2011). Seizures are also commonly associated with FXS, affecting

approximately 20% of patients (Wisniewski et al., 1991, Musumeci et al., 1999, Incorpora et al., 2002), however this association is not unique to FXS since most developmentally disabled populations have a high prevalence of epilepsy. Interestingly, the use of animal models to better understand cognitive dysfunction in FXS has inadvertently also provided insights on the molecular mechanisms underlying FXS-associated seizures with evidence linking loss of FMRP to neuronal hyperexcitability, and the involvement of metabotropic glutamate and GABA receptor pathways (Hagerman and Stafstrom, 2009, Pfeiffer and Huber, 2009).

There is also a strong connection between FXS and ASD with up to 60%-90% of FXS patients exhibiting at least some autistic behaviors (Merenstein et al., 1996, Harris et al., 2008). When using ADI-R, ADOS, and DSM-IV gold standard diagnostic criteria, 30% of FXS patients meet the criteria for autism and an additional 30% for pervasive developmental disorder not otherwise specified (PDD-NOS) (Harris et al., 2008, Cordeiro et al., 2011). FXS is also the leading single gene cause of ASD with reports of the *FMR1* mutation being found in up to 8% of autistic children (Li et al., 1993, Estecio et al., 2002). The heterogeneity of ASD has made scientific progress within this field difficult, however FXS offers a well-defined single gene model for which to study ASD related mechanisms, and indeed significant overlap has been found in the molecular pathways of both disorders (Wang et al., 2010b, Darnell et al., 2011, De Rubeis and Bagni, 2011).

1.1.2 Genetics of FXS

FXS is an X-linked disorder with an unusual inheritance pattern. The term "fragile X" actually originated from observations of a chromosomal constriction on the

long arm of the X chromosome that appeared to segregate in families with X-linked intellectual disability (Lubs, 1969, O'Donnell and Warren, 2002). These chromosomal constrictions were later termed "fragile sites" and their link to FXS was confirmed in 1981 (Richards et al., 1981). 10 years later, the exact genetic locus was narrowed down to a CGG trinucleotide repeat region within the *FMR1* gene, and it still remains as the single gene responsible for this syndrome (Verkerk et al., 1991). The inheritance of FXS is atypical from other X-linked disorders in that 1) there are non-affected obligate carrier males and 2) the risk of inheritance increases with each generation (Sherman et al., 1985). This genetic anticipation event was termed the "Sherman Paradox" and remained unexplainable until the cloning of the *FMR1* CGG repeat expansion mutation.

The variable CGG repeat region is located within the 5' UTR of *FMR1* and is quite polymorphic with normal alleles spanning anywhere from 6 to 54 repeats (Fu et al., 1991). Due to the nature of repeat DNA being difficult to replicate (Richards and Sutherland, 1994), this region is susceptible to repeat expansion resulting in premutation alleles of 55-200 repeats, and full mutation alleles of >200 repeats (Fu et al., 1991). Within premutation carriers, the larger the repeat length, the more likely an expansion will occur in the subsequent generation, thus accounting for the Sherman Paradox and the unusual inheritance pattern of FXS (Fu et al., 1991). Once the repeat size exceeds 200 repeats, delayed replication upon entering metaphase causes the appearance of "fragile sites" on chromosome spreads (Yudkin et al., 2014), and the entire region undergoes extensive CpG methylation and chromatin condensation (Coffee et al., 2002). This epigenetic change is actually triggered by the *FMR1* mRNA itself. Early in embryogenesis when *FMR1* mRNA is still transcribed, the expanded CGG repeat in the

5'UTR of the mRNA forms an RNA•DNA duplex with the complementary CGG repeat on the *FMR1* DNA and this interaction is required in order to induce transcriptionally repressive histone marks at the *FMR1* promoter (Colak et al., 2014). The net result of these epigenetic changes is sustained transcriptional silencing of *FMR1* (Penagarikano et al., 2007). Thus, FXS is actually due to loss of the encoded protein, FMRP, which has been confirmed by lack of *FMR1* expression in FXS patients (Pieretti et al., 1991), and a handful of *FMR1* deletion and missense mutations (Gedeon et al., 1992, Wohrle et al., 1992, De Boulle et al., 1993, Myrick et al., 2014c).

1.2 Fragile X Mental Retardation Protein (FMRP)

1.2.1 Structure and domains

FMRP is a complex protein with several structural domains and multiple functions. The full-length protein is encoded from 17 exons to yield a 632 amino acid product (71.1 kDa), however alternative splicing between exons 11-17 can result in several smaller versions that range in size from 47.3 to 69.9 kDa (Eichler et al., 1994, Sittler et al., 1996). From amino terminus to cytoplasmic, FMRP is comprised of two tandem Agenet domains in exons 1-3 and 3-5, a nuclear localization sequence in exons 5-6, two tandem KH domains in exons 8-9 and 9-13, a nuclear export sequence in exon 14, and an RGG box in exon 15 (**Figure 1.1A**) (Santoro et al., 2012).

Perhaps the best-studied domains are the three RNA binding motifs, which include KH1, KH2 and the RGG box. These were first identified in 1993 and helped establish FMRP as an RNA binding protein that selectively associates with approximately 4% of mRNA in the brain (Ashley et al., 1993). How FMRP uses these

domains to recognize a specific subset of messages has, however, been a long-standing question that will be discussed in **Section 1.2.2** and **Section 1.2.3** below. Less well studied is the amino terminus of FMRP, which encompasses two Agenet domains and a nuclear localization sequence, and will be discussed in **Section 1.2.4**.

1.2.2 KH domains

How does FMRP use the KH domains to recognize RNA? Crystallographic studies of other RNA binding proteins have shown that RNA binds to KH domains in a hydrophobic "RNA binding cleft" that is flanked by a G-X-X-G motif on one side and a variable loop on the other side (Valverde et al., 2008). The RNA binding cleft only accommodates up to 4 nucleic acids, however greater RNA binding specificity can be achieved by multiple tandem KH domains or other structural motifs that act in concert with the KH domain. The hydrophobic core of the RNA binding cleft is very important for RNA binding, and in fact, the I304N patient mutation lies directly within this hydrophobic core in FMRP's KH2 domain and is expected to disrupt all KH2 mediated RNA binding (Lewis et al., 2000, Ramos et al., 2003, Valverde et al., 2008).

Later studies identified that while most KH domains recognize a 4-7 nucleotide consensus sequence, FMRP's KH2 domain actually recognizes RNAs with a much more complex structure known as the "kissing complex" (Darnell et al., 2005). A kissing complex is comprised of two stem loops that form a 4 base pair interaction with one another into a loop-loop-pseudoknot. This association with kissing complex RNAs was specific to the KH2 domain because I304N mutation abolished the interaction but an equivalent KH1 mutation had no effect. Moreover, synthetic kissing complex RNAs were able to compete off FMRP binding with natural mRNA targets identified by HITS-CLIP,

confirming that kissing complex motifs are indeed critical for FMRP's RNA binding selectivity (Darnell et al., 2011). However, natural FMRP targets that harbor the kissing complex motif have yet to be identified.

Most recently a novel approach to isolate FMRP target binding sites, PAR-CLIP, was used in combination with next generation sequencing and computational analysis to identify possible RNA-recognition elements (RREs) within FMRP's bound mRNAs (Ascano et al., 2012). This study revealed that FMRP recognizes "ACUK" and "WGGA" motifs and that the KH2 domain is specifically responsible for ACUK recognition. FMRP with the I304N mutation and isoforms of FMRP that lack the extended variable loop in KH2 (alternative splicing that skips exon 12, see **Figure 1.1B**) both had reduced binding affinity for ACUK containing mRNAs, but not WGGA. Interestingly, the variable loop in exon 12 seems to play a developmental role in modifying the RNA binding properties of FMRP. Early in development, there is a 1:1 ratio between isoforms that exclude or include exon 12, however, by adulthood, exclusion of exon 12 is much more common and these isoforms are now at a 3:1 ratio (Brackett et al., 2013). Furthermore, higher levels of exon 12 retaining isoforms are found in cultured neural progenitor cells as well as brain regions that have significant neural stem cell populations (i.e. the hippocampus and olfactory bulb), all of which suggest that the extended variable loop in KH2 is important for neurogenesis and neural development. As mentioned above, the variable loop is an integral part of the RNA binding cleft within KH domains (Valverde et al., 2008), and therefore shortening of the loop through skipping of exon 12 could in theory modify the RNA binding specificity of FMRP's KH2 domain (Brackett et al., 2013). Thus, the hydrophobic core of the RNA binding cleft, kissing complex RNA structures,

ACUK motifs, and the variable loop have all been implicated in KH domain mediated RNA binding by FMRP.

1.2.3 RGG domain

At the C-terminus is another interesting FMRP RNA binding motif that has gathered a lot of attention, the RGG box. Similar to the KH2 domain, the RGG box is involved in binding mRNAs with a complex structural motif called the "G-quartet" (Darnell et al., 2001, Schaeffer et al., 2001). G-quartet RNAs are formed by four guanine nucleotides that form hydrogen bonds with each another into a square planar conformation and can stack on top of one another. Only a handful of G-quartet FMRP targets have been experimentally validated (Melko and Bardoni, 2010), however among the targets identified by Brown et al. that are both bound and translationally regulated by FMRP, a surprising 67% were predicted to contain the G-quartet motif (Brown et al., 2001, Darnell et al., 2001). In 2011, the NMR solution structure for the FMRP RGG box with bound G-quartet RNA confirms that the RGG box does indeed bind G-quartet RNAs (Phan et al., 2011), yet the full extent to which native FMRP targets harbor G-quartets still remains to be determined. The NMR structure also identified two arginine residues that make critical contacts with G-quartet RNA, and interestingly, these two residues are two out of the four arginines within the RGG box that are methylated *in vivo* and regulate FMRP's affinity for G-quartet RNA (Blackwell et al., 2010, Phan et al., 2011).

In addition to regulation of RNA binding by methylation, the position of the G-quartet within an mRNA sequence can dictate how FMRP binding will affect translation. For instance, for FMRP targets that have validated G-quartets in their 5'UTR, it has been proposed that FMRP binding stabilizes the G-quartet structure and could either prevent

polyribosome scanning or induce ribosome stalling, either way leading to translational repression of the target mRNA (Melko and Bardoni, 2010). This is certainly supported by reports of FMRP suppressing translation of a reporter gene with the G-quartet RNA sequence inserted into the 5'UTR (Schaeffer et al., 2001). However, FMRP does not always act as a translational repressor given that half the G-quartet containing targets identified by Brown et al. had decreased and the other half had increased association with polyribosomes in the absence of FMRP (Brown et al., 2001). Since G-quartets have been found within coding sequences and 3'UTRs as well, it is possible their variable location may contribute to different regulatory effects upon FMRP binding.

It should be noted that FMRP has two autosomal homologs, FXR1 and FXR2, that share significant sequence homology with FMRP, especially in exons 1-13 (Siomi et al., 1995, Zhang et al., 1995, Kirkpatrick et al., 2001). While all three contain the same basic protein structure of two Agenet domains, two KH domains, and an RGG box (Siomi et al., 1995, Zhang et al., 1995, Adams-Cioaba et al., 2010), only FMRP's RGG box has been demonstrated capable of binding G-quartet RNA, suggesting a functionally non-redundant role in mRNA metabolism that is served by FMRP and not its homologs (Darnell et al., 2009). In contrast, the KH2 domains from all three proteins are able to bind kissing complex RNAs. RGG motifs are loosely defined as three to four closely spaced arginine-glycine-glycine tripeptide repeats (Burd and Dreyfuss, 1994), which explains how FXR1/2 can contain RGG boxes despite their poor sequence homology with FMRP in the C-terminus, and also suggests that FMRP's specific recognition of G-quartets may be more sequence dependent. In fact, despite low C-terminal sequence

conservation with FXR1/2, the human FMRP RGG box shares significant conservation with the RGG boxes of 5 other FMRP species (Darnell et al., 2009).

Thus, FMRP can recognize G-quartet mRNAs through the RGG box, kissing complex RNAs at the KH2 domain, and ACUK and WGGA RNA sequence motifs throughout the transcriptome. Whether FMRP targets mRNAs with a combination of these features or separately across different mRNAs is a question that will require further exploration. However, since RNA binding is a critical function of FMRP, understanding the precise mechanisms that confer FMRP's RNA binding selectivity will undoubtedly help advance our understanding of FXS pathophysiology.

1.2.4 Amino-terminal domain

The amino-terminal domain comprises a large segment of the entire FMR protein, however its role in the pathophysiology of FXS has been understudied and is still largely unknown. It includes two tandem Agenet domains (Maurer-Stroh et al., 2003, Ramos et al., 2006), a nuclear localization sequence (Eberhart et al., 1996, Bardoni et al., 1997), and two distinct protein-protein interaction domains: the region spanning exons 4-5 that mediates interactions with NUFIP and 82-FIP (Bardoni et al., 1999, Bardoni et al., 2003), and the region spanning exon 7 that mediates interactions with CYFIP and FXR1/2 (Siomi et al., 1996, Schenck et al., 2001) (**Figure 1.1A**). This latter region has also been shown to be important for homo- and heterodimerization of FMRP with itself and the FXR1/2 proteins (Siomi et al., 1996, Adinolfi et al., 2003), and for shuttling FMRP between stress granules and the cytosol (Gareau et al., 2013), all of which have an unclear role in the pathophysiology of FXS.

Perhaps of most interest are the tandem Agenet domains, which despite their identification within FMRP over 10 years ago, have only recently been shown to mediate a nuclear FMRP function in chromatin binding and DNA damage response (Alpatov et al., 2014). The tandem Agenet domains preferentially recognize methylated lysine (Ramos et al., 2006), and at least two residues are critical for binding to chromatin, T102 and Y103 (Alpatov et al., 2014). The Agenet domains are also well conserved in the FXR1 and FXR2 proteins, which have been shown to bind trimethylated histone peptides as well (Adams-Cioaba et al., 2010). According to Alpatov et al., FMRP is recruited to the nucleus in response to replication stress where it binds chromatin via these Agenet domains and elicits H2A.X phosphorylation, a key signaling mechanism in the DNA damage response pathway (Alpatov et al., 2014). In the absence of FMRP, double stranded break repair was impaired and meiotic cells from *Fmr1* KO mice were shown to inappropriately retain many elements of the DNA damage response pathway on unrepaired regions of their chromosomes during meiosis. This nuclear role in the DNA damage pathway is strikingly different from FMRP's previously defined role as an RNA binding protein, but nonetheless is an important novel insight for FXS pathophysiology given the germ cell specific phenotypes of macroorchidism in FXS males (Chudley and Hagerman, 1987) and enlarged ovaries in *Fmr1* KO mice (Ascano et al., 2012). Whether FMRP's nuclear function also plays a role in intellectual disability or other neurological phenotypes still remains to be determined.

1.2.5 FMRP Function

mRNA transport and local translation within synapses is absolutely critical for synaptic plasticity and learning and memory. Thus, it is not surprising that a mutation in

an RNA binding protein, such as FMRP, would cause intellectual impairment. In fact, several other RNA binding proteins have been implicated in cognitive dysfunction as well, including FMR2 in FRAXE-associated ID (Bensaid et al., 2009), PQBP1 in several X-linked ID disorders such as Renpenning syndrome (Kunde et al., 2011), ZC3H14 in nonsyndromic autosomal recessive ID (Pak et al., 2011), EXOSC3 in ID with associated spasticity (Zanni et al., 2013), and UPF3B in syndromic and non-syndromic ID (Tarpey et al., 2007).

In the context of FXS, FMRP is necessary for binding to and regulating the translation of a specific subset of mRNA ligands at the synapse (Bassell and Warren, 2008, Santoro et al., 2012). Several lines of evidence support this role in local protein synthesis. First, FMRP has been localized to dendritic spines (Feng et al., 1997b, Antar et al., 2004), along with several of its mRNA targets including Arc, CamKIIα, $GluR_{1/2}$, Map1b, PSD95, and Sapap3/4 (Santoro et al., 2012). At the synapse, FMRP associates with actively translating polyribosomes (Feng et al., 1997b, Weiler et al., 1997), and in the absence of FMRP, there is excessive protein synthesis of several FMRP targets, including Arc, CamKIIα, $GluR_1$, Map1b, and PS95 (Zalfa et al., 2003, Muddashetty et al., 2007). Moreover, these targets fail to be translated in response to activity resulting in specific loss of activity dependent protein synthesis, a crucial component of synaptic learning and plasticity (Muddashetty et al., 2007). Perhaps the ultimate evidence comes from finding exaggerated group 1 metabotropic glutamate receptor dependent long term depression (mGluR-LTD) in *Fmr1* KO mice, the first and most thoroughly characterized synaptic plasticity defect reported in FXS (Huber et al., 2002).

mGluR-LTD is a form of synaptic plasticity in the hippocampus that depends on activity dependent local protein synthesis (Bear et al., 2004). In *Fmr1* KO mice, mGluR-LTD is enhanced rather than defective, which is consistent with the view that FMRP generally acts as a translational repressor (Laggerbauer et al., 2001, Li et al., 2001). Thus, in the absence of FMRP, there is no counterbalance to mGluR induced protein synthesis and mGluR-LTD becomes exaggerated (Bear et al., 2004). This model, commonly known as the "mGluR theory" of FXS, explains the connection between dysregulated translation of synaptic proteins and many of the synaptic and cognitive defects observed in FXS. Further experiments have since refined the model to state that FMRP is needed at basal states for translational suppression of specific synaptic proteins, and that this repression can be temporarily released to allow stimulus-induced episodes of protein synthesis that are timed with synaptic activity (Santoro et al., 2012). mGluR-mediated synaptic plasticity defects have now been reported in other areas of the brain outside the hippocampus including cerebellum (Koekkoek et al., 2005, Huber, 2006), neocortex (Wilson and Cox, 2007), and amgydala (Suvrathan et al., 2010), and furthermore, loss of stimulus-induced protein synthesis has also been seen in muscarinic acetylcholine (Volk et al., 2007), dopamine (Wang et al., 2010a), and TrkB (Osterweil et al., 2010) receptor signaling pathways. Thus, the loss of FMRP seems to cause a generalized deregulation of activity dependent protein synthesis across the brain, leading to elevated basal protein levels and absence of stimulus-induced translation (Bassell and Warren, 2008).

In addition to synaptic plasticity, these findings may also be particularly relevant for synaptic development. In fact, one of the only morphological changes seen in FXS brain is the hyperabundance of long, thin dendritic spines with immature morphology

(Rudelli et al., 1985, Comery et al., 1997, Irwin et al., 2001). These immature spines are reminiscent of what is seen in early development and are due to defects in spine maturation and stability with *Fmr1* KO mice showing delayed turnover from immature to mature spine formations and continual overproduction of transient spines (Cruz-Martin et al., 2010, Pan et al., 2010). Along these same lines, FMRP is required for experience-dependent axonal pruning (Tessier and Broadie, 2008), and has been shown to negatively regulate synapse number (Pfeiffer and Huber, 2007) and neuronal elaboration (Zhang et al., 2001, Pan et al., 2004). In essence, loss of FMRP leads to a generalized synaptic overgrowth phenotype during development that presumably is based on dysregulated protein synthesis, however a direct connection between translation regulation and FMRP's synaptic connectivity defects remains to be experimentally proven.

1.3 Conventional *FMR1* Mutations

1.3.1 Gross and small *FMR1* deletions

FXS is most often caused by trinucleotide CGG repeat expansion that induces transcriptional silencing of the *FMR1* gene, however conventional mutations affecting *FMR1* have also been reported. Two of the earliest cases come from reports in 1992 of patients with classic FXS phenotype, but without fragile X chromosomes or CGG repeat expansion (Gedeon et al., 1992, Wohrle et al., 1992). Both patients were intellectually disabled with macroorchidism and characteristic FXS facies. Southern blot analysis of their DNA with probes complementary to the CGG region of *FMR1* did not show any detectable autoradiographic signal, indicating a deletion of this region must have occurred. In the past, absence of the cytogenetic fragile X chromosomes would have led

to the conclusion that these patients did not have FXS. However the strong clinical suspicion for FXS led to further molecular analysis and revealed for the first time that deletions of *FMR1* can also give rise to the same clinical phenotype.

Since the initial report of these two patients, one of which who had a 2.5Mb deletion and the other who had a 250 kb deletion, a number of other large deletions have been reported ranging from 10kb up to 13Mb (reviewed in Coffee et al., 2008). Some of these large deletions can affect neighboring genes such as IDS or MTM1 (**Figure 1.2**), leading to FXS in combination with other clinical phenotypes such as Hunter syndrome or myotubular myopathy, respectively (Dahl et al., 1995, Birot et al., 1996). Smaller deletions that perturb only the *FMR1* gene sequence and not any flanking DNA, or deletions of the *FMR1* promoter region alone further clarify that isolated loss of *FMR1* gene expression is the underlying cause of FXS (Gu et al., 1994, Meijer et al., 1994, Trottier et al., 1994, Hammond et al., 1997). It is important to note that more distal deletions of *FMR1* that do not affect the 5' portion of the gene may also exist, however they are not usually surveyed for during FXS testing and therefore remain unidentified.

Only two very small intragenic deletions have ever been reported in *FMR1* (Lugenbeel et al., 1995). The patients carrying these mutations both had classic FXS phenotype including ID, autistic features, dysmorphic facies, and hypermobile joints. Neither patient had any fragile X chromosomes on cytogenetic examination, and molecular analysis by Southern blot and PCR both showed CGG repeats within normal limits. This would ordinarily rule out a diagnosis of FXS, however strong clinical suspicion led to the testing of the patients' blood by Western blot, which revealed absence of FMRP expression. Subsequent sequence analysis identified a 1 base pair

deletion in exon 5 of the first patient that causes a frameshift and early termination. In the second patient, a 2 base pair deletion was detected that changes a splice acceptor site in exon 2. This mutation also results in a frameshift and premature termination due to the splicing out of exon 2. Thus, both of these intragenic deletions cause an absence of the protein product, FMRP, and would not have been detected by standard cytogenetic and molecular FXS testing at the time.

1.3.2 *FMR1* mutation screening

The idea has been put forth that additional intragenic *FMR1* sequence variants, such as missense, nonsense, and small indels, may also exist within the population but have not been discovered due to lack of screening for these types of mutations. These variants could certainly cause dysfunctional or absent protein expression and may contribute significantly to disease, especially in individuals with ID who test negative for CGG repeat expansion or large deletions. In search of such mutations, there have been four studies to date that performed *FMR1* mutation screening. These studies are briefly discussed below, but the point mutations they have uncovered are discussed in greater detail in **Section 1.3.3** *FMR1* point mutations.

In 1997, Wang et al. screened 406 ID patients to find 27 patients with characteristic FXS phenotype but no chromosomal abnormality, CGG repeat expansion, or *FMR1* promoter deletion (Wang et al., 1997). These 27 patients were then screened for *FMR1* point mutations in exons 1-10 and 15, and only one splice site/frameshift mutation was found, however it was present in three unrelated individuals. In 2004, Shinahara et al. screened all 17 exons from 90 patients with either autism or ID. They found no mutations in any of the male individuals and only one splice site/frameshift mutation in a

female patient who had autism and severe ID (Shinahara et al., 2004). Collins et al. performed the largest scale study in 2010 using next generation sequencing techniques on 963 developmentally delayed males negative for *FMR1* CGG repeat expansion (Collins et al., 2010). The promoter, all 17 exons, and a substantial portion of the introns were sequenced to discover a single missense variant (R138Q), three promoter variants, and several non-coding variants of unknown functional significance. It is important to note that from this study there is incomplete evidence to determine whether any of these variants are the cause of disease; however, the novel missense variant, R138Q, is discussed further in **Chapters 3 & 4**.

The large-scale study performed by Collins et al. was very useful for the discovery of novel sequence variants, however we still do not know the true frequency of point mutations within FXS since ID can be caused by numerous different factors and FXS only accounts for ~2% of all ID. To more directly address this point, Luo et al. screened for *FMR1* sequence variants in 60 patients with ID and at least one other FXS symptom, such as dysmorphic facies, ADHD, or autistic features (Luo et al., 2014). They found only one coding sequence variant, but it was the same mutation that had already been reported by Shinahara et al. They concluded that *FMR1* point mutations do not seem to be highly prevalent in FXS, which suggests that they either give rise to atypical phenotypes or may induce a gain-of-function lethal effect in males. In light of recent discoveries pointing at a new role for FMRP in the DNA damage repair pathway (Alpatov et al., 2014), *FMR1* point mutations may actually result in negative selection against sperm with defective FMRP more so than simply the absence of FMRP, which could explain the low prevalence of point mutations even though males with deletion

mutations can clearly survive. In either case, screening females for heterozygous mutations may help unveil additional *FMR1* conventional mutations.

1.3.3 *FMR1* point mutations

To date, two splicing/frameshift, one nonsense, and three missense mutations have been reported within *FMR1* as disease causing mutations. The first splicing mutation, c.990+14C>T, was reported in three unrelated individuals with typical FXS presentation (Wang et al., 1997). This point mutation within intron 10 causes skipping of exon 10 and direct splicing of exon 9 to exon 11. Exon 11 is consequently in frameshift with a stop codon occurring shortly thereafter. The net result is a truncated transcript missing the coding sequence for the KH2 and RGG box RNA binding domains, however the authors did not confirm whether this protein is actually made. The second splicing mutation, c.879A>C, was found in two independent reports separated by 10 years, and is a synonymous mutation of exon 9 that destroys a splice donor site (Shinahara et al., 2004, Luo et al., 2014). Shinahara et al. originally reported the mutation in a female patient with autism and severe ID. They showed evidence that the destruction of the primary splice donor site activates a cryptic site in intron 9 that results in a 47 nucleotide insertion between exons 9 and 10, followed by premature termination shortly thereafter. This transcript is predicted to produce a truncated protein that is again missing the KH2 and RGG box domains. Even though the mutation was reported in a heterozygous female, they showed that the mutant allele was predominantly transcribed and therefore concluded that the patient's phenotype could be explained by truncated FMRP produced in the brain. Conversely, Luo et al. found the same mutation in a young boy with severe ID and developmental delay, however they were unable to detect any aberrantly spliced

transcripts or truncated protein from the patient's blood. This does not rule out the possibility for aberrant splicing and truncated FMRP products in the brain, however due to the discrepancy between reports it is unclear at this time whether the mutation actually causes cognitive impairment.

The only nonsense mutation that has been linked to FXS is c.80C>A and it results in a stop codon within exon 2, p.Ser27X (Gronskov et al., 2011). The patient presented with all the typical symptoms of FXS including ID, developmental delay, dysmorphic facies, macroorchidism, hyperextensible joints, epilepsy, and autistic features. Molecular FXS testing showed a normal 29 CGG repeat size; however no FMRP expression was detected in the patient's blood by Western blot, which prompted subsequent DNA sequencing. This revealed a nonsense mutation in the patient and in his heterozygous mother who was also mildly intellectually disabled. This study highlights the usefulness of evaluating protein expression in patients that test negative for *FMR1* repeat expansion or deletion mutations.

The first point mutation ever reported in *FMR1* was a missense mutation causing isoleucine substitution for asparagine at residue 304 (I304N) (De Boulle et al., 1993). This patient presented with severe ID (IQ < 20), seizures, dysmorphic facies, and extreme macroorchidism. Coincidentally, the patient also suffered from X-linked liver glycogenesis, which was highly prevalent in his family pedigree, and caused symptoms of growth retardation and hepatomegaly in his childhood. The FXS-like symptoms of ID and macroorchidism are not part of the clinical phenotype for X-linked liver glycogenesis and none of the other family members affected with this disorder had any neurological manifestations. Thus, the patient's severe ID and macroorchidism were highly suggestive

of a separate disorder and prompted FXS testing. Cytogenetic and molecular analysis revealed no fragile x chromosomes, normal CGG repeat length, and an unmethylated CpG island, however sequence analysis discovered a c.911T>A missense mutation that results in I304N substitution. This mutation was not present in any of the patient's family members or in 130 control individuals. Numerous studies have since shown that I304N missense mutation significantly disrupts FMRP function both *in vitro* and *in vivo* (Feng et al., 1997a, Brown et al., 1998, Laggerbauer et al., 2001, Pfeiffer and Huber, 2007, Valverde et al., 2007, Zang et al., 2009). The existence of this missense mutation also serves to show that not only absence of FMRP expression, but also dysfunctional FMRP expression, can yield the same FXS phenotype.

Since 1993, only two additional *FMR1* missense mutations have been identified. These include glycine substitution for glutamate at residue 266 (G266E), which is discussed further in **Chapter 2**, and arginine substitution for glutamine at residue 138 (R138Q), which is discussed further in **Chapters 3 & 4**. This is in stark contrast to the over 100 missense mutations reported in *MECP2*, a gene involved in the X-linked ID disorder known as Rett syndrome. It is arguable that *FMR1* missense mutations are less common because they may lead to less severe phenotypes, such as learning disability without any other classic FXS features, and therefore would not prompt extensive diagnostic pursuits. Or they may be less common because of potential dominant-negative or gain-of-function lethal effects. Regardless, whenever missense mutations are identified it is important to determine how they affect protein function. Unlike deletion, frameshift, or nonsense mutations, the functionality of missense mutations is often difficult to predict without experimental evidence.

1.3.4 Proposed research

Prior to this current body of research, the direct involvement of G266E and R138Q in FXS pathophysiology was unknown. Therefore, the goal of this dissertation is to examine whether these two novel *FMR1* missense variants are pathological mutations that affect the function of FMRP.

G266E missense was discovered in a patient with prototypical FXS phenotype in the absence of CGG repeat expansion. The patient's classic FXS phenotype along with the position of the mutation within an important RNA binding domain, led to the hypothesis that this mutation would abolish FMRP function similar to the I304N mutation. This was indeed true and the effects of G266E mutation on FMRP function are addressed in **Chapter 2**.

R138Q missense was discovered in a patient that was also negative for CGG repeat expansion, but with less characteristic FXS symptoms, which included ID and seizures. The patient's milder phenotype and position of the mutation in a domain with unclear function made hypotheses about the effect of this mutation more difficult. It was determined that R138Q disrupts parts, but not all, of FMRP function and these effects are discussed in **Chapter 3**.

The amino terminal domain of FMRP, where R138Q mutation is located, is not well understood in terms of structure or function. To better understand the potential effects that R138Q might have on FMRP structure, structural data for the amino terminal domain encompassing this residue is needed. The wild-type and R138Q amino terminal domain structures are described in **Chapter 4**.

The outcomes of this research provide a deeper understanding of FMRP function and identify key residues that are important for specific functions of FMRP. FMRP is an important molecule involved in learning and memory, and knowledge of its function and dysfunction has clinical relevance for the pathophysiology of FXS as well as broader biological significance for understanding the neurobiology of cognitive function.

Figure 1.1: *FMR1* gene structure and protein domains

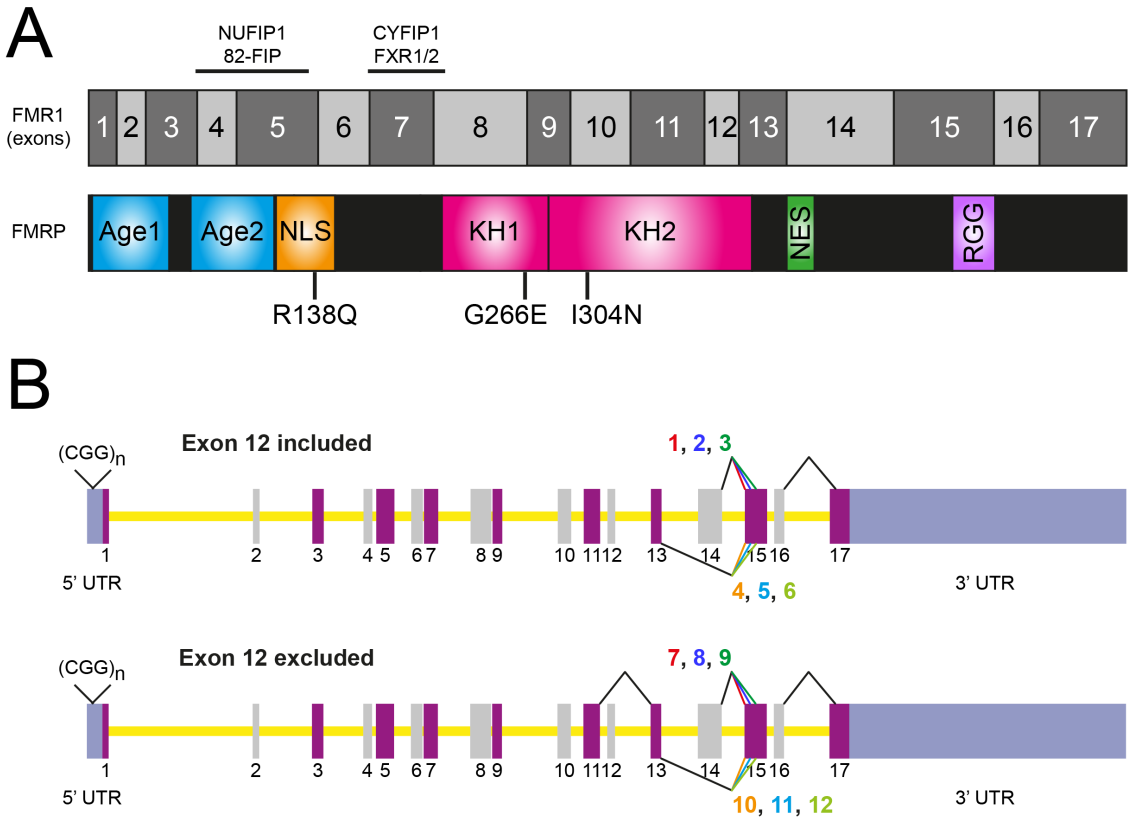

Figure 1.1: *FMR1* gene structure and protein domains

A: FMRP domain boundaries (bottom panel) with corresponding *FMR1* exon boundaries (top panel). Agenet1 and 2 are in blue, nuclear localization sequence (NLS) is in orange, KH1 and 2 are in pink, nuclear export sequence (NES) is in green, and RGG box is in purple. Locations of patient mutations are also denoted: R138Q in NLS, G266E in KH1, and I304N in KH2.

B: *FMR1* gene structure and alternative splicing. Exons 1-17 are shown in alternating fuchsia and gray, introns are shown in yellow (at $1/25^{th}$ scale compared to exons), and untranslated regions (UTR) are shown in blue-gray. 5' UTR includes variable CGG repeat length. Top panel indicates transcript isoforms that include exon 12, and bottom panel indicates transcript isoforms that exclude exon 12. For both conditions, exon 15 can be spliced at either the first, second, or third sites. Isoforms 1, 2, 3, 7, 8, and 9 include exon 14, while isoforms 4, 5, 6, 10, 11, and 12 skip exon 14.

Figure 1.2: *FMR1* neighboring genes

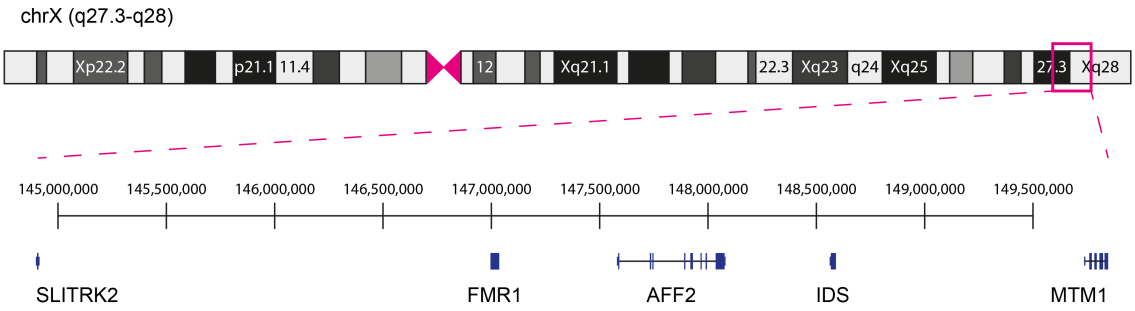

Figure 1.2: *FMR1* neighboring genes

Chromosome X with expanded q27.3 - q28 region and gene locations. Upstream of *FMR1* is largely a gene desert with *SLITRK2* as the closest upstream gene. Downstream of *FMR1* are the *AFF2*, *IDS*, and *MTM1* genes. Mutations in IDS cause Hunter syndrome, and mutations in MTM1 are associated with myotubular myopathies.

Chapter 2. Fragile X syndrome due to a G266E missense mutation[1]

[1] Adapted from Myrick LK, Nakamoto-Kinoshita M, Lindor NM, Kirmani S, Cheng X, Warren ST. (2014c). Fragile X syndrome due to a missense mutation. *Eur J Hum Genet* **22**:1185-1189.

Author Contributions: Myrick designed the lentiviral constructs and performed the polyribosome association and mRNA binding assays. Nakamoto-Kinoshita performed the AMPAR assay. Lindor and Kirmani evaluated the patient. Cheng assisted with crystallographic modeling of the G266E mutation.

2.1 Abstract

Fragile X syndrome is a common inherited form of intellectual disability and autism spectrum disorder. Most patients exhibit a massive CGG-repeat expansion mutation in the *FMR1* gene that silences the locus. In over two decades since the discovery of *FMR1*, only a single missense mutation (I304N) has been reported as causing fragile X syndrome. Here we describe a 16-year old male presenting with fragile X syndrome but without the repeat expansion mutation. Rather, we find a missense mutation, c.797G>A, that replaces glycine 266 with glutamic acid (G266E). The G266E FMR protein abolished many functional properties of the protein. This patient highlights the diagnostic utility of *FMR1* sequencing.

2.2 Introduction

Fragile X syndrome (FXS) is an X-linked disorder presenting in males and, less frequently, females with developmental delay. It is characterized by intellectual disability, speech and language delay, and a characteristic physical appearance of a long narrow face with prominent ears and jaw and macroorchidism in males (Santoro et al., 2012). Most patients suffer from severe social anxiety and hyperarousal with 60% of patients meeting diagnostic criteria for some form of autism spectrum disorder (ASD). Indeed, FXS is the most common single gene cause of ASD (Wang et al., 2010b).

FXS was one of the first examples of a trinucleotide repeat expansion disorder with the discovery of its causal gene, *FMR1* (Verkerk et al., 1991). This gene harbors a CGG-repeat in its 5' untranslated region. In normal individuals, repeat length is polymorphic with 29-30 repeats being the most common allele (Fu et al., 1991). In patients with FXS, there is a large expansion of the repeat sequence to over 200 repeats, referred to as the full mutation. Once the repeat length reaches 200, an epigenetic event is triggered that results in methylation of the entire *FMR1* gene and silences transcription (Santoro et al., 2012).

The absence of *FMR1* transcription leads to the loss of the encoded protein, FMRP. FMRP is a selective RNA-binding protein that regulates translation of its target mRNAs at the synapse in an activity-dependent manner (Bassell and Warren, 2008). Precise translation of these messages modulates synaptic strength and in the absence of FMRP, synaptic strength is defective with excess internalization of AMPA receptors from the synaptic membrane (Bhakar et al., 2012). This mimics excessive group 1 metabotropic glutamate receptor signaling, which is an insight that has initiated several

FXS clinical trials with therapeutic approaches directly targeting this pathway (Berry-Kravis et al., 2009, Jacquemont et al., 2011, Berry-Kravis et al., 2012).

FXS is almost exclusively diagnosed by molecular testing for CGG repeat expansion, even though the causal link to FXS is not due directly to repeat expansion, but rather loss of the encoded FMR protein. This CGG repeat test is among the most frequently ordered genetic tests and is standard of care for any child not meeting developmental milestones. Consequently, the actual diagnostic yield is only 1-2% (Strom et al., 2007). While it is clear that CGG-repeat expansion is the most frequent cause of FXS, more conventional mutations, particularly *FMR1* deletions, have also been reported in FXS (Coffee et al., 2008). Deletions are typically found as an anomaly of the CGG-repeat test or by microarray analysis, and sequencing of *FMR1* is not frequently done. This lack of clinical *FMR1* sequencing is not surprising as it was assumed sequencing would not uncover a significant number of mutations and therefore negatively affected insurance coverage of diagnostic sequencing. The lack of *FMR1* sequence testing has led to a marked deficit of conventional mutations, particularly missense mutations, even though the full mutation is a null allele like many conventional mutations. Indeed, in over two decades since the discovery of *FMR1* only a single missense mutation, isoleucine 304 to asparagine (I304N), has been reported (De Boulle et al., 1993). Here we report a second missense mutation in *FMR1,* glycine 266 to glutamic acid (G266E), leading to FXS. This highlights the clinical utility of *FMR1* sequencing, particularly at a time when gene sequencing is now more affordable and targeted therapeutics for FXS are being developed.

2.3 Methods

2.3.1 Cloning and lentivirus production

Full length human *FMR1* (iso-13 variant that uses second splice acceptor site in exon 17 (Sittler et al., 1996)) with an N-terminal Flag tag was cloned into the BamHI/EcoRI sites of the FUGW lentiviral vector and the c.797G>A (G266E) mutation was introduced using the Quikchange Lightning Site-Directed Mutagenesis Kit (Agilent). Both WT and G266E lentiviral constructs were verified by restriction enzyme digest and sequencing of the *FMR1* insert prior to being sent to the Emory University Viral Vector Core for lentivirus production.

2.3.2 Cell culture

Primary neuron cultures were dissected from WT and *Fmr1* KO mice at embryonic day 16.5 and cultured as described previously (Henderson et al., 2012) in accordance with the Institutional Animal Care and Use Committee guidelines. For imaging experiments, hippocampal neurons were plated at low density (5e3 cells/cm^2) onto poly-L-lysine coated coverslips (1mg/mL) and cocultured with glia. For biochemical experiments, cortical neurons were plated at high density (84e3 cells/cm^2) directly onto poly-L-lysine coated dishes (0.2mg/mL). Immortalized mouse embryonic fibroblasts (MEFs) from *Fmr1* KO mice were cultured in DMEM with 10% FBS.

2.3.3 AMPA receptor trafficking

Hippocampal neurons were transduced with lentivirus at 18 DIV. Six hours post-transduction, live neurons were processed for constitutive AMPA receptor internalization

as described previously (Henderson et al., 2012). For each experimental condition, 30 individual dendrites were analyzed using a one-way ANOVA.

2.3.4 Polyribosome profiling and western blotting

MEFs were plated in T225 flasks (Corning), transduced with lentivirus at approximately 40 to 50% confluency for 16 h, and then collected for polyribosome assay 24 h after virus removal. Immediately before harvest, cells were treated with cycloheximide (100 μg/mL, Acros Organics) for 15 m at 37°C, and then lysed in 20 mM Tris-HCl pH 8.0, 100 mM KCl, 5 mM $MgCl_2$, 0.3% IGEPAL (Sigma), supplemented with EDTA-free complete mini protease inhibitor (Roche), 100 U/mL SUPERaseIn (Ambion), and 100 μg/mL cycloheximide. Lysates were clarified by centrifugation at 13,000 x g for 10 m at 4°C, the supernatants loaded on top of 15−45% w/w linear sucrose gradients containing 20 mM Tris-HCl pH 8.0, 100 mM KCl, 5 mM $MgCl_2$, 20 U/mL SUPERaseIn, and 100 μg/mL cycloheximide, which were made using a Gradient Master 108 (BioComp), and centrifuged at 38,000 rpm (247,600 x g) for 2 h at 4°C using a SW41Ti rotor (Beckman Coulter). After centrifugation, the samples were fractionated into 10 x 1.1 mL fractions by bottom displacement using a Teledyne ISCO fractionator, with continuous monitoring at OD_{254} using an ISCO UA-6 UV detector, and then stored at -80°C.

Prior to western blotting, the samples were thawed on ice and 500 μL of each fraction were concentrated to approximately 40 μL with Amicon Ultra 30K centrifugal filters (Millipore). Concentrated samples were denatured in SDS sample buffer, separated by SDS-PAGE on 4-15% gradient polyacrylamide gels (BioRad), transferred onto nitrocellulose membranes, and probed with primary antibodies against FMRP (1:2000,

MAB2160, Millipore) and S6 ribosomal protein (1:1000, #2317, Cell Signaling Technologies) using standard techniques. Primary antibodies were labeled by HRP conjugated secondary antibody (1:50,000, Millipore) and the enhanced chemiluminescence signal detected using SuperSignal Femto Max Sensitivity Substrate (Thermo Scientific).

2.3.5 RNA co-immunoprecipitation and quantitative RT-PCR

Primary cortical neuron cultures were transduced with lentivirus at 10 DIV for 18 h, and then collected for RNA co-immunoprecipitation (co-IP) 72 h after virus removal. Neurons were lysed in 50 mM Tris-HCl pH 7.5, 300 mM NaCl, 30 mM EDTA, 0.5% Triton X-100 (Sigma), supplemented with complete mini protease inhibitor (Roche), and 100 U/mL SUPERaseIn (Ambion). Lysates were clarified by centrifugation at 20,000 x g for 15 m at 4°C, and the supernatant protein concentrations determined by Bradford assay (BioRad). Equal quantities of protein were used for all input (approximately 150 μg) and IP (approximately 1100 μg) samples within an experiment. For IP, the samples were incubated with EZview Red Anti-Flag M2 Affinity Gel (Sigma) for 2 h at 4°C, washed with the above lysis buffer 4 times, and RNA extracted using Trizol LS (Invitrogen). For input samples, RNA was extracted using TriReagent (Ambion). RNA was then stored at -80°C until processed for quantitative RT-PCR.

Prior to RNA extraction, a portion of both the input and IP samples were saved for Western blotting to verify that lentiviral infection produced equal FMRP expression and pull down across samples. Western blotting was performed as described above with the following exceptions: proteins were transferred onto PDVF membranes, probed with primary antibodies against FMRP (1:500, F4055, Sigma) and β-actin (1:1000, #4970,

Cell Signaling Technologies), labeled by HRP conjugated secondary antibody (1:10,000, Millipore), and the enhanced chemiluminescence signal detected using HyGlo Quick Spray (Denville Scientific). Densitometry was quantified using ImageJ.

For quantitative RT-PCR, 700 ng of total RNA was treated with DNase I (Invitrogen), and reverse transcribed using random hexamers and SuperScript III First Strand Synthesis System for RT-PCR (Invitrogen) according to manufacturer's instructions. PCR was performed with iQ SYBR® Green Supermix (BioRad) and 100 nM of forward and reverse primers (see **Section 2.3.6** for list of primers). mRNA quantification was determined using the standard curve method for relative quantification. A standard curve was established for each primer set, and the relative mRNA level for each input and IP sample was determined after normalizing each sample to its β-actin mRNA level and adjusting for FMRP protein expression level as determined by Western blot densitometry. The ratio between IP:input mRNA quantification was normalized to the WT value for each experiment to allow comparison across different experiments. Data were analyzed by two-way ANOVA with N = 4 for each group.

2.3.6 List of primer sequences

Map1b	for: 5'-CGATCGTGGGACACAAACCT-3' rev: 5'-GTGATCATCAAACGCACCTCA-3'
Psd95	for: 5'-CTATGAGACGGTGACGCAGA-3' rev: 5'-CGGGAGGAGACAAAGTGGTA-3'
CamKII	for: 5'-AATGGCAGATCGTCCACTTC-3' rev: 5'-ATGAGAGGTGCCCTCAACAC-3'

Actb (β-actin)	for: 5'-TGTTACCAACTGGGACGACA-3' rev: 5'-GGGGTGTTGAAGGTCTCAAA-3'

2.4 Results

2.4.1 Identification of a patient with a novel *FMR1* missense mutation (G266E)

The patient was delivered vaginally at 41 weeks gestation without complication and an occipital frontal circumference at 50th percentile. No abnormalities were noted except a bifid uvula. However, by 6 months developmental delay was noticed with walking achieved at 24 months. At age 13, the patient's gross motor skills, visual-motor problem solving, speech and language skills, and general conceptual abilities were all around the 3 – 4 year level. The patient achieved urinary continence at age 15. Examination at age 16 revealed a severely intellectually impaired male. The patient's height was 172.5 cm (45th percentile), weight 52.3 kg (17th percentile), and occipital frontal circumference 56 cm (66th percentile). Ear length was 7.5 cm (>95th percentile). The patient was diagnosed with an autistic spectrum disorder based upon observed or reported difficulty with eye contact, little interaction with peers, little social and emotional reciprocity, no indications of make-believe play, and difficulty with transitions and rituals in activities of daily living. Multiple dysmorphic features were noted (**Figure 2.1A**) including a tall forehead, long face, large ears, hypermobility of the elbows and small joints of the hands, flat feet, several café-au-lait macules, and macroorchidism. In adolescence, the patient began having disruptive outbursts with some aggression, poor attention span and hyperactivity, and was diagnosed with attention deficit with

hyperactivity disorder (ADHD) that responded favorably to treatment with methylphenidate. There is no history of seizures. There is no other family history of developmental disorder in the proband's parents, three brothers and two sisters, or two maternal uncles.

The patient was negative for FXS testing of CGG-repeat length (23 repeats). Karyotype analysis showed normal 46, XY. Array comparative genomic hybridization studies showed no copy number variants, metabolic studies were all within normal limits, and brain MRI was normal. Full sequencing of the patient's *FMR1* gene revealed a guanine to adenine transition at position chrX:g.147014110G>A (NM_002024.5:c.797G>A) leading to a missense mutation at amino acid 266, converting the highly conserved glycine residue to glutamic acid (**Figure 2.1B-C**). The patient's mother is unaffected but found to carry the Gly266Glu mutation, and all three of his unaffected brothers do not carry the mutation. This variant has been submitted to the *FMR1* variant database (http://databases.lovd.nl/shared/genes/FMR1).

2.4.2 Functional analysis of mutant G266E-FMRP

In order to determine if the c.797G>A (G266E) mutation is pathological, we tested the mutation using various established functions of FMRP *in vitro*. One of the penultimate consequences of FMRP loss is exaggerated AMPA receptor internalization (Bassell and Warren, 2008). Cultured mouse hippocampal neurons derived either from wild-type (WT) or *Fmr1* knockout (KO) mice have been shown to exhibit marked differences in AMPA receptor trafficking, with the KO neurons showing significantly greater internalization than WT neurons (Nakamoto et al., 2007). We infected *Fmr1* KO neurons with either WT or G266E-FMRP lentivirus and measured AMPA receptor

internalization. We found that G266E-FMRP was unable to rescue the exaggerated AMPA receptor internalization in KO neurons, indicating that this mutant protein leads to impaired synaptic function (**Figure 2.2A**).

Impaired synaptic function by Gly266Glu suggests that the ability of FMRP to regulate protein synthesis may be defective. A canonical property of this protein in translation is its association with polyribosomes (Stefani et al., 2004). To determine whether G266E-FMRP is able to associate with polyribosomes, we observed the distribution of FMRP in sucrose gradients of lysates from *Fmr1* KO MEFs that were infected with either WT or G266E-FMRP. WT-FMRP showed robust FMRP staining in polyribosome fractions while G266E-FMRP was virtually absent in these fractions (**Figure 2.2B**). Thus, mutant G266E-FMRP is defective in its ability to associate with polyribosomes.

FMRP associates with polyribosomes, in part, due to its selective binding of mRNA (Ashley et al., 1993), and a number of specific targets have been extensively validated (Santoro et al., 2012). In order to determine if G266E-FMRP is able to bind mRNA, we analyzed the relative mRNA levels of three well-characterized FMRP targets in co-immunoprecipitation experiments from WT or G266E-FMRP infected *Fmr1* KO cortical neurons. We found that the relative mRNA enrichment for *Map1B*, *PSD95*, and *CamKII* mRNAs in G266E-FMRP pull down experiments was similar to the background levels from GFP infected negative controls (**Figure 2.2C**). These values were significantly lower than WT-FMRP pull down experiments, indicating that G266E-FMRP is unable to bind known FMRP mRNA targets.

2.4.3 Structural analysis of mutant G266E-FMRP

The Gly266Glu mutation resides within the well-conserved KH1 RNA-binding domain of FMRP. High-resolution crystal structure of FMRP's KH1-KH2 domain is available (Protein Data Bank code 2QND) (Valverde et al., 2007), and indicates that Gly266 is located at the carboxyl end of β-strand 3 which is part of the β-sheet consisting of anti-parallel strands 2, 3, 1 (**Figure 2.3A**). Modeling the glutamic acid substitution at residue 266 introduces a large and negatively charged side chain that clashes into neighboring A271 of the following α-helix C and V250 of β-strand 3 (**Figure 2.3C**). In addition, glutamic acid at 266 would be subject to repulsion forces from the surrounding negatively charged residues, E267 and D268 (**Figure 2.3B**). These data suggest that Gly266Glu mutation will cause significant disruptive structural change consistent with its loss of function in the above functional assays.

2.5 Discussion

We have identified a novel missense mutation in *FMR1* that leads to FXS in the absence of CGG repeat expansion. This marks only the second time a missense mutation has been reported to cause FXS since the identification of the *FMR1* gene over 20 years ago. This single nucleotide substitution, c.797G>A (G266E), was discovered in a male patient with characteristic FXS phenotype.

Several lines of a priori evidence indicate this is a pathologic change. Glycine 266 is highly conserved from human through *Drosophila* and the glutamic acid substitution is judged as damaging by the prediction algorithms SIFT, Polyphen-2, and Provean (0, 1, and -7.53, respectively). Moreover, Gly266, located in the KH1 RNA-binding domain of

FMRP, is found in the invariant β-stand 3 of KH domains in general. Indeed Gly266 is found conserved at position 60 in twelve out of fifteen KH domains from unrelated RNA-binding proteins (Lewis et al., 2000) and a missense mutation of this residue in the *Drosophila* Bicaudal-C protein (Gly295Arg) creates a loss-of-function mutation (Mahone et al., 1995). Structural analysis of the previously determined FMRP KH1-KH2 domain structure (Valverde et al., 2007) also suggests that Gly266Glu is damaging. The sharp turn between β-strand 3 and α-helix C where residue 266 is located requires a relatively small and flexible amino acid, such as glycine. Exchanging this glycine for glutamic acid will almost certainly interfere with normal KH folding due to the substantial steric disturbance that is created by the much larger and negatively charged side chain.

Consistent with a loss-of-function mutation, we have demonstrated that the Gly266Glu missense produces a functional null protein that is unable to perform many key FMRP functions including mRNA binding, polyribosome association, and mGluR mediated AMPA receptor trafficking. We conclude that the loss of these FMRP functions due to Gly266Glu mutation is the basis for the FXS phenotype in this patient.

This report of a Gly266Glu mutation joins the report of the only other pathogenic missense mutation known of FMRP, the Ile304Asn mutation (c.911T>A) reported in a patient in 1993 (De Boulle et al., 1993). One might ask why so few missense mutations have been identified in *FMR1*? This gene does not appear any less mutable than other typical X-linked genes. A recent study sequencing *FMR1* in 963 developmentally delayed males observed 5 silent (synonymous) sites and 2 replacement (nonsynonymous) sites (Collins et al., 2010), which compares favorably with X-linked genome-wide averages of approximately 3.7 silent sites and 2.5 replacement sites (International HapMap et al.,

2007). However, if one examines other X-linked monogenic causes of intellectual disability and/or developmental delay (ID/DD), the small number of *FMR1* missense mutations is striking. For example, there are 143 unique missense mutations of *MECP2*, leading to Rett syndrome (as of 7/2013; Human Gene Mutation Database). These two genes are of comparable size with *FMR1* having 1,896 coding bases and *MECP2* having 1,458 coding bases. The most parsimonious explanation is that the majority of patients presenting with a distinctive Rett syndrome phenotype do, in fact, have *MECP2* mutations, while for FXS this is not true. Indeed, only ~1.4% of patients clinically tested for the full mutation are positive (Strom et al., 2007). Partly this is due to the non-specific and variable phenotype of FXS and that testing for FXS is among the primary tests ordered for any child not reaching developmental milestones, therefore a low positive test rate is expected. Yet missense *FMR1* mutations must exist in the population, perhaps leading to phenotypes that are not usually brought to medical attention, such as children with learning disabilities or who struggle in regular classrooms but not considered intellectually impaired. *FMR1* mutations may also underlie non-specific ID/DD phenotypes without distinctive features to prompt *FMR1* sequencing.

It is clear that mutations of all classes that lead to classic FXS are essentially functional null mutations. The full mutation leads to transcriptional silencing of *FMR1* and is the most common cause of FXS with a prevalence of ~1 in 5,000 males (Coffee et al., 2009). Diagnostic testing for FXS is largely limited to full mutation screening. However, a number of conventional mutations have also been demonstrated to lead to FXS (De Boulle et al., 1993, Coffee et al., 2008). Many *FMR1* deletions have been reported, with most uncovered through absent or unexpected bands on a Southern blot

used to diagnose the full mutation, or by microarray analysis. Nonsense and splice site mutations have also been reported in a limited number of patients (Lugenbeel et al., 1995, Wang et al., 1997, Gronskov et al., 2011). However, the overall prevalence of conventional *FMR1* mutations among children with ID/DD is unclear, as diagnostic laboratories do not currently perform routine *FMR1* sequencing. If one posits that perhaps 1 per 500 males with ID/DD carry a deleterious conventional *FMR1* mutation, not an unreasonable estimate compared to other X-linked ID/DD genes (Tarpey et al., 2009), then the diagnostic yield for FXS testing could be improved by ~14%. Identification of conventional *FMR1* mutations is not only important for genetic counseling, educational and program planning, but also for treatment strategy as mechanism-targeted therapeutics for FXS are increasingly entering clinical trials. Patients with functional null mutations, such as the Gly266Glu patient described above, would be expected to benefit similarly to patients with the full mutation of *FMR1*. In an era where sequencing costs are dropping exponentially, *FMR1* sequencing should now be incorporated into the standard of care for any child presenting with developmental delay as an adjunct to repeat expansion testing. This will require that affordable, easily accessible, and insurance-covered testing be made available to clinicians.

Figure 2.1: Identification of a patient with a novel *FMR1* missense mutation (G266E)

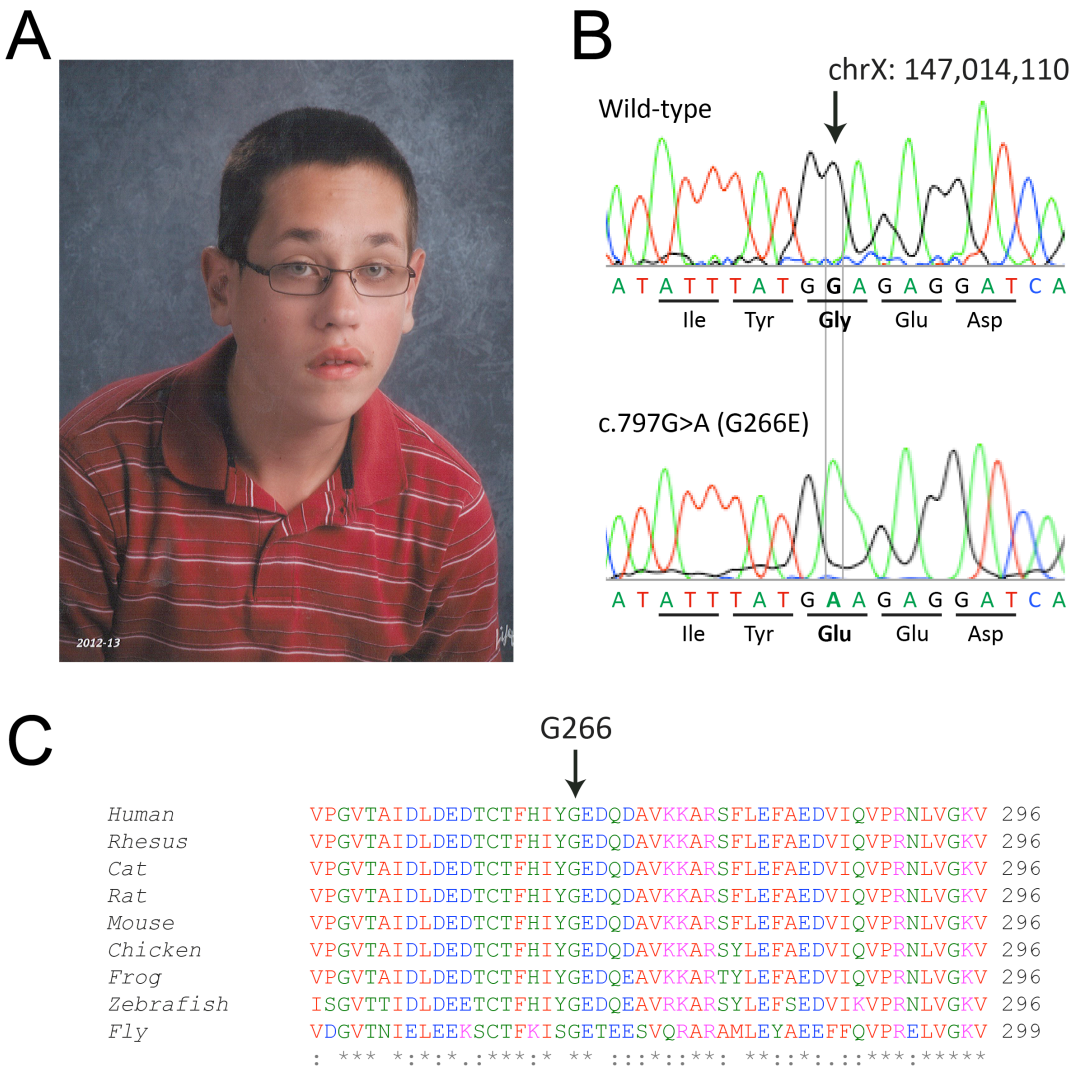

Figure 2.1: Identification of a patient with a novel *FMR1* missense mutation (G266E)

A: Patient's characteristic facial features that are consistent with Fragile X Syndrome, including tall forehead, elongated face, and large ears.

B: DNA chromatogram of the wild-type and patient alleles showing the single nucleotide substitution (NM_002024.5:c.797G>A) that replaces the glycine at residue 266 with glutamic acid (G266E).

C: ClustalW alignment across multiple species of FMRP amino acids 247-296. FMRP at residue 266 is highly conserved from human through *Drosophila*.

Figure 2.2: Functional analysis of mutant G266E-FMRP

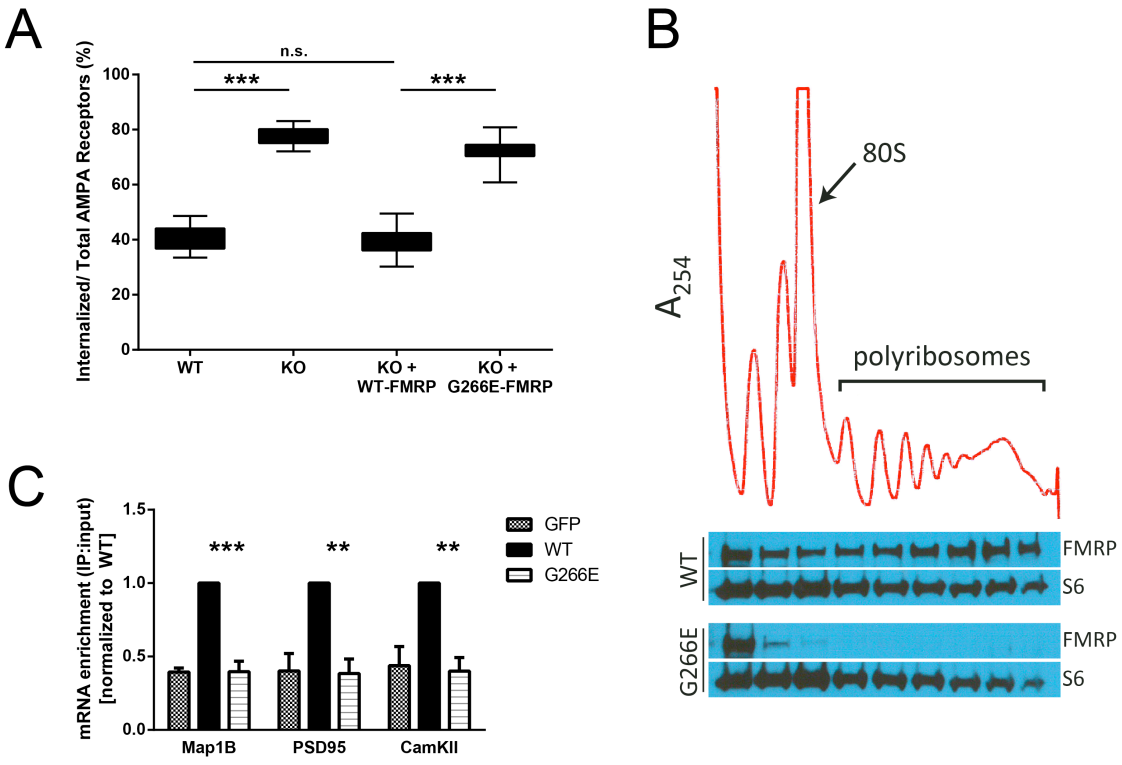

Figure 2.2: Functional analysis of mutant G266E-FMRP

A: Constitutive AMPA receptor assay showing that G266E-FMRP is unable to rescue exaggerated AMPA receptor internalization in KO neurons. Hippocampal neurons from *Fmr1* KO mice were cultured for 18 days, infected with either WT or G266E-FMRP, and the percentage of internalized to total AMPA receptors was calculated from individual dendrites. G266E-FMRP infected neurons were statistically different from WT-FMRP infected neurons (one-way ANOVA; $n = 30$; $F = 609.92$, $p < 0.001$, Tukey post hoc analysis: ***$p < 0.001$ for all pairwise comparisons except WT vs KO+WT-FMRP $p = 0.42$). Because the variance in uninfected KO neurons was so low, G266E-infected neurons were still statistically different from KO neurons even though the mutant protein clearly does not rescue AMPA receptor internalization like WT-FMRP. Data are represented as boxplot with whiskers from minimum to maximum.

B: Polyribosome assay showing that G266E-FMRP does not associate with polyribosome fractions. The top graph is a representative A254 absorbance profile from *Fmr1* KO MEF cells infected with either WT or G266E-FMRP, and the monosome (80S) and polyribosome peaks are indicated. Below is the distribution of FMRP by western blot analysis for each fraction corresponding to the same region of the linear sucrose gradient above. S6 ribosomal protein is also shown to verify sample loading in each well. These are representative blots from $n = 3$ experiments.

C: RNA co-immunoprecipitation showing that G266E-FMRP does not bind three well-validated FMRP targets using qPCR analysis of the relative mRNA enrichment of *Map1B*, *PSD95*, and *CamKII* mRNAs after FMRP immunoprecipitation. Cortical neurons from *Fmr1* KO mice were cultured for 10 days, infected with GFP, WT-FMRP, or

G266E-FMRP lentivirus, and then processed for FMRP-RNA co-immunoprecipitation. The relative mRNA level for each primer set was normalized to each sample's β-actin mRNA and also relative FMRP expression level as determined by western blot densitometry. When mRNA enrichment (IP:input) for WT-FMRP is set to equal 1.0, G266E-FMRP mRNA enrichment drops by 2-fold to the same levels as GFP infected neurons (paired Student's t test; n = 4; t = 16.92, ***p < 0.001 for *Map1B*; t = 12.544, **p = 0.001 for *PSD95*; t = 12.919, **p = 0.001 for *CamKII*). Data are represented as mean ± SD.

Figure 2.3: Structural analysis of mutant G266E-FMRP

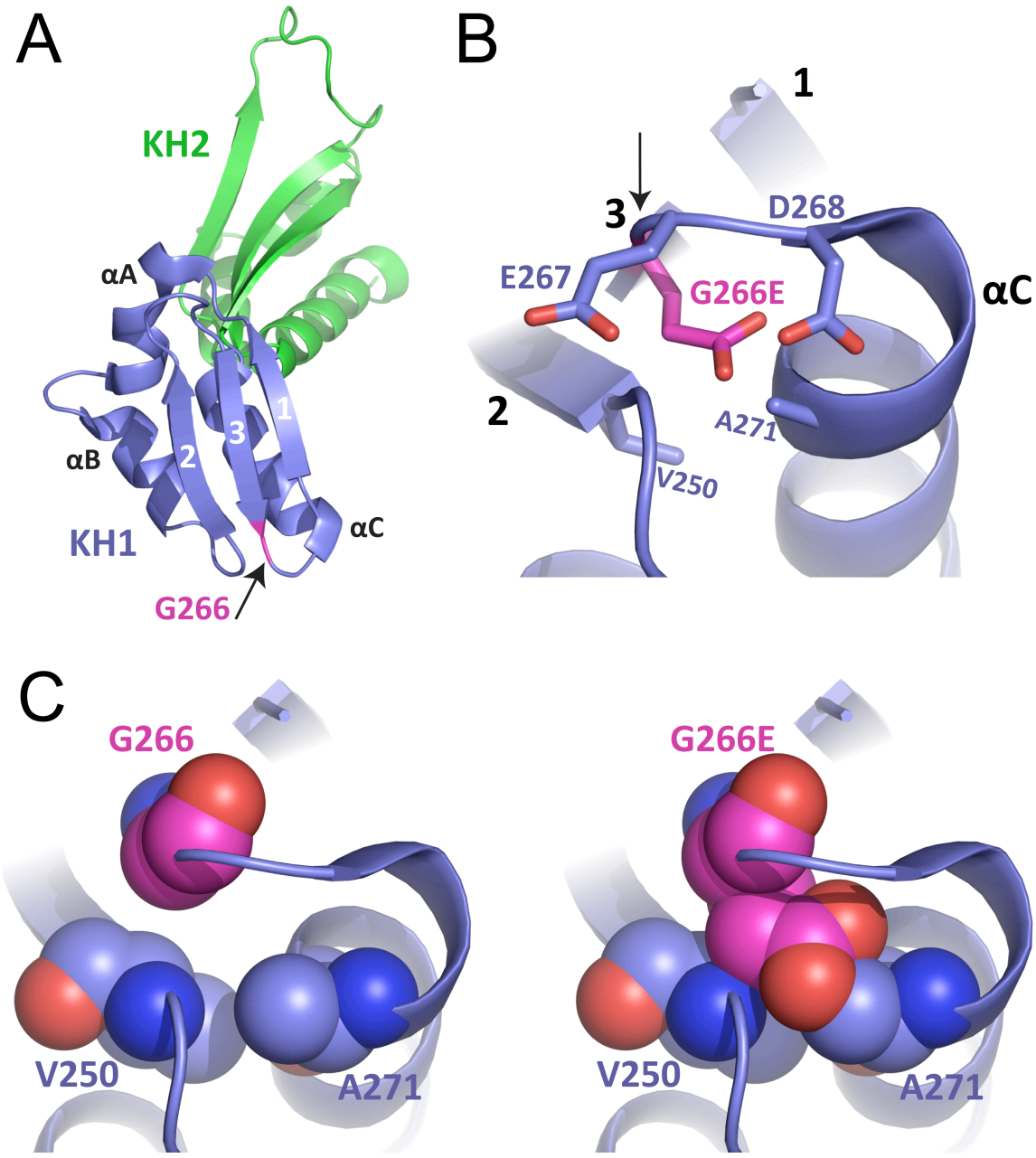

Figure 2.3: Structural analysis of mutant G266E-FMRP

A: Ribbon representation of the FMRP KH1 (blue) and KH2 (green) domains from Protein Data Bank code 2QND. The three β-strands (1, 2, 3) and three α-helices (αA, αB, αC) of KH1 are labeled, and the position of Gly266 is highlighted in pink as indicated by the arrow.

B: Stick representation of residues 266-268 showing the close proximity of three negatively charged amino acids when residue 266 is converted from glycine (neutral) to glutamic acid (negative). Arrow points to residue 266.

C: Sphere representations of glycine (left) or glutamic acid (right) at residue 266. There is high probability for glutamic acid to crash into residues V250 and A271 due to the space constraints predicted by this structural model.

Chapter 3. An independent role for presynaptic FMRP revealed by R138Q *FMR1* missense mutation associated with intellectual disability and seizures[2]

[2] Adapted from Myrick LK, Deng PY, Hashimoto H, Cho Y, Nakamoto-Kinoshita M, Poidevin MJ, Suhl JA, Visootsak J, Cavalli V, Jin P, Cheng X, Warren ST, Klyachko VA. (2014a). An independent role for presynaptic FMRP revealed by an FMR1 missense mutation associated with intellectual disability and seizures. *PNAS* **(in review)**.

Author Contributions: Myrick designed the lentiviral and protein expression constructs, performed the polyribosome association and mRNA binding assays, and purified recombinant FMRP. Deng performed the electrophysiology experiments. Hashimoto assisted with protein purification, Cho performed the binding assay, Nakamoto-Kinoshita performed the AMPAR assay, Poidevin performed the NMJ assays, and Suhl designed the *Drosophila* constructs. Visootsak evaluated the patient.

3.1 Abstract

Fragile X Syndrome (FXS) results in intellectual disability (ID) most often caused by a repeat expansion that silences the *FMR1* gene. The resulting absence of FMRP leads to both pre- and postsynaptic defects, yet whether the pre- and postsynaptic functions of FMRP are independent and have distinct roles in FXS neuropathology remains poorly understood. Here we demonstrate an independent presynaptic function for FMRP through the study of an ID patient with an *FMR1* missense mutation. This FMRP mutation, R138Q, preserves the postsynaptic functions of FMRP in RNA binding and translational regulation. However, neuronally driven expression of the mutant FMRP is unable to rescue neuromuscular junction defects in *dfmr1*$^{-/-}$ *Drosophila*, suggesting a presynaptic impairment. Furthermore, R138Q mutation renders FMRP incapable of rescuing presynaptic action potential broadening in *Fmr1* knockout mice, and disrupts its interactions with BK_{Ca} channels. These results revealed an independent presynaptic FMRP function linked to a specific subset of FXS phenotypes.

3.2 Introduction

Fragile X Syndrome (FXS) is the most common single-gene disorder responsible for intellectual disability (ID) in patients (Santoro et al., 2012). Along with cognitive dysfunction, the syndrome typically presents with several other comorbidities including behavioral and social impairments (anxiety, autism spectrum disorder), neurological defects (seizures, abnormal sleep patterns), and morphological abnormalities (dysmorphic facies, macroorchidism). Most patients inherit the syndrome through a maternal repeat expansion mutation that transcriptionally silences the *FMR1* gene and results in loss of the gene product, FMRP.

FMRP has complex multifaceted functions at synapses both in pre- and postsynaptic compartments. As an RNA binding protein, FMRP is best known for its function as a translation regulator in dendrites (Bassell and Warren, 2008). Loss of FMRP has been linked to various forms of long-term synaptic plasticity defects that depend on local protein synthesis in the postsynaptic neuron (Huber et al., 2002). In addition to disrupted mGluR signaling, which has been shown across multiple brain regions (Todd et al., 2003, Huber, 2006, Wang et al., 2009, Suvrathan et al., 2010), FMRP is also necessary for activity-dependent protein synthesis downstream of other signaling receptor pathways, including acetylcholine, dopamine, and TrkB (Volk et al., 2007, Wang et al., 2008, Osterweil et al., 2010).

While postsynaptic control of translation is believed to be the dominant function of FMRP, it is unable to explain all of the pathophysiology observed in FXS animal models. For instance, in *Drosophila*, presynaptic expression of the *FMR1* homolog, *dfmr1*, completely rescues the synaptic overgrowth phenotype at the neuromuscular

junction (NMJ) in *dfmr1* null mutants (Zhang et al., 2001, Pan et al., 2004, Gatto and Broadie, 2008). In mosaic *Fmr1* mice, the presynaptic presence of FMRP is sufficient to rescue synaptic connectivity defects in the hippocampal circuit (Hanson and Madison, 2007), and FMRP regulation of neurotransmitter release at excitatory hippocampal and cortical synapses has been shown to be cell-autonomous and translation-independent (Deng et al., 2013, Patel et al., 2013).

Both the pre- and postsynaptic functions of FMRP have also been linked to neuronal and circuit hyperexcitability in FXS animal models. Consistent with its role as a protein synthesis regulator, FMRP regulates the expression of a number of dendritic voltage-gated K+ channels in various brain circuits (Strumbos et al., 2010, Gross et al., 2011, Lee et al., 2011). In addition to translational regulation, FMRP has also been shown to influence neural excitability by directly modulating activity of a number of presynaptic voltage-gated ion channels. For example, FMRP interacts with the sodium-activated potassium channel, Slack, to directly control gating (Brown et al., 2010, Zhang et al., 2012), and directly interacts with the N-type voltage-gated calcium channel, $Ca_v2.2$, to control their surface expression (Ferron et al., 2014). FMRP also modulates activity of the large conductance, calcium-activated potassium channel, BK_{Ca}, in hippocampal and cortical excitatory neurons, which are critical for controlling action potential (AP) duration and neurotransmitter release (Deng et al., 2013). FMRP interacts with the regulatory β4 subunit of the BK_{Ca} channel to increase channel Ca^{2+} sensitivity and limit AP duration and neurotransmitter release. In brain slices from *Fmr1* KO mice, the absence of FMRP leads to excessive AP broadening, which can be acutely rescued with intracellular perfusion of an amino-terminal FMRP fragment containing amino acids

1-298 into the presynaptic neuron. These effects are independent of translation, suggesting a distinct presynaptic function of FMRP unrelated to translational control. Yet to what extent the functions of FMRP in pre- and postsynaptic compartments independently contribute to FXS neuropathology remains unknown. Moreover, the multitude and complexity of FMRP functions has made it difficult thus far to establish the link between specific FMRP functions and phenotypes in patients.

Distinguishing the roles of specific FMRP functions in FXS phenotypes could in principle be possible if partial loss-of-function mutations were found within the population that contributed to a limited subset of FXS phenotypes. However, to date only two missense mutations have been reported to cause FXS, and both mutations result in functional null forms of FMRP that phenocopy transcriptionally silenced repeat expansion mutations (De Boulle et al., 1993, Zang et al., 2009, Myrick et al., 2014c).

Here we studied the synaptic deficits associated with the *FMR1* missense mutation, c.413G>A (R138Q), which was recently identified in a screen of developmentally delayed males that were negative for repeat expansion (Collins et al., 2010). The identified patient has a history of intellectual disability and intractable seizures, but had no other features commonly associated with FXS. We show that R138Q is a partial loss-of-function mutation that specifically impairs presynaptic FMRP function while preserving postsynaptic translation regulation capabilities of FMRP. Postsynaptically, R138Q-FMRP is able to regulate normal AMPA receptor trafficking, as well as retain normal polyribosome association and mRNA binding functions. However, in *dfmr1* deficient *Drosophila*, neuronally driven expression of R138Q-FMRP is unable to rescue synaptic overgrowth at the NMJ, indicative of presynaptic deficits. In *Fmr1* KO

mice, R138Q-FMRP is unable to rescue AP broadening defects in hippocampal and cortical pyramidal neurons. Furthermore, biochemical studies revealed that R138Q mutation disrupts FMRP's interaction with BK_{Ca} channels, which mediate the effect of FMRP loss on AP duration. Together, these results suggest distinct functions for FMRP between pre- and postsynaptic compartments, and that a specific *FMR1* mutation linked to a limited subset of FXS phenotypes is associated with isolated loss of presynaptic function.

3.3 Methods

3.3.1 Patient description

The patient was born full-term without complication, but was hospitalized for five days immediately after birth for feeding and respiratory problems as well as to receive phototherapy for jaundice. No further complications were experienced until 1 month of age when the patient suffered non-accidental trauma, developed seizures immediately after the event, and was diagnosed with shaken baby syndrome. The MRI and CT were negative for any gross abnormalities at the time. At 18 months, the patient experienced another seizure episode that was associated with fever. At 24 months, the patient experienced a third seizure episode, without any precipitating event, and was started on - Trileptal anti-seizure medication. From age 2 to 8 years, the patient continued to have episodes of complex partial seizures every 3 to 4 months, with about 12 seizures per day for 2 to 3 days at a time. The seizures did not localize or lateralize to any particular brain region and remained uncontrolled despite treatment with multiple antiepileptic medications. The patient was consequently diagnosed with intractable unclassified

epilepsy; however, he is currently taking Trileptal and has not had any seizure episodes for the past 2.5 years.

In addition to epilepsy, the patient also has a history of developmental delay and intellectual disability. Some early motor developmental milestones were met, such as rolling over and sitting without support, though walking independently was not achieved until 18 months (mildly delayed). By 8 years, the patient had poor handwriting skills, could not write his name or numbers, and could not use utensils to feed himself. His language developmental milestones were also delayed as he did not speak his first words until 12 months, did not combine words until 3 years, and did not form complete sentences until 7 years. Cognitive function was formally tested twice at approximately 8 years of age, revealing a full scale IQ of 42 (moderately impaired function) by the Stanford-Binet Intelligence Scales, 5th edition and an IQ of 71 (mild intellectual disability) by the Kaufman Brief Intelligence Test, 2nd edition. The Vineland Adaptive Behavior Scales, 2nd edition and the Child Behavior Checklist were also conducted and found that the patient did not display any maladaptive behaviors commonly associated with FXS or autism, such as stereotypic behaviors, hyperactivity, impulsivity, physical aggressiveness, difficulty with changes or transitions, or problems with sleeping or eating. Currently, the patient is in 7th grade special education class and reading at the kindergarten level.

On physical exam, the patient is a non-dysmorphic male with height and weight in 25th percentile, head circumference in 95th percentile (mildly macrocephalic), and ears in 75th-95th percentile range. The patient did not display an elongated face, prominent

forehead or jaw (**Figure 3.1A**), macroorchidism, or any other dysmorphic feature commonly associated with FXS, except for one café-au-lait spot on his lower left chest.

There is a family history of learning problems on both the maternal and paternal sides (**Figure 3.1B**). The patient's father attended special education classes throughout childhood, with disabilities in reading and writing. He did not complete the 10th grade. The patient's mother completed 12th grade, however she had significant difficulty throughout school and also has a history of anxiety. The patient's maternal grandfather, now deceased, also had learning problems as a child and was only able to complete middle school. The mother was the only family member available for genetic testing and she was found to be a carrier of the c.413G>A (R138Q) mutation, indicating maternal transmission.

3.3.2 Constructs

For lentivirus production, full length human *FMR1* (iso-13 variant that uses second splice acceptor site in exon 17 (Sittler et al., 1996)) with an N-terminal Flag tag was cloned into the BamHI/EcoRI sites of the FUGW lentiviral vector and the c.413G>A (R138Q) mutation was introduced using the Quikchange Lightning Site-Directed Mutagenesis Kit (Agilent). WT and R138Q mutant lentiviral constructs were verified by restriction enzyme digest and sequencing of the *FMR1* insert prior to being sent to the Emory University Viral Vector Core for lentivirus production.

For *Drosophila* transgene injection, we first excised the *dfmr1* coding sequence from the pUAST-*dfmr1* vector by double restriction digest with EcoRI-HF and XbaI, and ligated this fragment into the TOPO v2.1 vector backbone with the same digested ends using the Takara DNA ligation kit (Takara). The *Drosophila* equivalent to the human

R138Q mutation requires two nucleotide substitutions, c.419_420delinsAG (R140Q), and they were introduced using the Quikchange Lightning Site-Directed Mutagenesis Kit (Agilent). Mutated *dfmr1*-R140Q was then excised from the TOPO vector by EcoRI-HF and XbaI, ligated back into the pUAST vector, and confirmed by sequencing of the *dfmr1* insert.

For protein expression, constructs were sent to the Emory Custom Cloning Core Facility for cloning. Truncated WT and R138Q human *FMR1* (residues 1-298) were cloned into the NdeI/BamHI sites of a modified pET28b expression vector (Novagen) harboring an upstream 6xHis-Smt3 (yeast SUMO) between the NcoI/NdeI sites. The 6xHis-SUMO-*FMR1* fusion constructs were verified by sequencing the *FMR1* insert. For binding assay experiments, an additional 6xHis tag was inserted between the SUMO and *FMR1* sequences to generate 6xHis-SUMO-6xHis-*FMR1*.

3.3.3 Animals

For cell culture experiments, control (C57BL/6J, Jackson Laboratory, stock #664) and *Fmr1* KO mice (generated on the same background), were housed and maintained according to the Emory University Institutional Animal Care and Use Committee guidelines. For electrophysiology, *Fmr1* KO (FVB.129P2-*Fmr1*^{tm1Cgr}/J; stock #4624) and control (FVB.129P2-*Pde6b*$^{+}$*Tyr*$^{c\text{-}ch}$/AntJ; stock #4828) mice were housed and maintained according to the Washington University Animal Studies Committee guidelines.

3.3.4 Cell culture

Immortalized mouse embryonic fibroblasts (MEFs) were generated from *Fmr1* KO mice and maintained in culture with DMEM (Corning) supplemented with 10% FBS (HyClone).

Primary cortical neuronal cultures were generated from embryonic day 16.5 *Fmr1* KO mice. Cortices were dissected in Hibernate E without Ca^{2+} (BrainBits), digested in 2mg/mL papain (Worthington Biochemical), and the dissociated neurons plated at 8.4e4 cells/cm^2 directly onto poly-L-lysine coated (0.2mg/mL) 100mm dishes in Adhesion media: 1X MEM (Gibco) supplemented with 10% FBS (HyClone), 30mM glucose, and 10mM HEPES. After 4 h to 6 h, Adhesion media was replaced with Neurobasal media (Gibco) supplemented with B27 (Invitrogen) and Glutamax (Invitrogen).

3.3.5 AMPA receptor trafficking

Constitutive AMPA receptor internalization assay (Nakamoto et al., 2007) with R138Q-FMRP lentiviral infection has been previously reported (Alpatov et al., 2014) and the raw data re-analyzed and re-formatted here. Approximately 34 individual dendrites were measured for each group and data were analyzed by one-way ANOVA with Tukey post hoc analysis.

3.3.6 Polyribosome profiling and western blotting

MEFs were plated in T225 flasks (Corning), transduced with lentivirus at approximately 40 to 50% confluency for 16 h, and then collected for polyribosome assay 24 h after virus removal. Immediately before harvest, cells were treated with cycloheximide (100 μg/mL, Acros Organics) for 15 m at 37°C, and then lysed in 20 mM

Tris-HCl pH 8.0, 100 mM KCl, 5 mM $MgCl_2$, 0.3% IGEPAL (Sigma), supplemented with EDTA-free complete mini protease inhibitor (Roche), 100 U/mL SUPERaseIn (Ambion), and 100 μg/mL cycloheximide. Lysates were clarified by centrifugation at 13,000 x g for 10 m at 4°C, the supernatants loaded on top of 15−45% w/w linear sucrose gradients containing 20 mM Tris-HCl pH 8.0, 100 mM KCl, 5 mM $MgCl_2$, 20 U/mL SUPERaseIn, and 100 μg/mL cycloheximide, which were made using a Gradient Master 108 (BioComp), and centrifuged at 38,000 rpm (247,600 x g) for 2 h at 4°C using a SW41Ti rotor (Beckman Coulter). After centrifugation, the samples were fractionated into 10 x 1.1 mL fractions by bottom displacement using a Teledyne ISCO fractionator, with continuous monitoring at OD_{254} using an ISCO UA-6 UV detector, and then stored at -80°C. Prior to western blotting, the samples were thawed on ice and 500 μL of each fraction were concentrated to approximately 40 μL with Amicon Ultra 30K centrifugal filters (Millipore). Concentrated samples were denatured in SDS sample buffer, separated by SDS-PAGE on 4-15% gradient polyacrylamide gels (BioRad), transferred onto nitrocellulose membranes, and probed with primary antibodies against FMRP (1:2000, MAB2160, Millipore) and S6 ribosomal protein (1:1000, #2317, Cell Signaling Technologies) using standard techniques. Primary antibodies were labeled by HRP conjugated secondary antibody (1:50,000, Millipore) and the enhanced chemiluminescence signal detected using SuperSignal Femto Max Sensitivity Substrate (Thermo Scientific).

3.3.7 RNA co-immunoprecipitation and quantitative RT-PCR

Primary cortical neuron cultures were transduced with lentivirus at 10 DIV for 18 h, and then collected for RNA co-immunoprecipitation (co-IP) 72 h after virus removal.

Neurons were lysed in 50 mM Tris-HCl pH 7.5, 300 mM NaCl, 30 mM EDTA, 0.5% Triton X-100 (Sigma), supplemented with complete mini protease inhibitor (Roche), and 100 U/mL SUPERaseIn (Ambion). Lysates were clarified by centrifugation at 20,000 x g for 15 m at 4°C, and the supernatant protein concentrations determined by Bradford assay (BioRad). Equal quantities of protein were used for all input (approximately 150 μg) and IP (approximately 1100 μg) samples within an experiment. For IP, the samples were incubated with EZview Red Anti-Flag M2 Affinity Gel (Sigma) for 2 h at 4°C, washed with the above lysis buffer 4 times, and RNA extracted using Trizol LS (Invitrogen). For input samples, RNA was extracted using TriReagent (Ambion). RNA was then stored at -80°C until processed for quantitative RT-PCR.

Prior to RNA extraction, a portion of both the input and IP samples were saved for Western blotting to verify that lentiviral infection produced equal FMRP expression and pull down across samples. Western blotting was performed as described above with the following exceptions: proteins were transferred onto PDVF membranes, probed with primary antibodies against FMRP (1:500, F4055, Sigma) and β-actin (1:1000, #4970, Cell Signaling Technologies), labeled by HRP conjugated secondary antibody (1:10,000, Millipore), and the enhanced chemiluminescence signal detected using HyGlo Quick Spray (Denville Scientific). Densitometry was quantified using ImageJ.

For quantitative RT-PCR, 700 ng of total RNA was treated with DNase I (Invitrogen), and reverse transcribed using random hexamers and SuperScript III First Strand Synthesis System for RT-PCR (Invitrogen) according to manufacturer's instructions. PCR was performed with iQ SYBR® Green Supermix (BioRad) and 100 nM of forward and reverse primers (see **Section 3.3.13** for list of primers). mRNA

quantification was determined using the standard curve method for relative quantification. A standard curve was established for each primer set, and the relative mRNA level for each input and IP sample was determined after normalizing each sample to its β-actin mRNA level and adjusting for FMRP protein expression level as determined by Western blot densitometry. The ratio between IP:input mRNA quantification was normalized to the WT value for each experiment to allow comparison across different experiments. Data were analyzed by two-way ANOVA with N = 5, 4, 3, and 2 for GFP, WT, R138Q, and G266E groups respectively.

3.3.8 *Drosophila* neuromuscular junction immunostaining and analysis

All flies were maintained under standard culture conditions on Cornmeal-molasses-yeast medium at 25°C. Transgenic *dfmr1* WT and R140Q mutant flies were generated by standard P-element transgene injection (Bestgene Inc) into a w^{1118} strain, and then crossed with either Da-GAL4 or Elav-GAL4 lines (Bloomington Stock Center, #8641 and #458 respectively).

To perform immunostaining of the NMJ, third stage wandering larvae were harvested, washed, and dissected in PBS (Ca^{2+} free) as described (Brent et al., 2009). Dissected larvae were fixed for 1 h on ice with 4% paraformaldehyde, followed by permeabilization at room temperature with 3-4 x 10 min washes using 0.3% PTX (PBS + 0.3% Triton X-100). Tissues were then blocked for 30 min to 1 h with 0.1% PTX + 5% normal goat serum, incubated overnight at 4°C with anti-discs large primary antibody (Developmental Studies Hybridoma Bank, 4F3), washed 3 x 5 min with 0.1% PTX, and labeled for 1-2 h with Alexa Fluor® 488 anti-mouse secondary antibody (Invitrogen, A-11001). Tissues were then mounted onto slides using Vectashield (Vector Laboratories),

and NMJ length and number of branches were measured from micrographs taken of muscles 6/7 of abdominal segment 2 or 3 using Axiovision software (Zeiss). Approximately 30 larvae were analyzed per genotype.

3.3.9 Electrophysiology slice preparation

Both male and female 15- to 25-day-old mice were used. Genotyping was performed according to the Jackson Laboratory protocols. All animal procedures conformed to the guidelines approved by the Washington University Animal Studies Committee. After being deeply anesthetized with CO_2, mice were decapitated and their brains were dissected out in ice-cold saline solution that contained the following: 130 mM NaCl, 24 mM $NaHCO_3$, 3.5 mM KCl, 1.25 mM NaH_2PO_4, 0.5 mM $CaCl_2$, 5.0 mM $MgCl_2$, and 10 mM glucose, pH 7.4 (saturated with 95% O_2 and 5% CO_2). Horizontal brain slices (350 μm) including the hippocampus were cut using a vibrating microtome (Leica VT1200S). Slices were initially incubated in the above solution at 35°C for 1 h for recovery and then kept at room temperature until use.

3.3.10 Action potential recordings and analysis

APs were recorded using an Axopatch 700B amplifier (Molecular Devices) in whole-cell configuration from hippocampal CA3 pyramidal neurons or Layer 5 pyramidal neurons in the entorhinal cortex visually identified with infrared video microscopy (Olympus BX50WI; Dage-MTI) and differential interference contrast optics. All the recordings were conducted at near-physiological temperature (33–34°C). The recording electrodes were filled with the following: 130 mM K-gluconate, 0.5 mM EGTA, 2 mM $MgCl_2$, 5 mM NaCl, 2 mM ATP_2Na, 0.4 mM GTPNa, and 10 mM HEPES,

pH 7.3. The extracellular solution contained the following: 130 mM NaCl, 24 mM $NaHCO_3$, 3.5 mM KCl, 1.25 mM NaH_2PO_4, 2 mM $CaCl_2$, 1 mM $MgCl_2$, and 10 mM glucose, pH 7.4 (saturated with 95% O_2 and 5% CO_2). APV (50 μM), DNQX (10 μM) and gabazine (5 μM) were included in the perfusate to block the effect of synaptic transmission on AP properties and long-term effects. APs were evoked by repetitive injection of a 1-ms current to evoke 25-AP train at 60 Hz. Membrane potential was set at -65 mV by automatic slow current injection to ensure stability of the resting potential and to prevent spontaneous AP firing. Each AP train was evoked four to six times in each neuron, and each train was separated by ~2-min rest periods. AP duration during bursts was normalized to an averaged duration of four low- frequency baseline APs (0.2 Hz) evoked before each burst.

Recordings were filtered at 2 kHz, digitized at 20 kHz, acquired using custom software written in LabView, and analyzed using programs written in Matlab. Data are presented as mean ± SEM. Student's paired or unpaired t test or ANOVA were used for statistical analysis as appropriate; p values are reported throughout the text, and significance was set as $p < 0.05$.

3.3.11 Protein expression and purification

All proteins were expressed as 6xHis-SUMO fusion proteins to facilitate protein expression and purification. WT and R138Q FMRP fragments (residues 1-298), with or without an additional 6xHis tag immediately amino-terminal to FMRP, were expressed in *E.coli* BL21 (DE3)-Gold cells with the RIL-Codon plus plasmid (Stratagene). Cultures were first grown at 37°C in LB supplemented with 50 μg/mL Kanomycin until OD_{600}

reached between 0.4-0.8. The temperature was then shifted to 16°C and protein expression was induced with 0.4 mM isopropyl β-D-1-thiogalactopyranoside (IPTG) for 16 h. Cells were harvested and resuspended in 4 volumes of 300 mM NaCl, 20 mM sodium phosphate pH 7.4, 20 mM imidazole, 1 mM dithiothreitol (DTT), and 0.3 mM phenylmethyl-sulphonyl fluoride, and then lysed using sonication for 5 min (1 s on, 2 s off), followed by centrifugation at 38,000g for 1 h. The fusion proteins were isolated on a nickel charged HiTrap Chelating column (GE Healthcare), eluted with 500 mM imidazole, and the 6xHis-SUMO tag removed by overnight incubation with Ulp1 protease at 4°C. The cleaved proteins were then diluted with 6 volumes of 20 mM HEPES pH 7.0 and 1 mM DTT, loaded over a HiTrap-Q column (GE Healthcare), and eluted at ~170-280 mM NaCl with a linear gradient of 100 mM to 800 mM NaCl. Fractions containing the FMRP fragments were pooled together, and concentrated using Spin-X UF 30k MWCO concentrators (Corning). The proteins were then loaded onto a Superdex 75 (16/60) column that was pre-equilibrated with 200 mM NaCl, 20 mM HEPES pH 7.0, and 1 mM DTT. The fractions containing purified FMRP fragment were pooled together, concentrated to 100 μM, and stored in aliquots at -80°C.

3.3.12 Binding Assay

Whole mouse brain was dissected and transferred to a dounce homogenizer containing 5 mL lysis buffer on ice (50 mM HEPES, pH 7.4, 300 mM NaCl, 1% Triton X-100, supplemented with protease and phosphatase inhibitors). After homogenization, brain lysates were clarified by centrifugation at 14000 rpm for 1 hr at 4°C. Supernatants were then pre-cleared to reduce non-specific binding by incubation with HisPur Cobalt Resin (Pierce) for 1 hr at 4°C. Beads were removed and total protein concentration was

determined by BCA method. 100 µg of His-tagged WT-$FMRP_{298}$ or R138Q-$FMRP_{298}$ fragments were incubated with 1 mg of lysate with rotation for 4 hr – overnight at 4°C. HisPur Cobalt Resin (Pierce) was then added and incubated for 1 hr at 4°C, followed by centrifugation at 2000 rpm for 1 min. Beads were washed five times with washing buffer (50 mM HEPES, pH 7.4, 500 mM NaCl, 1% Triton X-100, 10 mM imidazole), denatured with 1X SDS PAGE loading buffer, and processed for western blotting by standard techniques.

3.3.13 List of primer sequences

Map1b	for: 5'-CGATCGTGGGACACAAACCT-3' rev: 5'-GTGATCATCAAACGCACCTCA-3'
Psd95	for: 5'-CTATGAGACGGTGACGCAGA-3' rev: 5'-CGGGAGGAGACAAAGTGGTA-3'
CamKII	for: 5'-AATGGCAGATCGTCCACTTC-3' rev: 5'-ATGAGAGGTGCCCTCAACAC-3'
Actb (β-actin)	for: 5'-TGTTACCAACTGGGACGACA-3' rev: 5'-GGGGTGTTGAAGGTCTCAAA-3'

3.4 Results

3.4.1 Identification of ID patient with R138Q missense mutation

In a previous sequencing study of 963 developmentally delayed males, we identified a patient with an R138Q missense mutation in the *FMR1* gene without the

CGG-repeat expansion (Collins et al., 2010). This patient has a history of global developmental delay, intellectual disability, and intractable seizures, but no other behavioral, neurological, or dysmorphic features commonly associated with FXS (**Figure 3.1A**). Molecular FXS testing showed 45 CGG repeats, which is within the normal range (Fu et al., 1991), however full sequencing of the patient's *FMR1* gene revealed a c.413G>A transition that causes the highly conserved arginine (R) 138 residue to be replaced by glutamine (Q) (**Figures 3.1C-D**). Both maternal and paternal sides of the family have a history of learning problems, however this mutation was passed through the mother who was found to be a carrier of the c.413G>A (R138Q) mutation (**Figure 3.1B**). For a full patient description and clinical history, see Methods **Section 3.3.1**.

3.4.2 R138Q mutation does not affect postsynaptic functions of FMRP

To test the functional significance of the R138Q missense mutation, we first assayed whether this mutation impairs FMRP's established role as a protein synthesis regulator. In hippocampal neurons, postsynaptic AMPA receptor trafficking is influenced by FMRP-mediated control of local protein synthesis such that, in the absence of FMRP, there is exaggerated AMPA receptor internalization (Muddashetty et al., 2007, Nakamoto et al., 2007). To determine if the R138Q mutation affects FMRP's ability to regulate AMPA receptor trafficking, we measured AMPA receptor internalization in *Fmr1* KO mouse hippocampal neurons that were infected with either R138Q-FMRP or WT-FMRP lentivirus. We found that AMPA receptor internalization in R138Q-FMRP infected neurons was not significantly different from wild-type (WT) neurons or WT-FMRP infected *Fmr1* KO neurons, although *Fmr1* KO neurons alone were significantly different from all the other groups as expected (**Figure 3.2A**; one-way ANOVA; $F = 451.9$, $p <$

0.0001, Tukey post hoc analysis: **** $p < 0.0001$ for all pairwise comparisons with KO group). Since regulation of AMPA receptor trafficking is a function of FMRP's ability to control protein synthesis, this finding suggests that R138Q-FMRP retains its canonical function of regulating mRNA translation.

In line with its role as a protein synthesis regulator, FMRP is known to bind polyribosomes and specific mRNA targets (Stefani et al., 2004, Santoro et al., 2012). To determine if R138Q-FMRP can bind polyribosomes, we infected *Fmr1* KO mouse embryonic fibroblasts (MEFs) with R138Q-FMRP or WT-FMRP lentivirus and probed for FMRP distribution after sucrose gradient fractionation. We found that R138Q-FMRP is robustly present in polyribosome fractions, similar to WT-FMRP (**Figure 3.2B**). To determine if R138Q-FMRP can bind mRNA, we infected *Fmr1* KO cortical neurons with R138Q-FMRP or WT-FMRP lentivirus and performed FMRP-RNA co-immunoprecipitation (co-IP) to measure the relative mRNA levels of three validated FMRP targets: *Map1B*, *PSD95*, and *CamKII* (Santoro et al., 2012). We found R138Q-FMRP associated with these targets to a similar level as WT-FMRP, while neurons infected with the functional null G266E-FMRP mutant (Myrick et al., 2014c), or GFP alone, did not pull down these mRNAs and were significantly different from WT-FMRP as expected (**Figure 3.2C**; two-way ANOVA with significant main effect of lentivirus infection; $F = 66.57$, $p < 0.0001$, Dunnett's post hoc analysis: * $p < 0.0001$ for pairwise comparison with WT-FMRP control group for each mRNA target.) Together, these data indicate that the R138Q mutation does not impair FMRP's postsynaptic function as a translation regulator as evidenced by rescue of AMPA receptor trafficking, intact polyribosome association, and mRNA pull-down.

3.4.3 R140Q mutation impairs presynaptic function in *Drosophila*

The preservation of FMRP's canonical function as a protein synthesis regulator in the above biochemical studies led us to consider that the R138Q mutation might simply be a rare benign variant without any functional consequences. To further test this possibility, the function of R138Q-FMRP was assessed in an animal model. *Drosophila* provides a uniquely powerful system for studying FMRP function because there is only a single ortholog from the fragile X-related gene family, *dfmr1* (Wan et al., 2000), and therefore subtle phenotypes are more likely to be revealed due to loss of compensatory action from the fragile-x related proteins, FXR1 or FXR2. The *Drosophila* equivalent to the R138Q mutation is R140Q according to ClustalW alignment (**Figure 3.1D**).

One particularly robust phenotype is the overelaboration of synaptic branching and number of boutons at the NMJ in *dfmr1* null flies (Zhang et al., 2001). To determine if R140Q-FMRP is able to rescue synaptic overgrowth at the *Drosophila* NMJ, we used Da-Gal4 to drive ubiquitous expression of UAS-*dfmr1* R140Q in *dfmr1* deficient *Drosophila*. To our surprise, we found that R140Q-FMRP was unable to rescue overgrowth of NMJ length or branching, unlike WT-FMRP (**Figure 3.3B**). Since these NMJ structural defects are known to be a function of presynaptic FMRP (Gatto and Broadie, 2008), we also used Elav-Gal4 to drive pan-neuronal expression of UAS-*dfmr1* R140Q in *dfmr1* deficient *Drosophila*. We found that presynaptic specific expression of R140Q-FMRP was also unable to rescue overgrowth of NMJ length or branching, unlike WT-FMRP (**Figure 3.3C**; one-way ANOVA for NMJ length, branching; $F = 272.5$, 68.32, $p < 0.0001$, Tukey's post hoc analysis: **** $p < 0.0001$ for comparison with *dfmr1* −/−). Quantitative PCR for *dfmr1* on whole larvae show two to three fold higher

expression of R140Q-FMR1 compared to WT-FMR1 (**Figure 3.3D**), indicating that the lack of rescue in NMJ overgrowth was not due to inadequate R140Q-FMRP expression.

3.4.4 R138Q mutation impairs presynaptic function in mouse central neurons

To validate the presynaptic specific loss-of-function we observed with R138Q-FMRP in *Drosophila*, we sought to corroborate these findings within a mammalian system. We previously discovered that FMRP modulates AP duration via BK_{Ca} channels in hippocampal and cortical excitatory neurons in a cell-autonomous presynaptic manner (Deng et al., 2013). We showed that excessive AP broadening in *Fmr1* KO neurons can be acutely rescued with presynaptic intracellular perfusion of a commercially available amino-terminal FMRP fragment consisting of amino acids 1-298, and importantly, that these effects were independent of translation. To determine if R138Q-FMRP can rescue AP broadening in *Fmr1* KO neurons, we created and purified the same amino-terminal FMRP fragment consisting of amino acids 1-298, with and without the R138Q mutation (R138Q-$FMRP_{298}$ and WT-$FMRP_{298}$, respectively). We then performed AP rescue experiments in current-clamped CA3 hippocampal pyramidal cells in acute slices from 15- to 17-day-old *Fmr1* KO mice. AP trains were evoked by repetitive injection of a 1-ms current to evoke a 25-AP train at 60 Hz. FMRP fragment was introduced into the cells via a patch pipette using a micro-perfusion system that permitted us to control the exact time point at which perfusion was initiated. Only recordings in which AP duration could be recorded before and after FMRP fragment perfusion were used in this analysis. As in our previous studies, perfusion of WT-$FMRP_{298}$ into CA3 neurons of *Fmr1* KO mice rapidly rescued excessive AP broadening, at both baseline and during the train (**Figure 3.4A**, N = 6, P = 0.012 for baseline APs, P = 0.007 for the averaged last 2 APs in the train). In

contrast, intracellular perfusion of R138Q-$FMRP_{298}$ fragment was unable to reduce AP broadening in these neurons (**Figure 3.4B**, N = 6, P = 0.40 (baseline AP), P= 0.44 (end of train)). We note that the rescue effect of WT FMRP fragment was measurable within ~5 minutes after perfusion initiation. Together with the fact that the $FMRP_{298}$ fragment lacks the KH2 domain critical for association with polyribosomes, this rapid rescue provides further support for our earlier findings that the mechanism of these presynaptic FMRP actions is translation-independent. These results indicate that the R138Q mutation disrupts FMRP's ability to regulate AP duration in a presynaptic neuron.

We have previously shown that FMRP regulation of AP duration is a widespread phenomenon observed both in excitatory hippocampal and cortical neurons. We thus tested whether inability of R138Q-$FMRP_{298}$ to rescue AP broadening defect in *Fmr1* KO mice is also observed in cortical pyramidal neurons. AP measurements were performed in 15- to 17-day-old, Layer 5 cortical pyramidal neurons of the entorhinal cortex of *Fmr1* KO mice using the same intracellular perfusion approach described above. Similarly to hippocampal neurons, intracellular perfusion of WT-$FMRP_{298}$ rapidly reduced AP broadening in cortical pyramidal neurons, while perfusion of R138Q-$FMRP_{298}$ did not have a significant effect (**Figures 3.4C-D**; WT: N = 6, P = 0.015 (baseline), P= 0.028 (end of train); R138Q: N = 7, P= 0.69 (baseline), P= 0.72 (end of train)). These results support the above evidence that the R138Q mutation disrupts the presynaptic function of FMRP to regulate AP duration in both hippocampal and cortical pyramidal neurons.

3.4.5 R138Q mutation disrupts FMRP interaction with BK_{Ca} channels

What is the mechanism by which R138Q mutation renders FMRP incapable of regulating AP duration? We have previously shown that FMRP regulates AP duration

and neurotransmitter release in excitatory pyramidal neurons through FMRP's interaction with the BK_{Ca} channels, particularly their regulatory β4 subunit (Deng et al., 2013). The above observations therefore suggest that R138Q mutation may interfere with FMRP/BK_{Ca} channel interactions. To test this possibility, we used an in vitro binding assay in which His-tagged WT-$FMRP_{298}$ or R138Q-$FMRP_{298}$ fragments were used to pull-down BK_{Ca} channels from brain lysates prepared from WT mice. WT-$FMRP_{298}$ fragment interacted with the BK_{Ca} channel β4 subunit (**Figure 3.5**) in agreement with our previous observations (Deng et al., 2013) and revealed that FMRP-β4 interaction is mediated by the FMRP amino-terminus. In contrast to WT-$FMRP_{298}$, we observed no detectable β4 subunit association with R138Q-$FMRP_{298}$ (**Figure 3.5**, N = 4). We also observed binding of the BK_{Ca} channel α subunit with WT-$FMRP_{298}$, and this interaction was reduced for R138Q-$FMRP_{298}$ (**Figure 3.5**, N = 4). These results suggest that R138Q mutation strongly affects FMRP interaction with the BK_{Ca} channels, with nearly complete loss of interaction with the BK_{Ca} β4 subunit.

We note that an earlier study suggested that FMRP does not interact with the BK_{Ca} channel α subunit in heterologous cells (Brown et al., 2010). Because our current results indicate that FMRP interacts with both BK_{Ca} α and β4 subunits in neurons, we further tested whether FMRP interaction with BK_{Ca} α subunit requires β4, using β4 KO mice. When FMRP was IP-ed from the brain lysate of β4 KO mice and tested for BK_{Ca} α subunit, we detected a strong interaction, suggesting the FMRP can interact with BK_{Ca} α subunit in the absence of β4. These results provide further confirmation that FMRP interacts independently with both α and β4 subunits of BK_{Ca} channels, and the R138Q mutation weakens interactions with both BK_{Ca} channel α and β4 subunits.

3.5 Discussion

3.5.1 Summary of results

The pathophysiology of FXS is complex, involving both pre- and postsynaptic defects. Yet the interdependence and specific contributions of pre- and postsynaptic FMRP functions to various FXS phenotypes has been difficult to determine. Through the study of a novel *FMR1* missense mutation, R138Q, we have demonstrated that FMRP plays an important presynaptic role that is independent from its canonical postsynaptic function in mRNA translation. Our experiments indicate that R138Q mutation retains the postsynaptic translation regulation capabilities of FMRP, but is incapable of rescuing presynaptic structural defects at the *dfmr1* deficient *Drosophila* NMJ, nor rescuing presynaptic AP broadening defects in *Fmr1* KO mouse central neurons. Furthermore, we found that R138Q mutation strongly reduces FMRP's ability to interact with the BK_{Ca} channels that mediate FMRP's regulation of AP duration and glutamate release. The finding that R138Q is a partial loss-of-function mutation that abolishes specifically presynaptic but not postsynaptic FMRP function is consistent with the patient's limited FXS phenotype consisting of ID and seizures, but not any other symptoms commonly associated with FXS. Taken together, these results suggest that pre- and postsynaptic functions of FMRP are independent, and link the isolated loss of presynaptic FMRP function with a specific subset of FXS clinical features.

3.5.2 Insights into FXS pathophysiology from *FMR1* missense mutations

To date, there have only been two other reported missense mutations within *FMR1*, G266E (Myrick et al., 2014c) and I304N (De Boulle et al., 1993). Both of these mutations reside within the RNA binding domains of FMRP and result in loss of RNA binding and polyribosome association (Zang et al., 2009, Myrick et al., 2014c). Studies of these mutations provide strong evidence that FMRP's inability to regulate protein synthesis is a critical component of FXS pathophysiology given that both of these patients presented with very characteristic FXS phenotype including marked ID, developmental delay, macroorchidism, and dysmorphic facies. Conversely, the R138Q mutation does not reside within an RNA binding domain, but rather is located at the amino-terminal domain of FMRP. In contrast with the G266E and I304N patients, the R138Q patient only displays ID and seizures, which corresponds well with our observation that R138Q is a partial loss-of-function mutation. These results suggest that presynaptic FMRP function may be specifically connected to ID and seizure pathology in FXS, possibly through the amino-terminal domain.

3.5.3 BK_{Ca} channel dysfunction in ID and seizures

We have previously shown that FMRP binds to and modulates the activity of BK_{Ca} channels in order to regulate AP duration and neurotransmitter release (Deng et al., 2013). These functions are abolished by the R138Q mutation, thereby potentially linking FMRP and BK_{Ca} channel modulation to the ID and seizure phenotype exhibited by the R138Q patient. BK_{Ca} channels have in fact already been linked to ID and seizures separately in several previous reports. For instance, an autistic patient with severe ID was found to have a balanced translocation resulting in disruption of the KCNMA1 gene that

encodes the BK_{Ca} channel (Laumonnier et al., 2006). Dysregulation of BK_{Ca} channel isoform expression has also been linked to a mild form of autosomal recessive nonsyndromal mental retardation (Higgins et al., 2008). Probably the most compelling evidence comes from another report showing that the SNPs with the highest risk for ASD were found in *KCNMB4*, the gene encoding the β4 subunit of the BK_{Ca} channel (Skafidas et al., 2014).

BK_{Ca} channels have also been implicated in epilepsy and seizure disorders in numerous cases both through loss-of-function and gain-of-function mechanisms (N'Gouemo, 2011). Since BK_{Ca} channels play a critical role in repolarizing the membrane potential after AP firing, loss of BK channel function typically results in increased seizure susceptibility (Hu et al., 2001, Faber and Sah, 2003). In line with this, pharmacological inhibition of BK_{Ca} channels trigger seizures (Young et al., 2003), down-regulation of BK_{Ca} channel expression is associated with the development of temporal lobe epilepsy in rats (Ermolinsky et al., 2008, Pacheco Otalora et al., 2008), and a particular *KCNMB4* SNP is strongly correlated with temporal lobe epilepsy in humans (Cavalleri et al., 2007). Interestingly, some gain-of-function mutations in BK channels have also been implicated in seizure etiology, primarily absence epilepsy, by rapidly repolarizing the membrane and allowing for faster firing rates (Brenner et al., 2005, Du et al., 2005). Nevertheless, BK_{Ca} channel activity is clearly intimately connected with seizure pathology. In fact, presynaptic BK_{Ca} channels have recently been shown to preferentially localize to and regulate neurotransmitter release at glutamatergic, but not GABAergic, synapses, further supporting their critical role in modulating circuit hyperexcitability (Martire et al., 2010). Whether FMRP-BK_{Ca} channel interactions are

directly responsible for seizure and/or ID phenotypes, and whether targeting BK_{Ca} channels could be a useful component of FXS therapy remains to be determined.

3.5.4 Amino-terminal domain and FMRP function

Our studies suggest that this translation-independent presynaptic function of FMRP, abolished by the R138Q mutation, depends on an intact amino-terminal domain. Indeed, an amino-terminal fragment of FMRP (1-298) was sufficient to rescue excessive AP broadening in *Fmr1* KO cortical and hippocampal neurons as well as mediate FMRP binding with BK_{Ca} channel subunits. This 298 amino acid fragment is comprised of the FMRP amino-terminal domain (1-215) in addition to the full KH1 and a small portion of the KH2 RNA-binding domains. While we cannot rule out the possibility that FMRP's presynaptic function may be mediated by the KH1 domain, it is highly unlikely given that we have previously shown the presynaptic effects of FMRP on AP duration and glutamate release are independent of translation and therefore unlikely to involve any RNA binding domain function (Deng et al., 2013). Furthermore, we have shown that R138Q mutation does not disrupt FMRP's RNA binding ability, yet does impair presynaptic FMRP function at the *Drosophila* NMJ and in mouse cortical and hippocampal neurons. Thus we propose that the amino-terminal domain mediates FMRP's presynaptic function, yet the exact locus that is responsible for FMRP's modulation of AP duration or interaction with BK_{Ca} channels will require further studies.

The FMRP amino-terminal domain also mediates interaction of FMRP with a number of its binding partners (Siomi et al., 1996, Bardoni et al., 1999, Schenck et al., 2001, Bardoni et al., 2003), and also contains two tandem Tudor/Agenet motifs (Maurer-Stroh et al., 2003, Ramos et al., 2006) that mediate a nuclear FMRP function in

chromatin binding and DNA damage response (Alpatov et al., 2014). Interestingly, the R138Q mutation also abolished nucleosome binding, indicating this mutation may play a role in the pathophysiology of FXS through transcriptional changes (Alpatov et al., 2014). We are currently in the process of testing whether FMRP's ability to regulate AP duration involves transcription. Regardless, our work suggests a novel function for the amino-terminal domain of FMRP in the pathophysiology of FXS by modulating AP duration in a cell-autonomous presynaptic manner and presumably contributing to circuit hyperexcitability via interactions with the BK_{Ca} channels. In summary, our study of a novel missense mutation in *FMR1*, associated with a limited subset of FXS clinical features, provides a first step in teasing out the domain specific functions of FMRP in pre- and postsynaptic compartments, and their contribution to various elements of FXS pathophysiology.

Figure 3.1: Identification of ID patient with R138Q missense mutation

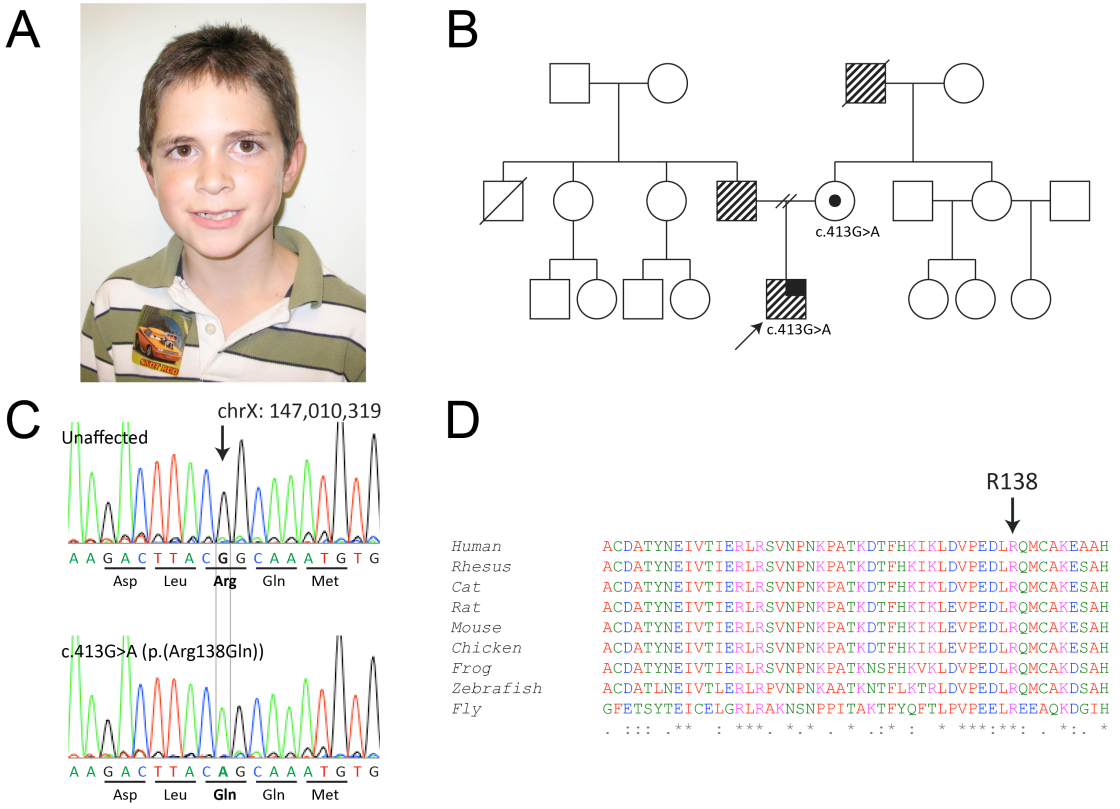

Figure 3.1: Identification of ID patient with R138Q missense mutation

A: Patient's does not have any dysmorphic facial features commonly associated with Fragile X Syndrome. Note the absence of an elongated face, prominent forehead, or large ears.

B: Family pedigree of the proband (indicated by arrow). Stripe pattern indicates learning disability and solid black indicates seizure disorder. The proband's mother was found a carrier of the c.413G>A (R138Q) mutation. No other family members were available for genetic testing.

C: DNA chromatogram of the wild-type and patient alleles showing the single nucleotide substitution (NM_002024.5:c.413G>A) that replaces the arginine at residue 138 with glutamine (R138Q).

D: ClustalW alignment across multiple species of FMRP amino acids 98-147. FMRP at residue 138 is highly conserved from human through *Drosophila*.

Figure 3.2: R138Q mutation does not affect postsynaptic functions of FMRP

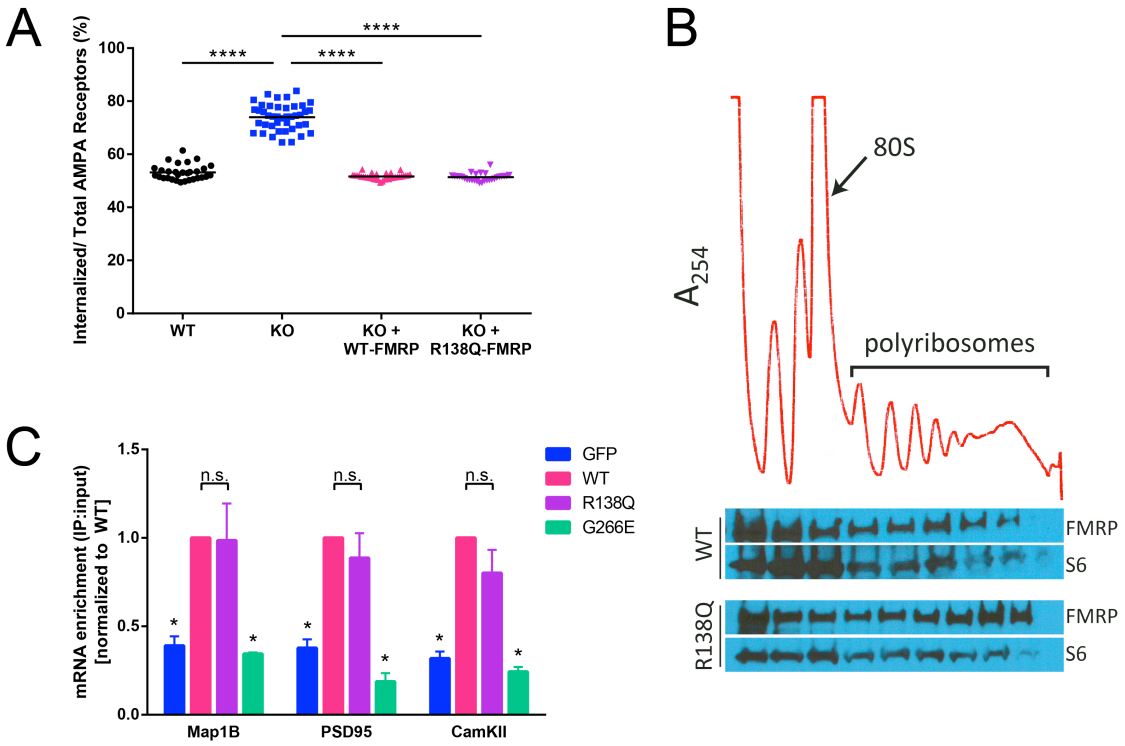

Figure 3.2: R138Q mutation does not affect postsynaptic functions of FMRP

A: Constitutive AMPA receptor assay indicating the percentage of internalized to total AMPA receptors measured from *Fmr1* KO hippocampal neurons that were infected with either WT or R138Q-FMRP. R138Q-FMRP infected neurons were not statistically different from WT neurons or WT-FMRP infected *Fmr1* KO neurons. The data are represented as scatter plot, with bars indicating the mean, and have been re-analyzed and re-formatted from (Alpatov et al., 2014). **** $p < 0.0001$ for pairwise comparisons with KO group.

B: Polyribosome assay on *Fmr1* KO MEF cells infected with either WT or R138Q-FMRP. Top graph is a representative A254 absorbance profile with the monosome (80S) and polyribosome peaks indicated. Below is the FMRP protein distribution showing that R138Q-FMRP associates with polyribosome fractions similar to WT-FMRP. Each fraction corresponds to the same region of the linear sucrose gradient above it. S6 ribosomal protein is shown to verify sample loading in each well. These are representative blots from N = 3 experiments.

C: RNA co-IP on *Fmr1* KO cortical neurons infected with GFP, WT-FMRP, R138Q-FMRP, or G266E-FMRP. The relative mRNA enrichment of FMRP targets *Map1B*, *PSD95*, and *CamKII* were analyzed by qPCR and show that R138Q-FMRP is able to pull down mRNA similar to WT-FMRP, while both negative controls, GFP and G266E-FMRP, did not significantly pull down mRNA. Data are represented as mean ± SEM, * $p < 0.0001$ for pairwise comparisons with WT-FMRP group.

Figure 3.3: R140Q mutation impairs presynaptic function in *Drosophila*

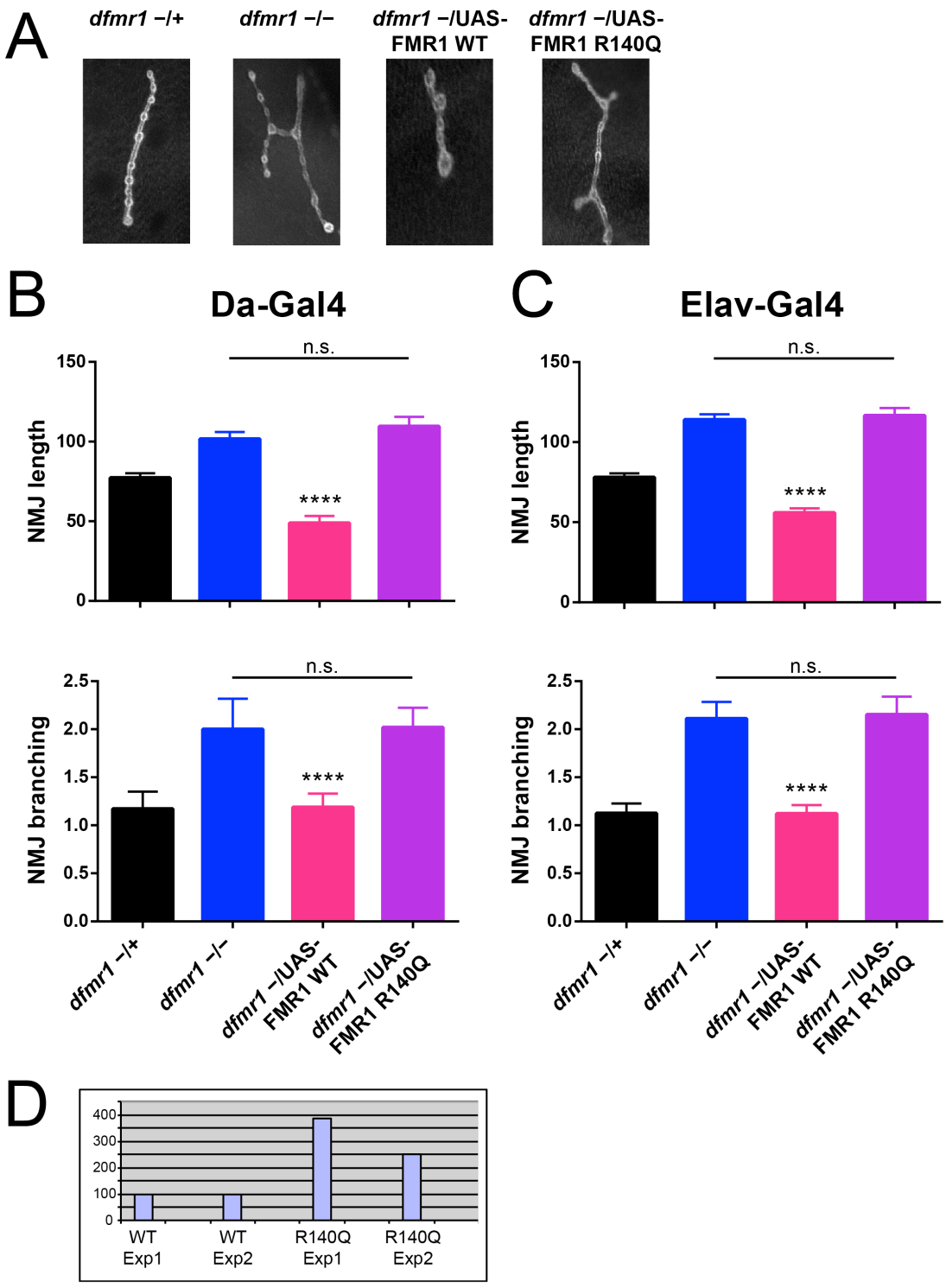

Figure 3.3: R140Q mutation impairs presynaptic function in *Drosophila*

A: Representative micrographs of the NMJ in *dfmr1* heterozygous wild-type flies (*dfmr1*−/+, indistinguishable from homozygous wild-type), *dfmr1* deficient mutants (*dfmr1* −/−), and *dfmr1* deficient mutants with either UAS-FMR1-WT or -R140Q (*Drosophila* equivalent of R138Q) driven expression. Note the higher branch number and longer NMJ length in UAS-FMR1-R140Q expressing flies.

B-C: Quantification of NMJ length and branching in *dfmr1* deficient flies with either ubiquitous (Da-Gal4, panel B) or neuronal (Elav-Gal4, panel C) expression of WT or R140Q FMRP. WT FMRP expression effectively reduces both NMJ length and branching, while R140Q fails to do so and has synaptic overgrowth similar to *dfmr1* deficient flies. Data are represented as mean ± 95% confidence interval, **** $p < 0.0001$ for comparison with *dfmr1* −/−.

D: *dfmr1* levels were measured from whole larvae in Elav-Gal4 driven UAS-FMR1-WT or -R140Q flies. R140Q mutants expressed *dfmr1* at equal or higher levels than WT, indicating the lack of rescue in NMJ length or branching was not due to inadequate R140Q-FMRP expression.

Figure 3.4 R138Q mutation impairs presynaptic function in mouse central neurons

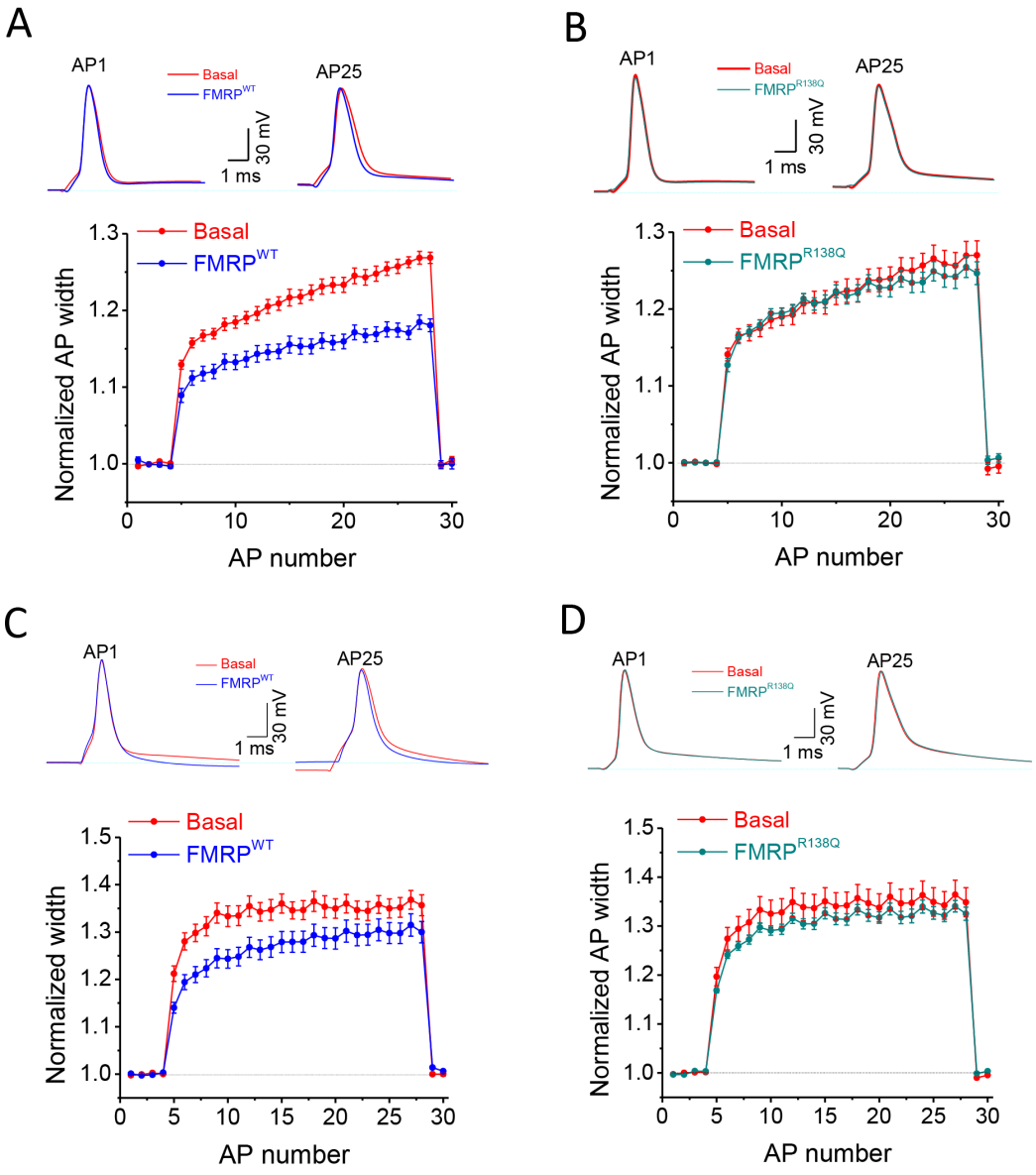

Figure 3.4 R138Q mutation impairs presynaptic function in mouse central neurons

AP trains were recorded from *Fmr1* KO mice in response to 25 stimuli at 60 Hz. The AP duration during each burst was normalized to the baseline AP duration determined from four low frequency stimuli (0.2 Hz) prior to each train.

A-B: Effect of intracellular perfusion of WT-$FMRP_{298}$ (A) or R138Q-$FMRP_{298}$ (B) on AP duration in *Fmr1* KO CA3 pyramidal neurons. WT-$FMRP_{298}$ rescues AP broadening (N = 6, p = 0.007), while R138Q-$FMRP_{298}$ does not have a significant effect (N = 6, p = 0.44).

C-D: Effect of intracellular perfusion of WT-$FMRP_{298}$ (C) or R138Q-$FMRP_{298}$ (D) on AP duration in *Fmr1* KO cortical pyramidal neurons. WT-$FMRP_{298}$ again rescues AP broadening (N = 6, p = 0.028), while R138Q-$FMRP_{298}$ does not have a significant effect (N = 7, p = 0.72).

Figure 3.5: R138Q mutation disrupts FMRP interaction with BK_{Ca} channels

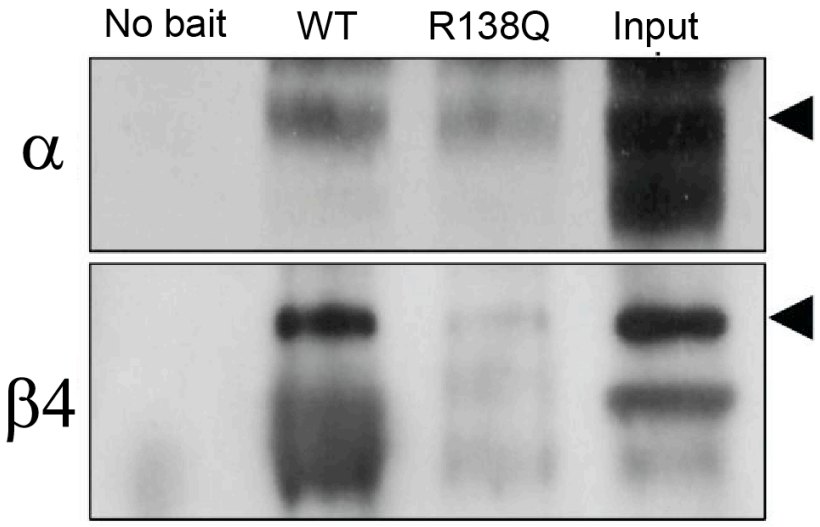

Figure 3.5: R138Q mutation disrupts FMRP interaction with BK_{Ca} channels

In vitro binding assay with His-tagged WT-$FMRP_{298}$ or R138Q-$FMRP_{298}$. Brain lysates from WT mice were incubated with His-tagged protein fragments, or no bait as control, and protein interactions with the FMRP fragments were pulled down using His resin. Samples were processed for SDS-PAGE followed by western blotting with antibodies against the BK_{Ca} channel α and β4 subunits. R138Q-$FMRP_{298}$ has no detectable association with β4 subunit and reduced association with the α subunit as well. These are representative blots from N = 4 experiments. Arrowheads indicate specific protein bands.

Chapter 4. Crystal structure of wild-type and R138Q mutant FMRP amino terminal domain[3]

[3] Adapted from Myrick LK, Hashimoto H, Cheng X, Warren ST. (2014b). FMRP contains an integral tandem Agenet (Tudor) and KH motif in the amino terminal domain. *Hum Mol Genet* **(in review)**.

Author Contributions: Myrick designed the protein expression constructs, purified protein, set up crystallization trays, and assisted with data collection. Hashimoto collected diffraction data and solved the structure using molecular replacement.

4.1 Abstract

Fragile X syndrome, a common cause of intellectual disability and autism, is due to mutational silencing of the *FMR1* gene leading to the absence of its gene product, FMRP. FMRP is a selective RNA-binding protein owing to two central KH domains and a C-terminal RGG box. However, several properties of the FMRP amino terminus are unresolved. It has been documented for over a decade that the amino terminus has the ability to bind RNA despite having no recognizable functional motifs. Moreover, the amino terminus has recently been shown to bind chromatin and influence the DNA damage response as well as function in the presynaptic space, modulating action potential duration. We report here the amino terminal crystal structures of wild-type FMRP, and a mutant (R138Q) that disrupts the amino terminus function, containing an integral tandem Agenet and discover a novel KH motif.

4.2 Introduction

Fragile X Mental Retardation Protein (FMRP) is an RNA binding protein that is responsible for regulating local protein synthesis within dendritic synapses (Bassell and Warren, 2008). Loss of FMRP results in fragile X syndrome (FXS), which is the most frequent inherited cause of intellectual disability (ID), and also one of the leading genetic causes of autism spectrum disorder (ASD) (Santoro et al., 2012).

Since the discovery of FMRP over 20 years ago, many insights about the functions of this protein have been gleaned by studying its various structural domains. For instance, FMRP has three RNA binding domains that include two centrally-located KH domains (KH1 and KH2) and a C-terminal RGG box (**Figure 4.1A**) (Ashley et al., 1993). These domains allow FMRP to bind and regulate the translation of a specific subset of mRNA targets involved in synaptic plasticity (Brown et al., 2001, Darnell et al., 2011). Tightly controlled local protein synthesis is important for many forms of synaptic plasticity, and in the absence of FMRP, defects in these protein-synthesis dependent synaptic plasticity pathways contribute significantly to the pathophysiology of FXS (Huber et al., 2002, Volk et al., 2007, Wang et al., 2008, Osterweil et al., 2010). Indeed, the only two *FMR1* missense mutations in patients presenting with FXS have been substitutions within the KH domains, illustrating the importance of FMRP's RNA binding domains in the pathophysiology of FXS (De Boulle et al., 1993, Myrick et al., 2014c).

The amino terminus of FMRP (defined here as amino acids 1-215) has been largely understudied and there are still many pending questions about its exact *in vivo* functions. It is the site for most of FMRP's protein-protein interactions, including

NUFIP1, 82-FIP, and CYFIP1/2 (Bardoni et al., 1999, Schenck et al., 2001, Bardoni et al., 2003), however the biological role of these protein interactions with FMRP are not well understood. Recently, an additional interaction between the FMRP amino terminus and the presynaptic BK channel β4 subunit has been demonstrated to modulate action potential duration, potentially linking the amino terminal domain with FMRP's presynaptic function (Deng et al., 2013). Moreover, it had been known for many years that FMRP shuttles between the nucleus and cytoplasm through its nuclear localization and export sequences (NLS and NES, respectively) (Eberhart et al., 1996). However, a clear nuclear function for FMRP had not been able to be specified until recently when nuclear FMRP was found to interact with chromatin and modulate the DNA damage response via its two amino terminal Agenet domains, also known as tandem Tudor domains (Alpatov et al., 2014). Interestingly, a patient missense mutation within the amino terminal domain, R138Q, disrupts both BK channel and chromatin binding (Alpatov et al., 2014, Myrick et al., 2014a, in preparation).

Of particular interest is how the FMRP amino terminal domain binds RNA. As early as 15 years ago, the FMRP amino terminus was demonstrated capable of binding to RNA homopolymers, even though this region did not contain any recognizable RNA binding motifs (Adinolfi et al., 1999, Adinolfi et al., 2003, Yan and Denman, 2011). Furthermore, brain cytoplasmic RNA BC1, and its primate analog BC200, have been shown to specifically bind the FMRP amino terminus and this interaction requires residues 180-217 (Zalfa et al., 2003, Zalfa et al., 2005). The subject of FMRP-BC1 RNA interaction has been quite controversial over the past 10 years and still remains unresolved. Several studies were unable to replicate BC1 and FMRP interaction (Wang et

al., 2005, Iacoangeli et al., 2008), while others have successfully replicated the interaction (Gabus et al., 2004, Johnson et al., 2006, Yan and Denman, 2011, Lacoux et al., 2012) but not the requirement of the amino terminus (Yan and Denman, 2011). Some insight comes from a recent attempt to molecularly model the BC1 RNA interaction with the FMRP amino terminal NMR structure of the first 134 residues (Lacoux et al., 2012). BC1 RNA was shown to interact with specific residues within Agenet2 on FMRP, and while these interactions were necessary, they were not sufficient for FMRP-BC1 RNA interaction. It was proposed that the complete RNA binding surface for BC1 interaction would require the downstream residues adjacent to the tandem Agenet domain, however structural data for FMRP between residues 135 – 215 was unavailable. Here we show the wild-type and R138Q mutant crystal structures of FMRP amino terminal fragment (residues 1-202). In addition to the expected Agenet domains, we surprisingly discovered a novel KH motif immediately preceding the KH1 and KH2 domains, which we have termed KH0. This previously unrecognized KH fold might contribute to this regions ability to bind RNA and could potentially resolve some unanswered questions about the functions of the FMRP amino terminal domain.

4.3 Methods

4.3.1 Protein expression and purification

We initially generated hexahistidine-SUMO-tagged constructs of human FMRP residues 1-234 and residues 1-298, for both wild-type (WT) and R138Q mutant. We performed proteolytic digestion on purified 1-234 fragment and found that trypsin generated a stable ~30 kDa protein (see below). The molecular mass was determined by

MALDI-TOF-MS, which corresponds to an FMRP protein fragment of residues 1-213, which was the construct used for crystallization.

The proteins were expressed in *E. coli* BL21 (DE3)-Gold cells with the RIL-Codon plus plasmid (Stratagene). Cultures were grown at 37 °C until the OD600 nm reached 0.5; the temperature was then shifted to 16 °C, and isopropyl β-D-1-thiogalactopyranoside (IPTG) was added to 0.4 mM to induce expression. After 16 h, cells were re-suspended with 4 volumes of 300 mM NaCl, 20 mM sodium phosphate, pH 7.4, 20 mM imidazole, 1 mM dithiothreitol (DTT) for wild-type or 0.5 mM tris(2-carboxyethyl)phosphine (TCEP) for R138Q, and 0.3 mM phenylmethyl-sulphonyl fluoride. The cells were sonicated for 5 min (1 s on and 2 s off) and the lysates clarified by centrifugation at 38,000g for 1 h. Hexahistidine fusion proteins were isolated on a nickel-charged HiTrap chelating column (GE Healthcare) and the His-SUMO tag was removed by incubating with Ulp1 for 16 h at 4 °C. The cleaved protein was further purified by HiTrap Q column (GE Healthcare) and eluted by increasing NaCl concentration from 0.1 to 1 M. The proteins were then loaded onto a Superdex 75 (16/60) column (equilibrated with 200 mM NaCl, 20 mM HEPES, pH 7.0, 1 mM DTT or 0.5 mM TCEP) where it eluted at ~75 mL as a single peak corresponding to a monomeric protein. We increased NaCl concentration up to 500 mM during protein concentration.

4.3.2 Protease digestion and mass spectrometry

FMRP 1-234 protein (4 μg) in 20 mM HEPES, pH 7.0, 200 mM NaCl, and 1 mM DTT was treated with serial dilutions of trypsin, chimotrypsin, and elastase for final protease conditions of 0, 0.1, 1, 10 and 100 ng/μL. Digestion occurred for 30 min at room temperature before being separated on a 12% SDS gel. Trypsin was found to form stable

cleavage product of the FMRP 1-234 protein and was used for further analysis by MALDI-TOF-MS. To prepare samples for MALDI, FMRP 1-234 protein was again digested with trypsin at 0, 1, and 10 ng/μL, for 30 min at room temperature. 1 μL of sinapic acid (dissolved in equal volumes of 0.1% TFA and acetonitrile) and 1 μL of digested protein were mixed together and spotted onto a MALDI plate and allowed to air dry overnight before determining the respective masses of the uncut and cut proteins by MALDI-TOF-MS using a Burker Ultra FlexII TOF/TOF instrument (Biochemistry Department, Emory University).

4.3.3 Crystallography

Crystallization was carried out in a 2 μL sitting drop with equal volumes of protein solution (40-60 mg/mL) and well solution. Crystals appeared within 16 h at 16 °C under the conditions of 27% (w/v) polyethylene glycol 3350, 0.2M ammonium sulfate, 0.1 M HEPES, pH 7.0, for wild-type crystal, and 25%-30% polyethylene glycol monomethyl ether 5000, 0.2M ammonium sulfate, 0.1M HEPES, pH 7.5 and 5 mM of $(CH_3)_3PbOAc$. Crystals were cryoprotected by soaking in mother liquor supplemented with 20% (v/v) ethylene glycol and by plunging into liquid nitrogen. X-ray diffraction data sets were collected at the SER-CAT beamline at the Advanced Photon Source, Argonne National Laboratory and processed using HKL2000 (Otwinowski et al., 2003).

We combined molecular replacement (PDB: 3O8V) and single anomalous diffraction (SAD) to obtain crystallographic phases using Pb containing R138Q crystals. A data set was collected at 100 K at a wavelength of 0.94390 Å, at a slightly higher energy (100 eV) than the Lead (Pb) absorption edge. Anomalous signal originally seemed to extend to only about 7.4 Å, but after combination with the partial model from

molecular replacement results, figure of merit and experimental phases were improved, and the resulting electron density map for KH0 domain was easily visible and the model was built using the program COOT (Emsley et al., 2010). Finally, PHENIX scripts (Adams et al., 2010) were used for model refinement against the native wild-type data and R138Q mutant data (**Table 4.1**), respectively, with an optimized weight for the X-ray target and the stereochemistry of the atomic displacement parameters during the last refinement cycles.

The secondary structure matching (SSM) script in COOT generated initial pair wise alignments, followed by visual inspections, between structures of FMRP 1-213 wild-type (PDB: 4QVZ), FMRP 1-213 R138Q (PDB: 4QW2), FMRP KH1-KH2 domain (PDB: 2QND) (Valverde et al., 2007), FXR1/2 tandem Agenet domains (PDB: 3O8V, 3H8Z) (Adams-Cioaba et al., 2010), SHH1 Tudor domain with H3K9me3 peptide (PDB: 4IUR) (Law et al., 2013), and UHRF1 tandem Tudor domain with H3K9me3 peptide (PDB: 3ASK) (Arita et al., 2012).

4.4 Results and Discussion

4.4.1 FMRP amino terminal region forms an integral domain containing two tandem Agenet modules and a novel KH module

We expressed, purified and crystallized wild-type and R138Q mutant of human FMRP residues 1-213 in two different space groups ($P4_32_12$ and $P4_12_12$) and determined the structures to the resolution of 3.2 Å and 3.0 Å, respectively (**Table 4.1**). For the structures of both space groups, the crystallographic asymmetric unit contains two molecules. The four monomeric structures are highly similar with a root mean square deviation of <0.6 when pairwise comparing two monomers. Thus, we will describe the

monomeric structure of slightly higher resolution (3.0 Å) R138Q mutant structure.

The FMRP amino terminal domain consists of three structural modules, a tandem array of two Agenet folds and a novel KH fold (**Figure 4.1B-C**). Each Agenet module contains a twisted β-sheet of five strands (β1-β5 for Agenet1 and β6-β10 for Agenet2). A 13-residue Loop-1 (residues 50-62) connects strand β5 of Agenet1 to strand β6 of Agenet2. The interface of the two Agenet modules is mediated by two ion pairs between side chains of E7 of strand β1 with R113 of strand β10, and E66 of strand β6 with R48 of strand β5 (**Figure 4.1D**). In addition, aromatic residues, F15 of strand β2 and W79 of strand β7, are packed against the aliphatic carbons of R48 and R113, respectively. These two ion pairs are conserved among the FMRP, FXR1, FXR2, and *Drosophila* FMR proteins (**Figure 4.2**), and mutations in residues R48C, E68K, R113C and R113H from a *Drosophila* forward genetic screen were unable to rescue FMRP overexpression induced lethality (Reeve et al., 2008) illustrating their importance for FMRP amino terminal function.

The KH0 module, residues 126-202, is composed of three antiparallel β strands of β11- β13 with three helices (αA-αC) packed on one side of the sheet (**Figure 4.1B-C**). The KH0 module is located on the right side of Agenet1, opposite of Agenet2. A 12-residue Loop-2 (residues 114-125) connects strand β10 of Agenet2 to strand β11 of KH0 and appears to be critical to the structural integrity of the molecule. The loop extends through the entire length of Agenet1 and provides hydrogen bonds via two asparagine residues, N116 and N118, connecting E7 of strand β1, main-chain carbonyl oxygen atoms of F49 of strand β5, and P50 of Loop-1 (**Figure 4.1E**).

The interface between Agenet1 and KH0 involves a large number of aromatic and hydrophobic interactions (**Figure 4.1F**). These interactions include F126, F157, L171, and I173 of KH0 and L4, V20, I28, F44 and F49 of Agenet1. Emphasizing the importance of these interactions is the observation that the three structural modules are integral parts of the entire structure, glued together by the interactions mediated by strand β5 in the center of the structure. To the left, R48 of strand β5 stabilizes a network of polar interactions involving Agenet2 (**Figure 4.1D**). To the right, F49 of strand β5 is part of the hydrophobic core involving KH0 (**Figure 4.1F**). In addition, the main-chain carbonyl oxygen atom of F49 interacts with residues in the middle of Loop-2 (**Figure 4.1E**). These intra-molecule interactions likely confer stability to the molecule.

4.4.2 FMRP tandem Agenet domain is structurally similar to other tandem Tudor domains that bind methylated lysine

DALI (distance matric alignment) search (Holm and Rosenstrom, 2010) against structures in the Protein Data Bank (PDB) showed that the FMRP tandem Agenet domain is structurally similar to the mammalian UHRF1 tandem Tudor domain and Arabidopsis SHH1 tandem Tudor-like domain (z score of 9.9 and 9.7, respectively) (**Figure 4.3**), both of which bind methylated lysine 9 of histone H3 (H3K9me) peptides via an aromatic cage.

The tandem Agenet domain of FMRP, particularly the second Agenet motif, was reported as a potential methylated lysine binder and has been shown to bind H3K79me2 both *in vivo* and *in vitro* (Ramos et al., 2006, Alpatov et al., 2014). Additionally, the structurally related FXR1/2 proteins have also been shown to recognize methylated lysine and bind H4K20me1/2/3 *in vitro* via their Agenet domains (Adams-Cioaba et al., 2010).

In support of a histone binding function for the FMRP amino terminal domain, we found that each Agenet fold contains an aromatic cage with potential for binding methylated lysine: Y16, F32, and W36 within Agenet1 and W80, Y96, and Y103 within Agenet2 (**Figure 4.3A**). Indeed, solution NMR spectrometry and *in vitro* binding assays have identified Y103 of Agenet2 (whose side chain is disordered in the absence of binding substrate) important for the recognition of trimethylated lysine (Ramos et al., 2006, Alpatov et al., 2014). Among the structurally characterized tandem Tudor domains, UHRF1, SHH1 and 53BP1 bind methylated lysine with their first Tudor domain (**Figure 4.3B-D**), whereas JMJD2A binds methylated lysine with its second Tudor domain (**Figure 4.3E**). For FMRP, both Agenet motifs contain a recognizable aromatic cage (**Figure 4.3A**), although only Agenet2 has been shown to interact with methylated lysine (Ramos et al., 2006, Alpatov et al., 2014).

4.4.3 FMRP has a KH0 module that may participate in binding of nucleic acids

A surprising structural motif was found at residues 126-202, for which the DALI server recognized as a KH fold (we named it as KH0). KH folds are well studied as DNA/RNA binding domains (Valverde et al., 2008), and FMRP already has two other tandem KH folds (KH1 and KH2) that follow immediately after KH0 (Valverde et al., 2007). Among the three FMRP KH folds, KH0 and KH1 (or KH2) share 20% (or 18%) sequence identity and a root-mean-square-deviation of 2.4 Å (or 2.6 Å). Both KH1 and KH2 have the canonical G-X-X-G motif between helices αA and αB, but KH0 does not have such a motif (**Figure 4.4A**). Instead, KH0 has an A-K-E-A between helices αA and αB (**Figure 4.4A**), and the K143-E144 is in corresponding positions as that of K299-N300 of KH2, as seen by the positively charged surface of KH0 and KH2 (**Figure 4.4C-**

D). The Agenet1 and the KH0 together form a continuous basic surface patch, while Agenet2 has an acidic surface (**Figure 4.4C**). If the aromatic cage of Agenet2 is indeed involved in binding positively charged histone lysine residues, then the basic surface patch of Agenet1 and KH0 could be involved in binding nucleosomal DNA. Alternatively, the basic surface patch of Agenet1 and KH0 could be involved in binding to RNA instead, which would potentially resolve some reports of the amino terminal domain's RNA binding capability despite the absence of any recognizable RNA binding motifs.

4.4.4 Functionally relevant mutation of the FMRP amino terminal domain

A FMRP missense mutation at arginine 138 to glutamine (R138Q), reported in a patient with intellectual disability and seizures (Collins et al., 2010), is located within KH0 helix αA. However, the wild-type and R138Q crystal structures were very similar with an root-mean-square-deviation of 0.8 Å (**Figure 4.5**). The R138Q missense is a partial loss-of-function mutation that impairs FMRP's ability to interact with BK channels and modulate action potential duration in hippocampal and cortical neurons (Myrick et al., 2014a, in preparation) as well as impairs chromatin binding (Alpatov et al., 2014). This mutation did not affect the ability of full length FMRP to bind RNA *in vivo*, at least not with the well-known FMRP targets: Map1b, PSD95, or CamKII (Myrick et al., 2014a, in preparation). We were able to express and purify the R138Q mutant 1-213 protein with similar purity and amount as that of wild-type protein. The one difference noted between wild-type and R138Q purification is that R138Q protein eluted slightly earlier from Q column (data not shown). This is evidence that the mutation may affect the protein-protein interactions of FMRP, which is also supported by biochemical

data indicating R138Q disrupts FMRP's interaction with BK channels (Myrick et al., 2014a, in preparation). Thus, we were unable to determine any gross structural changes that would cause R138Q mutation to lose chromatin or BK channel binding, however this positively charged arginine residue may be critical for specific protein-protein interactions that are unable to form when mutated to a negatively charged glutamine.

4.5 Summary

We determined the crystal structure of the wild-type and R138Q mutant FMRP amino terminal domains (residue 1-202). We found that the amino terminal fragment forms a stable domain that contains two tandem Agenet modules and a KH module. The three structural modules are arranged with Agenet1 flanked by Agenet2 and KH0 forming an integral structure, stabilized by intra-molecular polar interactions (Agenet2-Agenet1) and intra-molecular hydrophobic interactions (Agenet1-KH0). Both Agenet modules contain an aromatic cage and have potential for binding methylated histone lysines, while Agenet1 and KH0 possess a continuous basic surface patch with potential for binding nucleic acids. Thus, our work helps provide structural evidence for many of the proposed functions of the amino terminal domain including chromatin binding, protein-protein interactions, and RNA binding.

Table 4.1: Summary of X-ray diffraction and refinement statistics

FMRP (1-213)	Wild-type	R138Q	
Space Group	$P4_32_12$	$P4_12_12$	
Unit cell		α = β = γ = 90°	
a (Å)	89.5	89.1	89.3
b (Å)	89.5	89.1	89.3
c (Å)	118.1	122.0	122.5
Bemaline		APS 22-ID	
Wavelength (Å)	1.0000		0.9439
Resolution (Å)*	29.6-3.19 (3.30-3.19)	24.9-2.99 (3.10-2.99)	50-3.10 (3.21-3.19)
Rmerge*	0.153 (0.904)	0.147 (0.710)	0.196 (0.694)
I/<σI>*	13.3 (2.5)	12.0 (3.0)	27.0 (5.0)
Completeness (%)*	98.3 (98.5)	99.8 (100.0)	99.6 (96.8)
Redundancy*	9.5 (8.9)	6.3 (6.5)	46.0 (21.2)
Observed reflections	77,967	65,538	434,198
Unique reflections*	8234 (801)	10452 (1013)	9443 (891) (7564 have both I+ and I-)
			0.73 (FOM)
Refinement			
Resolution (Å)	3.19	2.99	
No. reflections	8207	10425	
R_{work} / R_{free}	25.4 / 30.4	22.7 / 28.3	
Molecules in ASU	2	2	
No. of atoms			
Protein	2933	3071	
Solvent	13	15	
B-factors (Å)			
Protein	98.3	64.3	
Solvent	71.6	51.9	
Clash score	5.2	5.2	
Ramachandran			
outliers	0.00%	0.00%	
allowed	1.28%	1.52%	
favored	98.72	98.48%	
Rotamer outliers	0.00%	0.32%	
R.m.s. deviations			
Bond length (Å)	0.002	0.003	
Bond angles (°)	0.7	0.7	

Table 4.1: Summary of X-ray diffraction and refinement statistics

*Values in parenthesis correspond to highest resolution shell;

$R_{merge} = \Sigma \mid I - \langle I \rangle \mid / \Sigma I$, where I is the observed intensity and $\langle I \rangle$ is the averaged intensity from multiple observations;

$\langle I/\sigma I \rangle$ = averaged ratio of the intensity (I) to the error of the intensity (σI);

$R_{work} = \Sigma \mid F_{obs} - F_{cal} \mid / \Sigma \mid F_{obs} \mid$, where F_{obs} and F_{cal} are the observed and calculated structure factors, respectively;

R_{free} was calculated using a randomly chosen subset (5%) of the reflections not used in refinement.

Figure 4.1: Structure of FMRP amino terminal domain

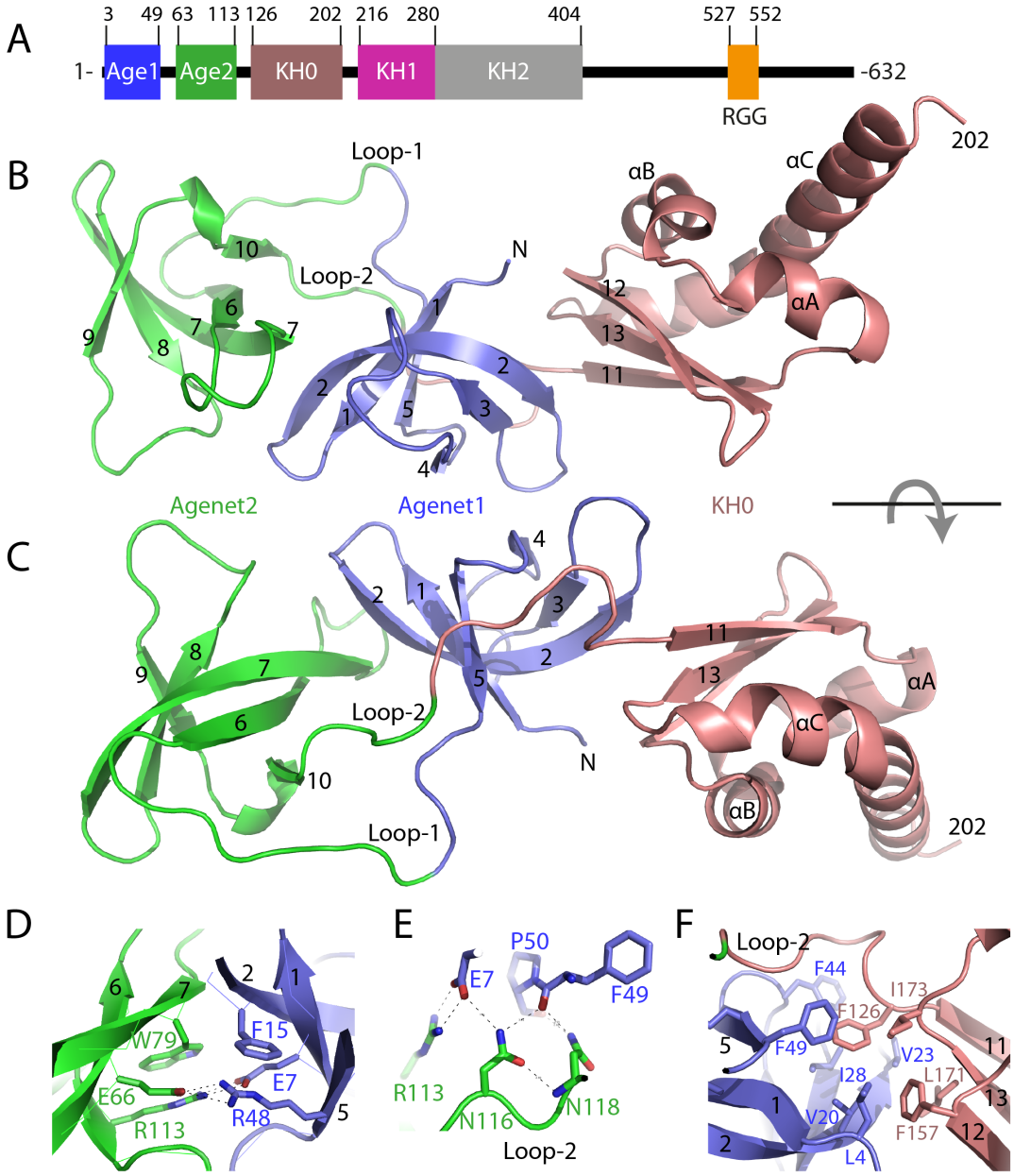

Figure 4.1: Structure of FMRP amino terminal domain

A: Schematic of human FMRP structure. Tandem Agenet and KH0 domain, KH1 and KH2 domains, and RGG box are shown. Position of R138Q mutation within KH0 domain and G-X-X-G motifs within KH1 and KH2 are indicated.

B-C: Two views of FMRP amino terminal structure, with Agenet1 in blue, Agenet2 in green, and KH0 in brown.

D: Intra-molecular polar interactions on the interface of Agenet1 (blue) and 2 (green).

E: Intra-molecular polar interactions between strand β5 of Agenet1 (blue) and Loop-2 (green).

F: Intra-molecular hydrophobic interactions on the interface of Agenet1 (blue) and KH0 (brown).

Figure 4.2: Sequence and secondary structure alignment of human FMRP, FXR1, FXR2, dFmr1, and zFmr1

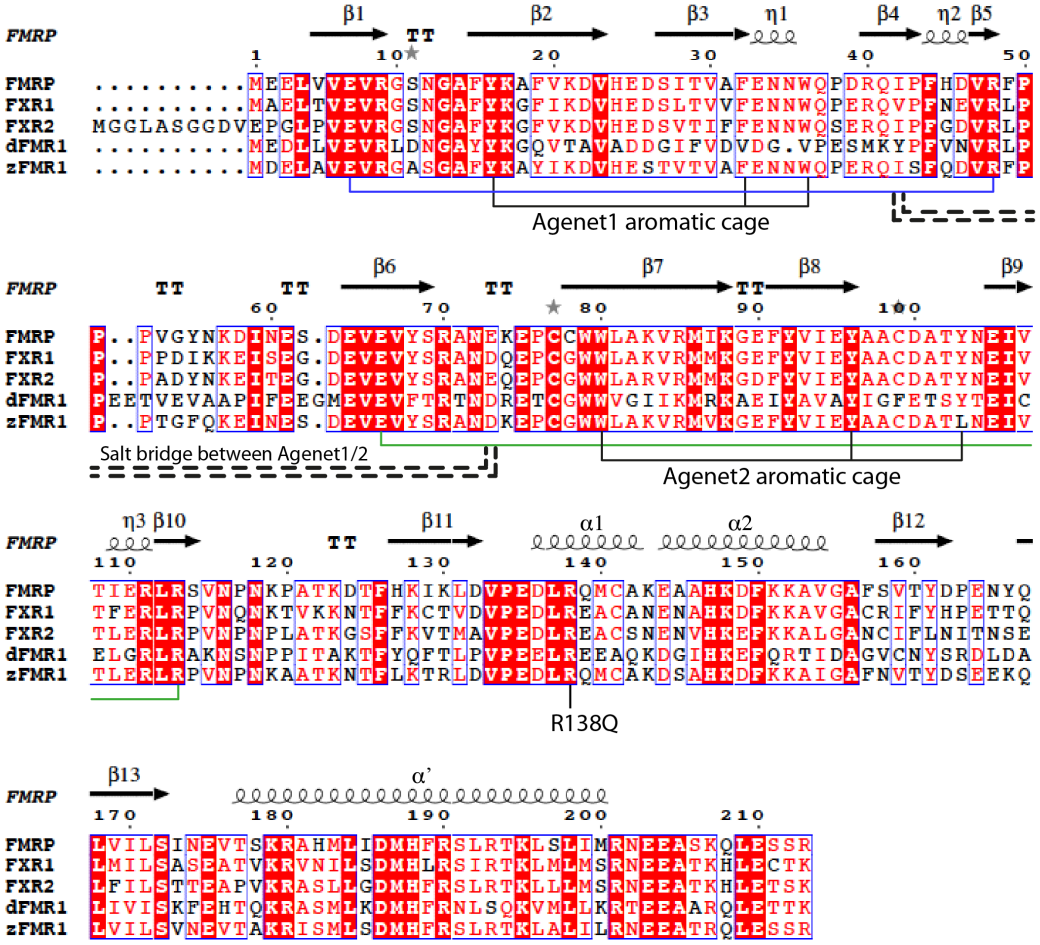

Figure 4.2: Sequence and secondary structure alignment of human FMRP, FXR1, FXR2, dFmr1, and zFmr1

Alignment of human FMRP (AGO02165.1), FXR1 (NP_001013456.1), FXR2 (NP_004851.2), *Drosophila* Fmr1 (NP_001247017.1), and zebrafish Fmr1 (NP_694495.1) are shown. Salt bridge interacting residues in Agenet1 and Agenet2 (E7, R48, E66, R113), potential methylated lysine binding aromatic cage residues (Y16, F32, W36 in Agenet1 and W80, Y96, Y103 in Agenet2), and the R138Q patient mutation are indicated.

Figure 4.3: Structural similarity of FMRP tandem Agenet with other tandem Tudor domains

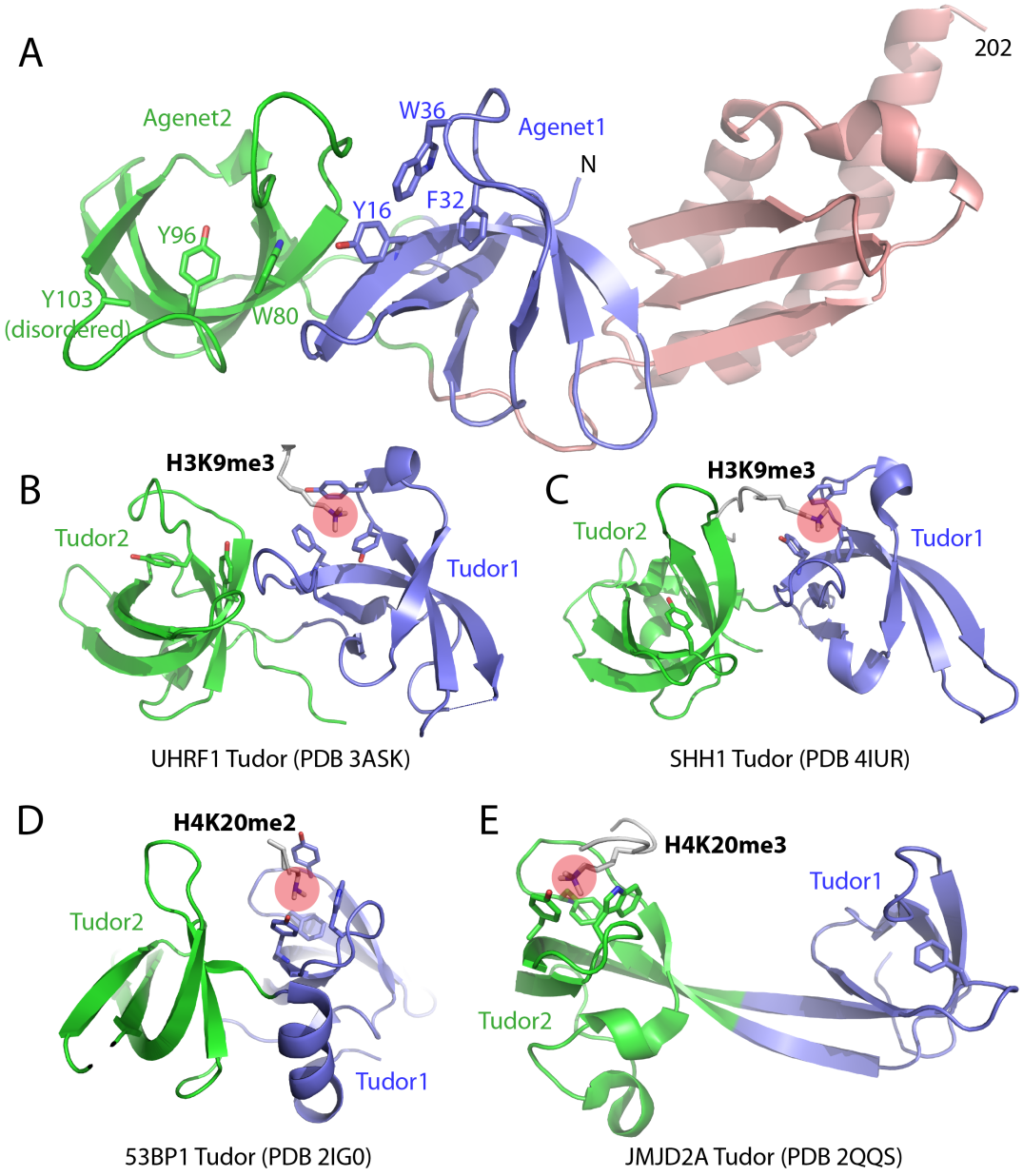

Figure 4.3: Structural similarity of FMRP tandem Agenet with other tandem Tudor domains

A: FMRP amino terminal structure with aromatic cage residues in Agenet1 (blue) and Agenet2 (green) indicated.

B-D: Tandem Tudor domains of UHRF1, SHH1, and 53BP1 bind methylated lysine in the Tudor1 aromatic cage (corresponds to Agenet1 of FMRP).

E: Tandem Tudor domain of JMJD2A binds methylated lysine in the Tudor2 aromatic cage (corresponds to Agenet2 of FMRP).

Figure 4.4: FMRP KH0 motif is an integral part of the amino terminal structure

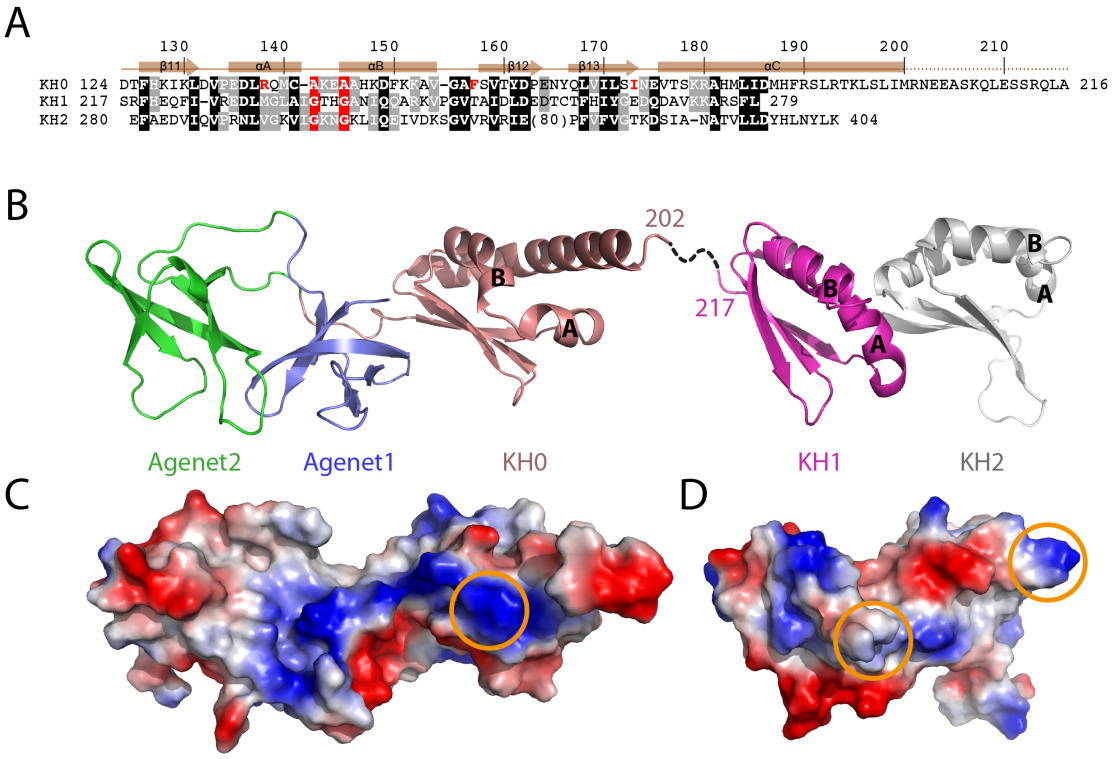

Figure 4.4: FMRP KH0 motif is an integral part of the amino terminal structure

A: Sequence and structural alignments of FMRP KH0, KH1, and KH2. White letters on black are identical or conserved residues among all three KH modules, and white on gray are identical or conserved in at least two. The G-X-X-G motifs of KH1 and KH2 and A-X-X-A motif of KH0 are depicted in white on red background. The position of the patient mutation (R138) and hydrophobic residues involved in the hydrophobic core (Fig. 4.1F) unique to KH0 are shown in red. Conserved residues are as defined by the following groupings: V, L, I and M; F, Y and W; K and R, E and D; Q and N; E and Q; D and N; S and T, and A, G and P.

B: Cartoon structure of Agenet1-Agenet2-KH0 (PDB: 4QW2) connected to KH1-KH2 (PDB: 2QND) by a flexible linker.

C-D: The surface charge distribution of amino terminal Agenet1-Agenet2-KH0 (panel C) and KH1-KH2 (panel D) at neutral pH, displayed as blue for positive, red for negative, and white for neutral, in a similar orientation as shown in panel B. The orange circles indicate the position of A-X-X-A or G-X-X-G.

Figure 4.5: Comparison of wild-type and R138Q structures

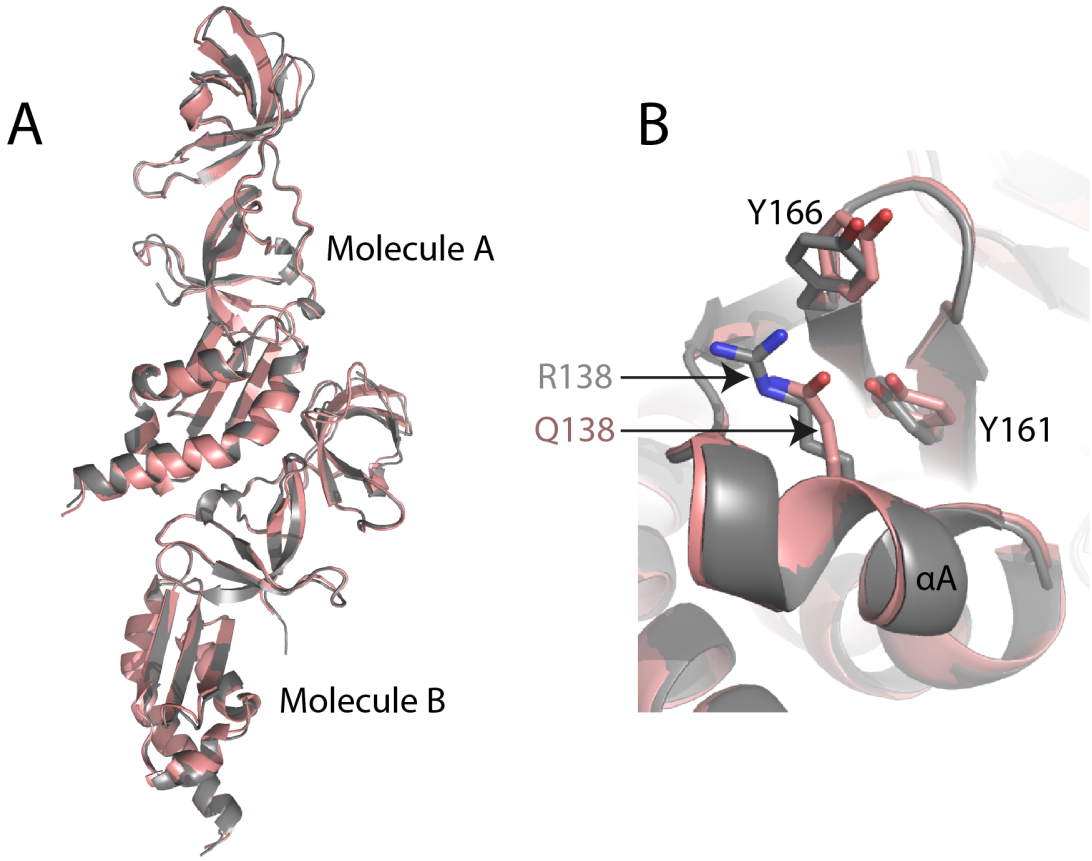

Figure 4.5: Comparison of wild-type and R138Q structures

A: Wild-type (grey, space group: $P4_32_12$) and R138Q (brown, space group: $P4_12_12$) crystal structures are highly similar with a r.m.s.d. of 0.8 Å.

B: Superposition of wild-type (grey) and R138Q (brown). Residues R138 and Q138 of helix αA are indicated.

Chapter 5. Discussion

5.1 Summary of Findings

The aim of this dissertation was to determine how two novel *FMR1* missense mutations, G266E and R138Q, contribute to the function of FMRP and their involvement in the pathogenesis of intellectual disability. In **Chapter 2**, the effect of G266E mutation on FMRP function was assessed in the postsynaptic compartment through monitoring AMPA receptor trafficking. This particular assay depends on FMRP-mediated translation of specific mRNA targets that in turn regulate AMPA receptor internalization. G266E failed to control AMPA receptor internalization, which was then confirmed by failure to associate with polyribosomes or bind mRNA. It was concluded from these data that G266E mutation abolishes FMRP's ability to regulate mRNA translation, a critical function for FMRP in the pathophysiology of FXS, and therefore explains the FXS phenotype observed in the patient. Thus, G266E is indeed a functional null mutation, and joins I304N as the second missense mutation to cause FXS (**Figure 5.1**).

In **Chapter 3**, the effect of R138Q mutation on FMRP function was assessed in both pre- and postsynaptic compartments. All of the canonical functions of FMRP in regulating postsynaptic translation that were disrupted by G266E mutation were found to remain intact by R138Q mutation. Further investigation revealed that R138Q was unable to rescue synaptic overgrowth at the *Drosophila* NMJ, a presynaptic specific function of FMRP. This presynaptic defect was confirmed by failure of R138Q to control AP duration or interact with BK_{Ca} channels in mouse cortical and hippocampal neurons. It was concluded from these data that R138Q mutation causes loss of FMRP's presynaptic function while leaving postsynaptic translational control intact. The partial loss of FMRP function is consistent with the partial FXS phenotype observed in the patient and allows

us to speculate that perhaps the role of FMRP in the presynaptic space specifically contributes to ID and seizure related aspects of FXS, while the postsynaptic functions of FMRP may be more relevant for the other FXS associated phenotypes not present in this patient. Of course, these are speculations based on a single patient mutation and any true associates would need to be determined experimentally. Regardless, these data do identify R138Q as a pathological missense mutation that contributes to at least a subset of FXS pathophysiology (**Figure 5.1**).

To support experimental observations, structural data is often used to help determine how a missense mutation might affect protein function. In the case of G266E, the crystal structure for the tandem KH1 and KH2 domains where residue 266 is located was already publically available. Mutational analysis at residue 266 clearly indicated that a substitution from a small glycine side chain to a large and negatively charged glutamate would cause significant steric hindrance. Thus the experimental loss of function by G266E is supported by a structurally predicted unstable mutation. In the case of R138Q, there was no structural data available for this residue prior to this work. In **Chapter 4**, the crystal structure is determined for both wild-type and R138Q mutant amino terminal domains up to residue 202. This work led to the discovery of a novel KH0 fold within the FMRP amino terminal domain that may help explain reports of this domain's RNA binding capability in spite of any recognizable RNA binding motifs (**Figure 5.2**). Interestingly, there were no observable structural differences between the wild-type and R138Q structures, suggesting that the functional defects mediated by this mutation may occur through subtle disruption of protein-protein interactions rather than large conformational changes in structure.

5.2 Future Directions

5.2.1 Separation of pre- and postsynaptic FMRP function

G266E was shown to be a functional null mutant, rendering FMRP incapable of performing its canonical function of regulating local protein synthesis. Loss of this function was sufficient to recapitulate the entire FXS phenotype, as demonstrated by both G266E and I304N missense mutations. It is, however, possible that G266E may still retain some functions, especially those that are independent of translation regulation. All of the assays that were performed to test G266E function in this dissertation were related to FMRP's role as a translation regulator. However, both the presynaptic and nuclear functions of FMRP are independent of translation, as demonstrated by this dissertation (see **Chapter 3**) and by others (Deng et al., 2013, Alpatov et al., 2014), and could theoretically remain undisrupted by G266E mutation.

The amino terminal domain mediates both the presynaptic and nuclear functions of FMRP, however we do not currently know whether the predicted structural disruption of the KH1-KH2 domains by G266E mutation would also affect the amino terminal domain. It is possible that the entire protein is folded improperly, or alternatively, the KH domains may be disrupted in isolation leaving the amino terminal domain intact to perform the presynaptic and nuclear functions of FMRP. Evidence that supports a possible intact presynaptic function for G266E mutant FMRP comes from the *Drosophila* equivalent mutation, G269E, which was identified in a *Drosophila* forward genetic screen (Reeve et al., 2008). This mutant was unable to rescue excessive defasciculation in *dfmr1* null mutants, however when overexpressed the G269E mutant behaved similar to

wild-type in reducing axonal elaboration in a gain-of-function assay, both of which are presynaptic specific effects of FMRP. This suggests the G269E mutation may have simply caused a reduction in protein level without altering protein function, at least in this particular assay that measures presynaptic FMRP function.

One immediate experiment to assess whether G266E can retain FMRP's presynaptic function would be to measure AP duration in *Fmr1* KO mouse neurons after presynaptic perfusion of a purified G266E-FMRP 1-298 fragment. If G266E rescues AP duration, it would indicate this mutation preserves presynaptic function and that the amino terminal domain remains intact. However, even though the 1-298 fragment contains the full amino terminal domain and KH1, it does not keep KH2 intact with KH1. Therefore it would not be possible to determine whether the amino terminal domain remained intact because G266E causes isolated disruption of the KH domains, or if the absence of the KH2 domain altogether does not allow G266E to induce the same structural disruptions. A better experiment would be to create transgenic mice with the G266E mutation and compare their AP durations to wild-type littermates. Ultimately, the goal would be to identify missense mutations that abolish postsynaptic but not presynaptic FMRP function, so that together with R138Q loss of presynaptic but not postsynaptic FMRP function, there would be clear evidence that the functions of FMRP in the different synaptic spaces are distinct and independent of one another.

5.2.2 Links between FMRP presynaptic function and seizure susceptibility

R138Q was shown to be a partial loss-of-function mutant that affects FMRP presynaptic function while leaving translational function intact. R138Q specifically impaired FMRP's ability to interact with and modulate BK_{Ca} channels, the major players

involved in controlling AP duration and neurotransmitter release. While loss of FMRP had already been linked to exaggerated AP duration and neurotransmitter release (Deng et al., 2013), a missense mutation that recapitulates this effect verifies that it is the interaction between FMRP and BK channels that is necessary for modulating AP duration and not simply a general consequence of FMRP's absence.

There is a great body of literature linking loss of FMRP with circuit hyperexcitability (Gibson et al., 2008, Pfeiffer and Huber, 2009) and BK_{Ca} dysfunction with epilepsy (N'Gouemo, 2011), however the exact molecular mechanisms underlying seizure pathology within FXS are not well understood and whether FMRP-BK_{Ca} channel interactions are directly responsible for seizure and/or ID phenotypes still remains to be determined. The model proposed here is that FMRP acts to enhance BK_{Ca} channel antiepileptic activity such that in the absence of FMRP-BK_{Ca} channel interaction, diminished BK_{Ca} channel activity then contributes to circuit hyperexcitability. This model, could in theory, provide the molecular basis for at least some of the seizure pathology seen in FXS, however a direct connection between FMRP-BK_{Ca} channel activity and seizures needs to be established first. Deng et al. have begun to address this issue and found that genetic upregulation of BK_{Ca} channel activity can rescue seizure susceptibility in *Fmr1* KO mice (Deng and Klyachko, in preparation).

However, further studies are still needed to determine whether FMRP's presynaptic activity can be specifically linked with seizure pathology. It is tempting to think so because the R138Q patient has an ID and seizure phenotype that correlates with a mutation specifically expected to increase seizure susceptibility, but a single patient mutation is not sufficient evidence from which to make genotype to phenotype

conclusions. A necessary experiment is to first determine the exact FMRP locus that binds to BK_{Ca} channels, and then analyze the spectrum of phenotypes that occur in mice when this locus is mutated or removed. If isolated disruption of FMRP's interaction with BK_{Ca} channels gives rise to increased seizure susceptibility in mice in the absence of other FXS-like phenotypes such as elongated dendritic spines and aberrant synaptic plasticity, then a possible link between presynaptic function and seizures could be made. Conversely, if there were mutations that caused isolated disruption of FMRP's postsynaptic translation regulation function without affecting presynaptic activity, then these could also be tested in animal models for loss of seizure susceptibility while other FXS-related phenotypes still persisted. The link between FMRP's presynaptic activity on BK_{Ca} channels and ID/seizure pathology could also be further explored with pharmacological manipulation of BK_{Ca} channels. Two anticonvulsant drugs currently on the market include zonisamide (BK_{Ca} activator) and paxilline (BK_{Ca} blocker). If the model that FMRP is needed to enhance BK_{Ca} channel activity is correct, then *Fmr1* KO mice treated with a BK_{Ca} activator like zonisamide should respond better than mice given a BK_{Ca} blocker such as paxilline. In fact, BK_{Ca} channel openers have already been patented for use in the treatment of FXS (Briault and Perche, 2013), however preclinical and clinical data is still needed to determine whether this type of pharmacological intervention could be useful as targeted FXS therapy.

It is important to note that the work presented in this dissertation does not provide sufficient evidence to claim that R138Q mutation is solely a defect in BK_{Ca} channel activity. In fact, it is already known that R138Q mutation also disrupts histone binding (Alpatov et al., 2014), however the path by which chromatin modulation would lead to

neurological impairment is unclear in this context. Additionally, FMRP has other presynaptic functions, such as axonal protein synthesis (Li et al., 2009), that were not specifically assayed in this dissertation and could theoretically be disrupted by R138Q mutation as well. Especially if the novel KH0 fold participates in RNA binding, then it is possible that R138Q might disrupt interactions with these currently unknown mRNA targets to impair presynaptic protein synthesis. Thus, in addition to BK_{Ca} channel abnormalities, the symptoms experienced by the patient may also be partially accounted for by defects in histone binding with the Agenet domains or presynaptic translation through the KH0 domain. Only further experimentation to understand the full consequences of R138Q mutation will answer these questions.

5.2.3 Amino terminal domain interactions with chromatin and RNA

The amino terminal domain of FMRP (residues 1-213) was shown to be a stable domain that consists of two tandem Agenet motifs and a novel KH0 fold. Histone and RNA binding were predicted functions of the amino terminal domain and the structure of this region indicated the potential for both a histone recognizing aromatic cage within Agenet2 and a positively charged nucleic acid binding surface by KH0 in connection with Agenet1. However, the structure of the Agenet2 aromatic cage was not ideal for histone binding, and indeed may require a ligand to form the proper binding conformation. Furthermore, the positively charged binding surface, while suitable for RNA binding, may participate in protein-protein interactions with negatively charged proteins instead. Thus it is important to not over interpret the current data until co-crystal structures can be solved showing true histone and/or RNA binding interactions.

The novel KH0 fold was actually very surprising to find because this particular region of FMRP had not been predicted to contain any recognizable structural motifs. KH0 is indeed a non-canonical KH fold that does not contain the G-X-X-G motif traditionally required KH domains to bind RNA. Therefore, if KH0 participates in RNA binding, it most certainly does so in a manner different from the other KH1 and KH2 domains in FMRP. In addition to a crystal structure of the KH0 fold with bound RNA, a crystal structure of all three KH domains together, with and without bound RNA, would be very useful to determine how they work together to confer RNA binding specificity to FMRP. The binding cleft of KH domains by themselves can only accommodate four nucleotides, so when more binding specificity is needed, it has been proposed that multiple tandem KH domains act together to increase the RNA binding surface and specificity (Valverde et al., 2008). In fact, many KH containing RNA binding proteins have been reported to crystallize as dimers or tetramers, and this self-association with either neighboring KH proteins or tandem KH domains within the same protein has been suggested to play an important part in mediating RNA specificity (Ramos et al., 2002, Valverde et al., 2008). KH0 is able to form an antiparallel coiled-coil dimerization, which supports the idea that KH0 interacts with itself or with the other KH1 and KH2 domains, however crystal analysis of the three tandem KH domains with bound RNA will ultimately reveal whether these domains act independently or in concert with one another.

5.3 Significance

The work presented in this dissertation indicates that both G266E and R138Q missense mutations contribute to the pathophysiology of FXS. G266E has been identified as a functional null, while R138Q is a partial loss-of-function mutant, and taken together this research clearly separates the pre- and postsynaptic functions of FMRP. Research on *FMR1* missense mutations, particularly partial loss-of-function mutations, provides new avenues of insight about the physiological functions of FMRP and allows us to speculate about their correlations with specific FXS clinical features. Teasing out the domain specific functions of FMRP and their contribution to various elements of FXS pathophysiology will be important to advancing our understanding of not only FXS, but also of ID disorders at large. While missense mutations of *FMR1* are quite rare compared to other X-linked causes of ID (see **Section 1.3.2** *FMR1* mutation screening and **Section 1.3.3** *FMR1* point mutations), they are critical in determining the subtle functions of FMRP and should be considered not only when the clinical evidence for FXS is strong but also in cases where ID may be the only prevailing symptom.

Figure 5.1: Model of FMRP pre- and postsynaptic function with G266E and R138Q mutations

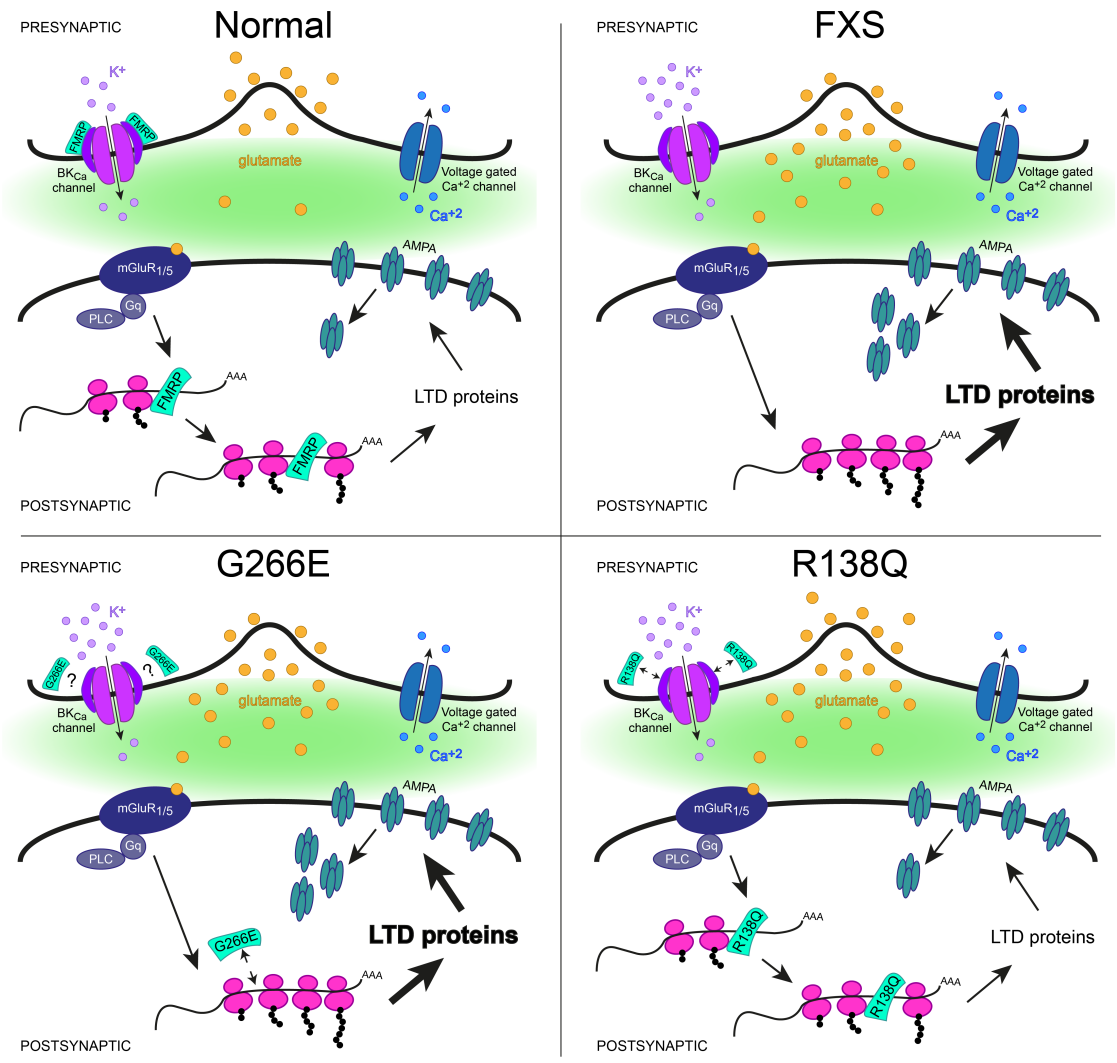

Figure 5.1: Model of FMRP pre- and postsynaptic function with G266E and R138Q mutations

FMRP has both pre- and postsynaptic functions. In the postsynaptic compartment, FMRP (turquoise) regulates the translation of bound mRNA targets by directly associating with the mRNA (black strand) and polyribosomes (pink). FMRP generally acts as a translation repressor until synaptic activity, such as $mGluR_{1/5}$ stimulation, signals the need for protein synthesis. FMRP then releases its suppression and allows the temporary synthesis of specific proteins important for synaptic plasticity (i.e. LTD proteins). Ultimately this local protein synthesis leads to changes in the synaptic architecture (i.e. surface AMPA receptor internalization) and is the foundation for synaptic plasticity. In the presynaptic compartment, FMRP plays a role in regulating AP duration by modulating BK_{Ca} activity. BK_{Ca} channels (purple) are critical for repolarizing the cell membrane after an action potential and are activated by Ca^{2+} influx and voltage depolarization. When open, they allow for large conductance of K^+ efflux, which quickly repolarizes the cell membrane and limits AP duration. FMRP specifically binds to the β4 subunit (dark purple) of the BK_{Ca} channel and facilitates channel activity.

In the absence of FMRP, as in the case of FXS, both pre- and postsynaptic defects arise. In the postsynaptic space, loss of FMRP leads to dysregulated translation of synaptic proteins, elevated protein synthesis at basal states, and loss of activity dependent increases in protein synthesis. Elevated levels of, for example, LTD proteins, cause increased AMPA receptor internalization and consequently synaptic plasticity defects. In the presynaptic space, loss of FMRP interaction with BK_{Ca} channels negatively affects

the activity of the channels so then repolarization of the cell membrane is delayed, AP duration is prolonged, and excessive neurotransmitter is released (i.e. glutamate).

G266E mutation produces a functional null form of FMRP, so even though FMRP is present within the neuron, it cannot bind mRNA or polyribosomes, and therefore results in unregulated protein synthesis and excessive AMPA receptor internalization just like absence of FMRP in FXS. Whether G266E can still interact with and modulate BK_{Ca} channels in the presynaptic compartment is currently unknown. Conversely, R138Q mutation preserves FMRP's postsynaptic function as a translation regulator, but is unable to interact with BK_{Ca} channels or modulate AP duration, therefore resulting in an isolated loss of FMRP presynaptic function. These mutations confirm that FMRP plays separate and independent roles between the pre- and postsynaptic compartments.

Figure 5.2: New FMRP structural domain boundaries

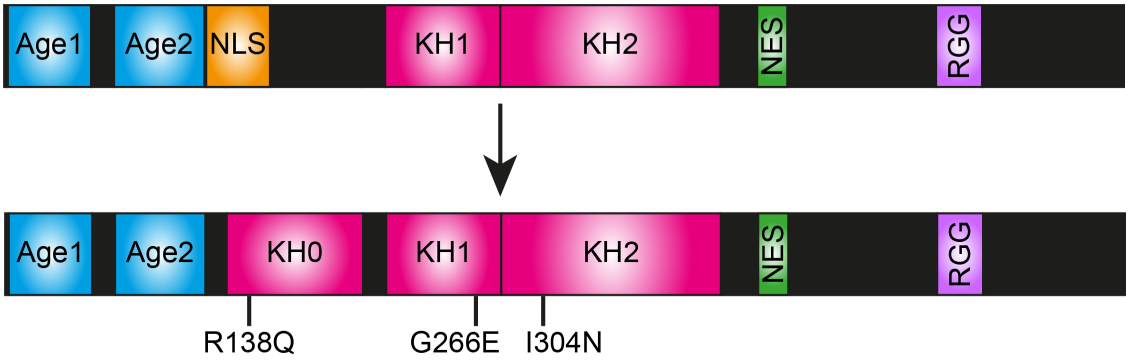

Figure 5.2: New FMRP structural domain boundaries

Structural analysis of the FMRP amino terminal domain (residues 1-213) revealed a novel KH motif that follows the Agenet2 module and immediately precedes the KH1 module, thus rendering FMRP a protein with now three KH domains. The nuclear localization sequence (NLS) is still present but not shown in the new model for simplicity. Each KH module has been associated with a patient mutation: R138Q in KH0, G266E in KH1, and I304N in KH2.

Abrams MT, Reiss AL, Freund LS, Baumgardner TL, Chase GA, Denckla MB. (1994). Molecular-neurobehavioral associations in females with the fragile X full mutation. *American journal of medical genetics* **51**:317-327.

Adams PD, Afonine PV, Bunkoczi G, Chen VB, Davis IW, Echols N, Headd JJ, Hung LW, Kapral GJ, Grosse-Kunstleve RW, McCoy AJ, Moriarty NW, Oeffner R, Read RJ, Richardson DC, Richardson JS, Terwilliger TC, Zwart PH. (2010). PHENIX: a comprehensive Python-based system for macromolecular structure solution. *Acta Crystallogr D Biol Crystallogr* **66**:213-221.

Adams-Cioaba MA, Guo Y, Bian C, Amaya MF, Lam R, Wasney GA, Vedadi M, Xu C, Min J. (2010). Structural studies of the tandem Tudor domains of fragile X mental retardation related proteins FXR1 and FXR2. *PLoS One* **5**:e13559.

Adinolfi S, Bagni C, Musco G, Gibson T, Mazzarella L, Pastore A. (1999). Dissecting FMR1, the protein responsible for fragile X syndrome, in its structural and functional domains. *RNA* **5**:1248-1258.

Adinolfi S, Ramos A, Martin SR, Dal Piaz F, Pucci P, Bardoni B, Mandel JL, Pastore A. (2003). The N-terminus of the fragile X mental retardation protein contains a novel domain involved in dimerization and RNA binding. *Biochemistry* **42**:10437-10444.

Alpatov R, Lesch BJ, Nakamoto-Kinoshita M, Blanco A, Chen S, Stutzer A, Armache KJ, Simon MD, Xu C, Ali M, Murn J, Prisic S, Kutateladze TG, Vakoc CR, Min J, Kingston RE, Fischle W, Warren ST, Page DC, Shi Y. (2014). A chromatin-dependent role of the fragile X mental retardation protein FMRP in the DNA damage response. *Cell* **157**:869-881.

Antar LN, Afroz R, Dictenberg JB, Carroll RC, Bassell GJ. (2004). Metabotropic glutamate receptor activation regulates fragile x mental retardation protein and FMR1 mRNA localization differentially in dendrites and at synapses. *J Neurosci* **24**:2648-2655.

Arita K, Isogai S, Oda T, Unoki M, Sugita K, Sekiyama N, Kuwata K, Hamamoto R, Tochio H, Sato M, Ariyoshi M, Shirakawa M. (2012). Recognition of modification status on a histone H3 tail by linked histone reader modules of the epigenetic regulator UHRF1. *Proc Natl Acad Sci U S A* **109**:12950-12955.

Ascano M, Jr., Mukherjee N, Bandaru P, Miller JB, Nusbaum JD, Corcoran DL, Langlois C, Munschauer M, Dewell S, Hafner M, Williams Z, Ohler U, Tuschl T. (2012). FMRP

targets distinct mRNA sequence elements to regulate protein expression. *Nature* **492**:382-386.

Ashley CT, Jr., Wilkinson KD, Reines D, Warren ST. (1993). FMR1 protein: conserved RNP family domains and selective RNA binding. *Science* **262**:563-566.

Bardoni B, Castets M, Huot ME, Schenck A, Adinolfi S, Corbin F, Pastore A, Khandjian EW, Mandel JL. (2003). 82-FIP, a novel FMRP (fragile X mental retardation protein) interacting protein, shows a cell cycle-dependent intracellular localization. *Hum Mol Genet* **12**:1689-1698.

Bardoni B, Schenck A, Mandel JL. (1999). A novel RNA-binding nuclear protein that interacts with the fragile X mental retardation (FMR1) protein. *Hum Mol Genet* **8**:2557-2566.

Bardoni B, Sittler A, Shen Y, Mandel JL. (1997). Analysis of domains affecting intracellular localization of the FMRP protein. *Neurobiol Dis* **4**:329-336.

Bassell GJ, Warren ST. (2008). Fragile X syndrome: loss of local mRNA regulation alters synaptic development and function. *Neuron* **60**:201-214.

Bear MF, Huber KM, Warren ST. (2004). The mGluR theory of fragile X mental retardation. *Trends Neurosci* **27**:370-377.

Bensaid M, Melko M, Bechara EG, Davidovic L, Berretta A, Catania MV, Gecz J, Lalli E, Bardoni B. (2009). FRAXE-associated mental retardation protein (FMR2) is an RNA-binding protein with high affinity for G-quartet RNA forming structure. *Nucleic Acids Res* **37**:1269-1279.

Berry-Kravis E, Hessl D, Coffey S, Hervey C, Schneider A, Yuhas J, Hutchison J, Snape M, Tranfaglia M, Nguyen DV, Hagerman R. (2009). A pilot open label, single dose trial of fenobam in adults with fragile X syndrome. *J Med Genet* **46**:266-271.

Berry-Kravis EM, Hessl D, Rathmell B, Zarevics P, Cherubini M, Walton-Bowen K, Mu Y, Nguyen DV, Gonzalez-Heydrich J, Wang PP, Carpenter RL, Bear MF, Hagerman RJ. (2012). Effects of STX209 (arbaclofen) on neurobehavioral function in children and adults with fragile X syndrome: a randomized, controlled, phase 2 trial. *Sci Transl Med* **4**:152ra127.

Bhakar AL, Dolen G, Bear MF. (2012). The pathophysiology of fragile X (and what it teaches us about synapses). *Annu Rev Neurosci* **35**:417-443.

Birot AM, Delobel B, Gronnier P, Bonnet V, Maire I, Bozon D. (1996). A 5-megabase familial deletion removes the IDS and FMR-1 genes in a male Hunter patient. *Hum Mutat* **7**:266-268.

Blackwell E, Zhang X, Ceman S. (2010). Arginines of the RGG box regulate FMRP association with polyribosomes and mRNA. *Hum Mol Genet* **19**:1314-1323.

Brackett DM, Qing F, Amieux PS, Sellers DL, Horner PJ, Morris DR. (2013). FMR1 transcript isoforms: association with polyribosomes; regional and developmental expression in mouse brain. *PLoS One* **8**:e58296.

Brenner R, Chen QH, Vilaythong A, Toney GM, Noebels JL, Aldrich RW. (2005). BK channel beta4 subunit reduces dentate gyrus excitability and protects against temporal lobe seizures. *Nat Neurosci* **8**:1752-1759.

Brent JR, Werner KM, McCabe BD. (2009). Drosophila larval NMJ dissection. *J Vis Exp*.

Briault S, Perche O (2013) Compositions for the treatment of Fragile X syndrome; Publication No. EP2540295 A1; published Jan 2, 2013.

Brown MR, Kronengold J, Gazula VR, Chen Y, Strumbos JG, Sigworth FJ, Navaratnam D, Kaczmarek LK. (2010). Fragile X mental retardation protein controls gating of the sodium-activated potassium channel Slack. *Nat Neurosci* **13**:819-821.

Brown V, Jin P, Ceman S, Darnell JC, O'Donnell WT, Tenenbaum SA, Jin X, Feng Y, Wilkinson KD, Keene JD, Darnell RB, Warren ST. (2001). Microarray identification of FMRP-associated brain mRNAs and altered mRNA translational profiles in fragile X syndrome. *Cell* **107**:477-487.

Brown V, Small K, Lakkis L, Feng Y, Gunter C, Wilkinson KD, Warren ST. (1998). Purified recombinant Fmrp exhibits selective RNA binding as an intrinsic property of the fragile X mental retardation protein. *J Biol Chem* **273**:15521-15527.

Burd CG, Dreyfuss G. (1994). Conserved structures and diversity of functions of RNA-binding proteins. *Science* **265**:615-621.

Cavalleri GL, Weale ME, Shianna KV, Singh R, Lynch JM, Grinton B, Szoeke C, Murphy K, Kinirons P, O'Rourke D, Ge D, Depondt C, Claeys KG, Pandolfo M, Gumbs C, Walley N, McNamara J, Mulley JC, Linney KN, Sheffield LJ, et al. (2007). Multicentre search for genetic susceptibility loci in sporadic epilepsy syndrome and seizure types: a case-control study. *Lancet Neurol* **6**:970-980.

Chudley AE, Hagerman RJ. (1987). Fragile X syndrome. *J Pediatr* **110**:821-831.

Coffee B, Ikeda M, Budimirovic DB, Hjelm LN, Kaufmann WE, Warren ST. (2008). Mosaic FMR1 deletion causes fragile X syndrome and can lead to molecular misdiagnosis: a case report and review of the literature. *Am J Med Genet A* **146A**:1358-1367.

Coffee B, Keith K, Albizua I, Malone T, Mowrey J, Sherman SL, Warren ST. (2009). Incidence of fragile X syndrome by newborn screening for methylated FMR1 DNA. *Am J Hum Genet* **85**:503-514.

Coffee B, Zhang F, Ceman S, Warren ST, Reines D. (2002). Histone modifications depict an aberrantly heterochromatinized FMR1 gene in fragile x syndrome. *Am J Hum Genet* **71**:923-932.

Colak D, Zaninovic N, Cohen MS, Rosenwaks Z, Yang WY, Gerhardt J, Disney MD, Jaffrey SR. (2014). Promoter-bound trinucleotide repeat mRNA drives epigenetic silencing in fragile X syndrome. *Science* **343**:1002-1005.

Collins SC, Bray SM, Suhl JA, Cutler DJ, Coffee B, Zwick ME, Warren ST. (2010). Identification of novel FMR1 variants by massively parallel sequencing in developmentally delayed males. *Am J Med Genet A* **152A**:2512-2520.

Comery TA, Harris JB, Willems PJ, Oostra BA, Irwin SA, Weiler IJ, Greenough WT. (1997). Abnormal dendritic spines in fragile X knockout mice: maturation and pruning deficits. *Proc Natl Acad Sci U S A* **94**:5401-5404.

Cordeiro L, Ballinger E, Hagerman R, Hessl D. (2011). Clinical assessment of DSM-IV anxiety disorders in fragile X syndrome: prevalence and characterization. *J Neurodev Disord* **3**:57-67.

Crawford DC, Acuna JM, Sherman SL. (2001). FMR1 and the fragile X syndrome: human genome epidemiology review. *Genet Med* **3**:359-371.

Cruz-Martin A, Crespo M, Portera-Cailliau C. (2010). Delayed stabilization of dendritic spines in fragile X mice. *J Neurosci* **30**:7793-7803.

Dahl N, Hu LJ, Chery M, Fardeau M, Gilgenkrantz S, Nivelon-Chevallier A, Sidaner-Noisette I, Mugneret F, Gouyon JB, Gal A, et al. (1995). Myotubular myopathy in a girl with a deletion at Xq27-q28 and unbalanced X inactivation assigns the MTM1 gene to a 600-kb region. *Am J Hum Genet* **56**:1108-1115.

Darnell JC, Fraser CE, Mostovetsky O, Darnell RB. (2009). Discrimination of common and unique RNA-binding activities among Fragile X mental retardation protein paralogs. *Hum Mol Genet* **18**:3164-3177.

Darnell JC, Fraser CE, Mostovetsky O, Stefani G, Jones TA, Eddy SR, Darnell RB. (2005). Kissing complex RNAs mediate interaction between the Fragile-X mental retardation protein KH2 domain and brain polyribosomes. *Genes Dev* **19**:903-918.

Darnell JC, Jensen KB, Jin P, Brown V, Warren ST, Darnell RB. (2001). Fragile X mental retardation protein targets G quartet mRNAs important for neuronal function. *Cell* **107**:489-499.

Darnell JC, Van Driesche SJ, Zhang C, Hung KY, Mele A, Fraser CE, Stone EF, Chen C, Fak JJ, Chi SW, Licatalosi DD, Richter JD, Darnell RB. (2011). FMRP stalls ribosomal translocation on mRNAs linked to synaptic function and autism. *Cell* **146**:247-261.

De Boulle K, Verkerk AJ, Reyniers E, Vits L, Hendrickx J, Van Roy B, Van den Bos F, de Graaff E, Oostra BA, Willems PJ. (1993). A point mutation in the FMR-1 gene associated with fragile X mental retardation. *Nat Genet* **3**:31-35.

De Rubeis S, Bagni C. (2011). Regulation of molecular pathways in the Fragile X Syndrome: insights into Autism Spectrum Disorders. *J Neurodev Disord* **3**:257-269.

Deng PY, Rotman Z, Blundon JA, Cho Y, Cui J, Cavalli V, Zakharenko SS, Klyachko VA. (2013). FMRP regulates neurotransmitter release and synaptic information transmission by modulating action potential duration via BK channels. *Neuron* **77**:696-711.

Du W, Bautista JF, Yang H, Diez-Sampedro A, You SA, Wang L, Kotagal P, Luders HO, Shi J, Cui J, Richerson GB, Wang QK. (2005). Calcium-sensitive potassium channelopathy in human epilepsy and paroxysmal movement disorder. *Nat Genet* **37**:733-738.

Eberhart DE, Malter HE, Feng Y, Warren ST. (1996). The fragile X mental retardation protein is a ribonucleoprotein containing both nuclear localization and nuclear export signals. *Hum Mol Genet* **5**:1083-1091.

Eichler EE, Richards S, Gibbs RA, Nelson DL. (1994). Fine structure of the human FMR1 gene. *Hum Mol Genet* **3**:684-685.

Emsley P, Lohkamp B, Scott WG, Cowtan K. (2010). Features and development of Coot. *Acta Crystallogr D Biol Crystallogr* **66**:486-501.

Ermolinsky B, Arshadmansab MF, Pacheco Otalora LF, Zarei MM, Garrido-Sanabria ER. (2008). Deficit of Kcnma1 mRNA expression in the dentate gyrus of epileptic rats. *Neuroreport* **19**:1291-1294.

Estecio M, Fett-Conte AC, Varella-Garcia M, Fridman C, Silva AE. (2002). Molecular and cytogenetic analyses on Brazilian youths with pervasive developmental disorders. *J Autism Dev Disord* **32**:35-41.

Faber ES, Sah P. (2003). Calcium-activated potassium channels: multiple contributions to neuronal function. *Neuroscientist* **9**:181-194.

Feng Y, Absher D, Eberhart DE, Brown V, Malter HE, Warren ST. (1997a). FMRP associates with polyribosomes as an mRNP, and the I304N mutation of severe fragile X syndrome abolishes this association. *Mol Cell* **1**:109-118.

Feng Y, Gutekunst CA, Eberhart DE, Yi H, Warren ST, Hersch SM. (1997b). Fragile X mental retardation protein: nucleocytoplasmic shuttling and association with somatodendritic ribosomes. *J Neurosci* **17**:1539-1547.

Ferron L, Nieto-Rostro M, Cassidy JS, Dolphin AC. (2014). Fragile X mental retardation protein controls synaptic vesicle exocytosis by modulating N-type calcium channel density. *Nat Commun* **5**:3628.

Fu YH, Kuhl DP, Pizzuti A, Pieretti M, Sutcliffe JS, Richards S, Verkerk AJ, Holden JJ, Fenwick RG, Jr., Warren ST, et al. (1991). Variation of the CGG repeat at the fragile X site results in genetic instability: resolution of the Sherman paradox. *Cell* **67**:1047-1058.

Gabus C, Mazroui R, Tremblay S, Khandjian EW, Darlix JL. (2004). The fragile X mental retardation protein has nucleic acid chaperone properties. *Nucleic Acids Res* **32**:2129-2137.

Gareau C, Houssin E, Martel D, Coudert L, Mellaoui S, Huot ME, Laprise P, Mazroui R. (2013). Characterization of fragile X mental retardation protein recruitment and dynamics in Drosophila stress granules. *PLoS One* **8**:e55342.

Gatto CL, Broadie K. (2008). Temporal requirements of the fragile X mental retardation protein in the regulation of synaptic structure. *Development* **135**:2637-2648.

Gedeon AK, Baker E, Robinson H, Partington MW, Gross B, Manca A, Korn B, Poustka A, Yu S, Sutherland GR, et al. (1992). Fragile X syndrome without CCG amplification has an FMR1 deletion. *Nat Genet* **1**:341-344.

Gibson JR, Bartley AF, Hays SA, Huber KM. (2008). Imbalance of neocortical excitation and inhibition and altered UP states reflect network hyperexcitability in the mouse model of fragile X syndrome. *J Neurophysiol* **100**:2615-2626.

Gronskov K, Brondum-Nielsen K, Dedic A, Hjalgrim H. (2011). A nonsense mutation in FMR1 causing fragile X syndrome. *Eur J Hum Genet* **19**:489-491.

Gross C, Yao X, Pong DL, Jeromin A, Bassell GJ. (2011). Fragile X mental retardation protein regulates protein expression and mRNA translation of the potassium channel Kv4.2. *J Neurosci* **31**:5693-5698.

Gu Y, Lugenbeel KA, Vockley JG, Grody WW, Nelson DL. (1994). A de novo deletion in FMR1 in a patient with developmental delay. *Hum Mol Genet* **3**:1705-1706.

Hagerman PJ, Stafstrom CE. (2009). Origins of epilepsy in fragile X syndrome. *Epilepsy Curr* **9**:108-112.

Hall SS, Burns DD, Lightbody AA, Reiss AL. (2008). Longitudinal changes in intellectual development in children with Fragile X syndrome. *J Abnorm Child Psychol* **36**:927-939.

Hammond LS, Macias MM, Tarleton JC, Shashidhar Pai G. (1997). Fragile X syndrome and deletions in FMR1: new case and review of the literature. *Am J Med Genet* **72**:430-434.

Hanson JE, Madison DV. (2007). Presynaptic FMR1 genotype influences the degree of synaptic connectivity in a mosaic mouse model of fragile X syndrome. *J Neurosci* **27**:4014-4018.

Harris SW, Hessl D, Goodlin-Jones B, Ferranti J, Bacalman S, Barbato I, Tassone F, Hagerman PJ, Herman H, Hagerman RJ. (2008). Autism profiles of males with fragile X syndrome. *Am J Ment Retard* **113**:427-438.

Henderson C, Wijetunge L, Kinoshita MN, Shumway M, Hammond RS, Postma FR, Brynczka C, Rush R, Thomas A, Paylor R, Warren ST, Vanderklish PW, Kind PC, Carpenter RL, Bear MF, Healy AM. (2012). Reversal of disease-related pathologies in the fragile X mouse model by selective activation of GABAB receptors with arbaclofen. *Sci Transl Med* **4**:152ra128.

Hessl D, Nguyen DV, Green C, Chavez A, Tassone F, Hagerman RJ, Senturk D, Schneider A, Lightbody A, Reiss AL, Hall S. (2009). A solution to limitations of cognitive testing in children with intellectual disabilities: the case of fragile X syndrome. *J Neurodev Disord* **1**:33-45.

Higgins JJ, Hao J, Kosofsky BE, Rajadhyaksha AM. (2008). Dysregulation of large-conductance Ca2+-activated K+ channel expression in nonsyndromal mental retardation due to a cereblon p.R419X mutation. *Neurogenetics* **9**:219-223.

Holm L, Rosenstrom P. (2010). Dali server: conservation mapping in 3D. *Nucleic Acids Res* **38**:W545-549.

Hu H, Shao LR, Chavoshy S, Gu N, Trieb M, Behrens R, Laake P, Pongs O, Knaus HG, Ottersen OP, Storm JF. (2001). Presynaptic Ca2+-activated K+ channels in glutamatergic hippocampal terminals and their role in spike repolarization and regulation of transmitter release. *J Neurosci* **21**:9585-9597.

Huber KM. (2006). The fragile X-cerebellum connection. *Trends Neurosci* **29**:183-185.

Huber KM, Gallagher SM, Warren ST, Bear MF. (2002). Altered synaptic plasticity in a mouse model of fragile X mental retardation. *Proc Natl Acad Sci U S A* **99**:7746-7750.

Iacoangeli A, Rozhdestvensky TS, Dolzhanskaya N, Tournier B, Schutt J, Brosius J, Denman RB, Khandjian EW, Kindler S, Tiedge H. (2008). On BC1 RNA and the fragile X mental retardation protein. *Proc Natl Acad Sci U S A* **105**:734-739.

Incorpora G, Sorge G, Sorge A, Pavone L. (2002). Epilepsy in fragile X syndrome. *Brain Dev* **24**:766-769.

International HapMap C, Frazer KA, Ballinger DG, Cox DR, Hinds DA, Stuve LL, Gibbs RA, Belmont JW, Boudreau A, Hardenbol P, Leal SM, Pasternak S, Wheeler DA, Willis TD, Yu F, Yang H, Zeng C, Gao Y, Hu H, Hu W, et al. (2007). A second generation human haplotype map of over 3.1 million SNPs. *Nature* **449**:851-861.

Irwin SA, Patel B, Idupulapati M, Harris JB, Crisostomo RA, Larsen BP, Kooy F, Willems PJ, Cras P, Kozlowski PB, Swain RA, Weiler IJ, Greenough WT. (2001). Abnormal dendritic spine characteristics in the temporal and visual cortices of patients with fragile-X syndrome: a quantitative examination. *Am J Med Genet* **98**:161-167.

Jacquemont S, Curie A, des Portes V, Torrioli MG, Berry-Kravis E, Hagerman RJ, Ramos FJ, Cornish K, He Y, Paulding C, Neri G, Chen F, Hadjikhani N, Martinet D, Meyer J, Beckmann JS, Delange K, Brun A, Bussy G, Gasparini F, et al. (2011). Epigenetic modification of the FMR1 gene in fragile X syndrome is associated with differential response to the mGluR5 antagonist AFQ056. *Sci Transl Med* **3**:64ra61.

Jacquemont S, Hagerman RJ, Hagerman PJ, Leehey MA. (2007). Fragile-X syndrome and fragile X-associated tremor/ataxia syndrome: two faces of FMR1. *Lancet Neurol* **6**:45-55.

Johnson EM, Kinoshita Y, Weinreb DB, Wortman MJ, Simon R, Khalili K, Winckler B, Gordon J. (2006). Role of Pur alpha in targeting mRNA to sites of translation in hippocampal neuronal dendrites. *J Neurosci Res* **83**:929-943.

Kirkpatrick LL, McIlwain KA, Nelson DL. (2001). Comparative genomic sequence analysis of the FXR gene family: FMR1, FXR1, and FXR2. *Genomics* **78**:169-177.

Koekkoek SK, Yamaguchi K, Milojkovic BA, Dortland BR, Ruigrok TJ, Maex R, De Graaf W, Smit AE, VanderWerf F, Bakker CE, Willemsen R, Ikeda T, Kakizawa S, Onodera K, Nelson DL, Mientjes E, Joosten M, De Schutter E, Oostra BA, Ito M, et al. (2005). Deletion of FMR1 in Purkinje cells enhances parallel fiber LTD, enlarges spines, and attenuates cerebellar eyelid conditioning in Fragile X syndrome. *Neuron* **47**:339-352.

Kunde SA, Musante L, Grimme A, Fischer U, Muller E, Wanker EE, Kalscheuer VM. (2011). The X-chromosome-linked intellectual disability protein PQBP1 is a component of neuronal RNA granules and regulates the appearance of stress granules. *Hum Mol Genet* **20**:4916-4931.

Lacoux C, Di Marino D, Boyl PP, Zalfa F, Yan B, Ciotti MT, Falconi M, Urlaub H, Achsel T, Mougin A, Caizergues-Ferrer M, Bagni C. (2012). BC1-FMRP interaction is modulated by 2'-O-methylation: RNA-binding activity of the tudor domain and translational regulation at synapses. *Nucleic Acids Res* **40**:4086-4096.

Laggerbauer B, Ostareck D, Keidel EM, Ostareck-Lederer A, Fischer U. (2001). Evidence that fragile X mental retardation protein is a negative regulator of translation. *Hum Mol Genet* **10**:329-338.

Laumonnier F, Roger S, Guerin P, Molinari F, M'Rad R, Cahard D, Belhadj A, Halayem M, Persico AM, Elia M, Romano V, Holbert S, Andres C, Chaabouni H, Colleaux L, Constant J, Le Guennec JY, Briault S. (2006). Association of a functional deficit of the BKCa channel, a synaptic regulator of neuronal excitability, with autism and mental retardation. *Am J Psychiatry* **163**:1622-1629.

Law JA, Du J, Hale CJ, Feng S, Krajewski K, Palanca AM, Strahl BD, Patel DJ, Jacobsen SE. (2013). Polymerase IV occupancy at RNA-directed DNA methylation sites requires SHH1. *Nature* **498**:385-389.

Lee HY, Ge WP, Huang W, He Y, Wang GX, Rowson-Baldwin A, Smith SJ, Jan YN, Jan LY. (2011). Bidirectional regulation of dendritic voltage-gated potassium channels by the fragile X mental retardation protein. *Neuron* **72**:630-642.

Lewis HA, Musunuru K, Jensen KB, Edo C, Chen H, Darnell RB, Burley SK. (2000). Sequence-specific RNA binding by a Nova KH domain: implications for paraneoplastic disease and the fragile X syndrome. *Cell* **100**:323-332.

Li C, Bassell GJ, Sasaki Y. (2009). Fragile X Mental Retardation Protein is Involved in Protein Synthesis-Dependent Collapse of Growth Cones Induced by Semaphorin-3A. *Front Neural Circuits* **3**:11.

Li SY, Chen YC, Lai TJ, Hsu CY, Wang YC. (1993). Molecular and cytogenetic analyses of autism in Taiwan. *Hum Genet* **92**:441-445.

Li Z, Zhang Y, Ku L, Wilkinson KD, Warren ST, Feng Y. (2001). The fragile X mental retardation protein inhibits translation via interacting with mRNA. *Nucleic Acids Res* **29**:2276-2283.

Lubs HA. (1969). A marker X chromosome. *Am J Hum Genet* **21**:231-244.

Lugenbeel KA, Peier AM, Carson NL, Chudley AE, Nelson DL. (1995). Intragenic loss of function mutations demonstrate the primary role of FMR1 in fragile X syndrome. *Nat Genet* **10**:483-485.

Luo S, Huang W, Xia Q, Du Q, Wu L, Duan R. (2014). Mutational Analyses of the FMR1 Gene in Chinese Pediatric Population of Fragile X Suspects: Low Tolerance for Point Mutation. *J Child Neurol*.

Mahone M, Saffman EE, Lasko PF. (1995). Localized Bicaudal-C RNA encodes a protein containing a KH domain, the RNA binding motif of FMR1. *EMBO J* **14**:2043-2055.

Martire M, Barrese V, D'Amico M, Iannotti FA, Pizzarelli R, Samengo I, Viggiano D, Ruth P, Cherubini E, Taglialatela M. (2010). Pre-synaptic BK channels selectively control glutamate versus GABA release from cortical and hippocampal nerve terminals. *J Neurochem* **115**:411-422.

Maurer-Stroh S, Dickens NJ, Hughes-Davies L, Kouzarides T, Eisenhaber F, Ponting CP. (2003). The Tudor domain 'Royal Family': Tudor, plant Agenet, Chromo, PWWP and MBT domains. *Trends Biochem Sci* **28**:69-74.

Meijer H, de Graaff E, Merckx DM, Jongbloed RJ, de Die-Smulders CE, Engelen JJ, Fryns JP, Curfs PM, Oostra BA. (1994). A deletion of 1.6 kb proximal to the CGG repeat of the FMR1 gene causes the clinical phenotype of the fragile X syndrome. *Hum Mol Genet* **3**:615-620.

Melko M, Bardoni B. (2010). The role of G-quadruplex in RNA metabolism: involvement of FMRP and FMR2P. *Biochimie* **92**:919-926.

Merenstein SA, Sobesky WE, Taylor AK, Riddle JE, Tran HX, Hagerman RJ. (1996). Molecular-clinical correlations in males with an expanded FMR1 mutation. *Am J Med Genet* **64**:388-394.

Muddashetty RS, Kelic S, Gross C, Xu M, Bassell GJ. (2007). Dysregulated metabotropic glutamate receptor-dependent translation of AMPA receptor and postsynaptic density-95 mRNAs at synapses in a mouse model of fragile X syndrome. *J Neurosci* **27**:5338-5348.

Musumeci SA, Hagerman RJ, Ferri R, Bosco P, Dalla Bernardina B, Tassinari CA, De Sarro GB, Elia M. (1999). Epilepsy and EEG findings in males with fragile X syndrome. *Epilepsia* **40**:1092-1099.

Myrick LK, Deng PY, Hashimoto H, Cho Y, Nakamoto-Kinoshita M, Poidevin MJ, Suhl JA, Visootsak J, Cavalli V, Jin P, Cheng X, Warren ST, Klyachko VA. (2014a). An independent role for presynaptic FMRP revealed by an FMR1 missense mutation associated with intellectual disability and seizures. *PNAS* **(in review)**.

Myrick LK, Hashimoto H, Cheng X, Warren ST. (2014b). FMRP contains an integral tandem Agenet (Tudor) and KH motif in the amino terminal domain. *Hum Mol Genet* **(in review)**.

Myrick LK, Nakamoto-Kinoshita M, Lindor NM, Kirmani S, Cheng X, Warren ST. (2014c). Fragile X syndrome due to a missense mutation. *Eur J Hum Genet* **22**:1185-1189.

N'Gouemo P. (2011). Targeting BK (big potassium) channels in epilepsy. *Expert Opin Ther Targets* **15**:1283-1295.

Nakamoto M, Nalavadi V, Epstein MP, Narayanan U, Bassell GJ, Warren ST. (2007). Fragile X mental retardation protein deficiency leads to excessive mGluR5-dependent internalization of AMPA receptors. *Proc Natl Acad Sci U S A* **104**:15537-15542.

O'Donnell WT, Warren ST. (2002). A decade of molecular studies of fragile X syndrome. *Annu Rev Neurosci* **25**:315-338.

Osterweil EK, Krueger DD, Reinhold K, Bear MF. (2010). Hypersensitivity to mGluR5 and ERK1/2 leads to excessive protein synthesis in the hippocampus of a mouse model of fragile X syndrome. *J Neurosci* **30**:15616-15627.

Otwinowski Z, Borek D, Majewski W, Minor W. (2003). Multiparametric scaling of diffraction intensities. *Acta Crystallogr A* **59**:228-234.

Pacheco Otalora LF, Hernandez EF, Arshadmansab MF, Francisco S, Willis M, Ermolinsky B, Zarei M, Knaus HG, Garrido-Sanabria ER. (2008). Down-regulation of BK channel expression in the pilocarpine model of temporal lobe epilepsy. *Brain Res* **1200**:116-131.

Pak C, Garshasbi M, Kahrizi K, Gross C, Apponi LH, Noto JJ, Kelly SM, Leung SW, Tzschach A, Behjati F, Abedini SS, Mohseni M, Jensen LR, Hu H, Huang B, Stahley SN, Liu G, Williams KR, Burdick S, Feng Y, et al. (2011). Mutation of the conserved polyadenosine RNA binding protein, ZC3H14/dNab2, impairs neural function in Drosophila and humans. *Proc Natl Acad Sci U S A* **108**:12390-12395.

Pan F, Aldridge GM, Greenough WT, Gan WB. (2010). Dendritic spine instability and insensitivity to modulation by sensory experience in a mouse model of fragile X syndrome. *Proc Natl Acad Sci U S A* **107**:17768-17773.

Pan L, Zhang YQ, Woodruff E, Broadie K. (2004). The Drosophila fragile X gene negatively regulates neuronal elaboration and synaptic differentiation. *Curr Biol* **14**:1863-1870.

Patel AB, Hays SA, Bureau I, Huber KM, Gibson JR. (2013). A target cell-specific role for presynaptic Fmr1 in regulating glutamate release onto neocortical fast-spiking inhibitory neurons. *J Neurosci* **33**:2593-2604.

Penagarikano O, Mulle JG, Warren ST. (2007). The pathophysiology of fragile x syndrome. *Annu Rev Genomics Hum Genet* **8**:109-129.

Pfeiffer BE, Huber KM. (2007). Fragile X mental retardation protein induces synapse loss through acute postsynaptic translational regulation. *J Neurosci* **27**:3120-3130.

Pfeiffer BE, Huber KM. (2009). The state of synapses in fragile X syndrome. *Neuroscientist* **15**:549-567.

Phan AT, Kuryavyi V, Darnell JC, Serganov A, Majumdar A, Ilin S, Raslin T, Polonskaia A, Chen C, Clain D, Darnell RB, Patel DJ. (2011). Structure-function studies of FMRP RGG peptide recognition of an RNA duplex-quadruplex junction. *Nat Struct Mol Biol* **18**:796-804.

Pieretti M, Zhang FP, Fu YH, Warren ST, Oostra BA, Caskey CT, Nelson DL. (1991). Absence of expression of the FMR-1 gene in fragile X syndrome. *Cell* **66**:817-822.

Ramos A, Hollingworth D, Adinolfi S, Castets M, Kelly G, Frenkiel TA, Bardoni B, Pastore A. (2006). The structure of the N-terminal domain of the fragile X mental retardation protein: a platform for protein-protein interaction. *Structure* **14**:21-31.

Ramos A, Hollingworth D, Major SA, Adinolfi S, Kelly G, Muskett FW, Pastore A. (2002). Role of dimerization in KH/RNA complexes: the example of Nova KH3. *Biochemistry* **41**:4193-4201.

Ramos A, Hollingworth D, Pastore A. (2003). The role of a clinically important mutation in the fold and RNA-binding properties of KH motifs. *RNA* **9**:293-298.

Reeve SP, Lin X, Sahin BH, Jiang F, Yao A, Liu Z, Zhi H, Broadie K, Li W, Giangrande A, Hassan BA, Zhang YQ. (2008). Mutational analysis establishes a critical role for the N terminus of fragile X mental retardation protein FMRP. *J Neurosci* **28**:3221-3226.

Richards BW, Sylvester PE, Brooker C. (1981). Fragile X-linked mental retardation: the Martin-Bell syndrome. *J Ment Defic Res* **25 Pt 4**:253-256.

Richards RI, Sutherland GR. (1994). Simple repeat DNA is not replicated simply. *Nat Genet* **6**:114-116.

Rudelli RD, Brown WT, Wisniewski K, Jenkins EC, Laure-Kamionowska M, Connell F, Wisniewski HM. (1985). Adult fragile X syndrome. Clinico-neuropathologic findings. *Acta Neuropathol* **67**:289-295.

Santoro MR, Bray SM, Warren ST. (2012). Molecular mechanisms of fragile X syndrome: a twenty-year perspective. *Annu Rev Pathol* **7**:219-245.

Schaeffer C, Bardoni B, Mandel JL, Ehresmann B, Ehresmann C, Moine H. (2001). The fragile X mental retardation protein binds specifically to its mRNA via a purine quartet motif. *EMBO J* **20**:4803-4813.

Schenck A, Bardoni B, Moro A, Bagni C, Mandel JL. (2001). A highly conserved protein family interacting with the fragile X mental retardation protein (FMRP) and displaying selective interactions with FMRP-related proteins FXR1P and FXR2P. *Proc Natl Acad Sci U S A* **98**:8844-8849.

Sherman SL, Jacobs PA, Morton NE, Froster-Iskenius U, Howard-Peebles PN, Nielsen KB, Partington MW, Sutherland GR, Turner G, Watson M. (1985). Further segregation analysis of the fragile X syndrome with special reference to transmitting males. *Hum Genet* **69**:289-299.

Shinahara K, Saijo T, Mori K, Kuroda Y. (2004). Single-strand conformation polymorphism analysis of the FMR1 gene in autistic and mentally retarded children in Japan. *J Med Invest* **51**:52-58.

Siomi MC, Siomi H, Sauer WH, Srinivasan S, Nussbaum RL, Dreyfuss G. (1995). FXR1, an autosomal homolog of the fragile X mental retardation gene. *EMBO J* **14**:2401-2408.

Siomi MC, Zhang Y, Siomi H, Dreyfuss G. (1996). Specific sequences in the fragile X syndrome protein FMR1 and the FXR proteins mediate their binding to 60S ribosomal subunits and the interactions among them. *Mol Cell Biol* **16**:3825-3832.

Sittler A, Devys D, Weber C, Mandel JL. (1996). Alternative splicing of exon 14 determines nuclear or cytoplasmic localisation of fmr1 protein isoforms. *Hum Mol Genet* **5**:95-102.

Skafidas E, Testa R, Zantomio D, Chana G, Everall IP, Pantelis C. (2014). Predicting the diagnosis of autism spectrum disorder using gene pathway analysis. *Mol Psychiatry* **19**:504-510.

Stefani G, Fraser CE, Darnell JC, Darnell RB. (2004). Fragile X mental retardation protein is associated with translating polyribosomes in neuronal cells. *J Neurosci* **24**:7272-7276.

Strom CM, Crossley B, Redman JB, Buller A, Quan F, Peng M, McGinnis M, Fenwick RG, Jr., Sun W. (2007). Molecular testing for Fragile X Syndrome: lessons learned from 119,232 tests performed in a clinical laboratory. *Genet Med* **9**:46-51.

Strumbos JG, Brown MR, Kronengold J, Polley DB, Kaczmarek LK. (2010). Fragile X mental retardation protein is required for rapid experience-dependent regulation of the potassium channel Kv3.1b. *J Neurosci* **30**:10263-10271.

Suvrathan A, Hoeffer CA, Wong H, Klann E, Chattarji S. (2010). Characterization and reversal of synaptic defects in the amygdala in a mouse model of fragile X syndrome. *Proc Natl Acad Sci U S A* **107**:11591-11596.

Tarpey PS, Raymond FL, Nguyen LS, Rodriguez J, Hackett A, Vandeleur L, Smith R, Shoubridge C, Edkins S, Stevens C, O'Meara S, Tofts C, Barthorpe S, Buck G, Cole J, Halliday K, Hills K, Jones D, Mironenko T, Perry J, et al. (2007). Mutations in UPF3B, a member of the nonsense-mediated mRNA decay complex, cause syndromic and nonsyndromic mental retardation. *Nat Genet* **39**:1127-1133.

Tarpey PS, Smith R, Pleasance E, Whibley A, Edkins S, Hardy C, O'Meara S, Latimer C, Dicks E, Menzies A, Stephens P, Blow M, Greenman C, Xue Y, Tyler-Smith C, Thompson D, Gray K, Andrews J, Barthorpe S, Buck G, et al. (2009). A systematic, large-scale resequencing screen of X-chromosome coding exons in mental retardation. *Nat Genet* **41**:535-543.

Tessier CR, Broadie K. (2008). Drosophila fragile X mental retardation protein developmentally regulates activity-dependent axon pruning. *Development* **135**:1547-1557.

Todd PK, Malter JS, Mack KJ. (2003). Whisker stimulation-dependent translation of FMRP in the barrel cortex requires activation of type I metabotropic glutamate receptors. *Brain Res Mol Brain Res* **110**:267-278.

Tranfaglia MR. (2011). The psychiatric presentation of fragile x: evolution of the diagnosis and treatment of the psychiatric comorbidities of fragile X syndrome. *Dev Neurosci* **33**:337-348.

Trottier Y, Imbert G, Poustka A, Fryns JP, Mandel JL. (1994). Male with typical fragile X phenotype is deleted for part of the FMR1 gene and for about 100 kb of upstream region. *Am J Med Genet* **51**:454-457.

Valverde R, Edwards L, Regan L. (2008). Structure and function of KH domains. *FEBS J* **275**:2712-2726.

Valverde R, Pozdnyakova I, Kajander T, Venkatraman J, Regan L. (2007). Fragile X mental retardation syndrome: structure of the KH1-KH2 domains of fragile X mental retardation protein. *Structure* **15**:1090-1098.

Verkerk AJ, Pieretti M, Sutcliffe JS, Fu YH, Kuhl DP, Pizzuti A, Reiner O, Richards S, Victoria MF, Zhang FP, et al. (1991). Identification of a gene (FMR-1) containing a CGG repeat coincident with a breakpoint cluster region exhibiting length variation in fragile X syndrome. *Cell* **65**:905-914.

Volk LJ, Pfeiffer BE, Gibson JR, Huber KM. (2007). Multiple Gq-coupled receptors converge on a common protein synthesis-dependent long-term depression that is affected in fragile X syndrome mental retardation. *J Neurosci* **27**:11624-11634.

Wan L, Dockendorff TC, Jongens TA, Dreyfuss G. (2000). Characterization of dFMR1, a Drosophila melanogaster homolog of the fragile X mental retardation protein. *Mol Cell Biol* **20**:8536-8547.

Wang H, Fukushima H, Kida S, Zhuo M. (2009). Ca2+/calmodulin-dependent protein kinase IV links group I metabotropic glutamate receptors to fragile X mental retardation protein in cingulate cortex. *J Biol Chem* **284**:18953-18962.

Wang H, Iacoangeli A, Lin D, Williams K, Denman RB, Hellen CU, Tiedge H. (2005). Dendritic BC1 RNA in translational control mechanisms. *J Cell Biol* **171**:811-821.

Wang H, Kim SS, Zhuo M. (2010a). Roles of fragile X mental retardation protein in dopaminergic stimulation-induced synapse-associated protein synthesis and subsequent alpha-amino-3-hydroxyl-5-methyl-4-isoxazole-4-propionate (AMPA) receptor internalization. *J Biol Chem* **285**:21888-21901.

Wang H, Wu LJ, Kim SS, Lee FJ, Gong B, Toyoda H, Ren M, Shang YZ, Xu H, Liu F, Zhao MG, Zhuo M. (2008). FMRP acts as a key messenger for dopamine modulation in the forebrain. *Neuron* **59**:634-647.

Wang LW, Berry-Kravis E, Hagerman RJ. (2010b). Fragile X: leading the way for targeted treatments in autism. *Neurotherapeutics* **7**:264-274.

Wang YC, Lin ML, Lin SJ, Li YC, Li SY. (1997). Novel point mutation within intron 10 of FMR-1 gene causing fragile X syndrome. *Hum Mutat* **10**:393-399.

Weiler IJ, Irwin SA, Klintsova AY, Spencer CM, Brazelton AD, Miyashiro K, Comery TA, Patel B, Eberwine J, Greenough WT. (1997). Fragile X mental retardation protein is translated near synapses in response to neurotransmitter activation. *Proc Natl Acad Sci U S A* **94**:5395-5400.

Wilson BM, Cox CL. (2007). Absence of metabotropic glutamate receptor-mediated plasticity in the neocortex of fragile X mice. *Proc Natl Acad Sci U S A* **104**:2454-2459.

Wisniewski KE, Segan SM, Miezejeski CM, Sersen EA, Rudelli RD. (1991). The Fra(X) syndrome: neurological, electrophysiological, and neuropathological abnormalities. *Am J Med Genet* **38**:476-480.

Wohrle D, Kotzot D, Hirst MC, Manca A, Korn B, Schmidt A, Barbi G, Rott HD, Poustka A, Davies KE, et al. (1992). A microdeletion of less than 250 kb, including the proximal part of the FMR-I gene and the fragile-X site, in a male with the clinical phenotype of fragile-X syndrome. *Am J Hum Genet* **51**:299-306.

Yan X, Denman RB. (2011). Conformational-dependent and independent RNA binding to the fragile x mental retardation protein. *J Nucleic Acids* **2011**:246127.

Young KL, Villar D, Carson TL, Ierman PM, Moore RA, Bottoff MR. (2003). Tremorgenic mycotoxin intoxication with penitrem A and roquefortine in two dogs. *J Am Vet Med Assoc* **222**:52-53, 35.

Yudkin D, Hayward BE, Aladjem MI, Kumari D, Usdin K. (2014). Chromosome fragility and the abnormal replication of the FMR1 locus in fragile X syndrome. *Hum Mol Genet* **23**:2940-2952.

Zalfa F, Adinolfi S, Napoli I, Kuhn-Holsken E, Urlaub H, Achsel T, Pastore A, Bagni C. (2005). Fragile X mental retardation protein (FMRP) binds specifically to the brain cytoplasmic RNAs BC1/BC200 via a novel RNA-binding motif. *J Biol Chem* **280**:33403-33410.

Zalfa F, Giorgi M, Primerano B, Moro A, Di Penta A, Reis S, Oostra B, Bagni C. (2003). The fragile X syndrome protein FMRP associates with BC1 RNA and regulates the translation of specific mRNAs at synapses. *Cell* **112**:317-327.

Zang JB, Nosyreva ED, Spencer CM, Volk LJ, Musunuru K, Zhong R, Stone EF, Yuva-Paylor LA, Huber KM, Paylor R, Darnell JC, Darnell RB. (2009). A mouse model of the human Fragile X syndrome I304N mutation. *PLoS Genet* **5**:e1000758.

Zanni G, Scotton C, Passarelli C, Fang M, Barresi S, Dallapiccola B, Wu B, Gualandi F, Ferlini A, Bertini E, Wei W. (2013). Exome sequencing in a family with intellectual disability, early onset spasticity, and cerebellar atrophy detects a novel mutation in EXOSC3. *Neurogenetics* **14**:247-250.

Zhang Y, Brown MR, Hyland C, Chen Y, Kronengold J, Fleming MR, Kohn AB, Moroz LL, Kaczmarek LK. (2012). Regulation of neuronal excitability by interaction of fragile X mental retardation protein with slack potassium channels. *J Neurosci* **32**:15318-15327.

Zhang Y, O'Connor JP, Siomi MC, Srinivasan S, Dutra A, Nussbaum RL, Dreyfuss G. (1995). The fragile X mental retardation syndrome protein interacts with novel homologs FXR1 and FXR2. *EMBO J* **14**:5358-5366.

Zhang YQ, Bailey AM, Matthies HJ, Renden RB, Smith MA, Speese SD, Rubin GM, Broadie K. (2001). Drosophila fragile X-related gene regulates the MAP1B homolog Futsch to control synaptic structure and function. *Cell* **107**:591-603.